Source Term Review for the Tailings Management Area and Reclaim Pond at the Proposed Crandon Mine, Forest County, Wisconsin

Edited by Craig H. Benson and Christopher P. Carlson

Contributions by

Craig H. Benson, Civil Engineering Consultants

David W. Blowes, Sala Groundwater

Kim A. Lappako, St. Paul, Minnesota

Kenneth D. Markart, Wisconsin Department of Natural Resources

Christopher P. Carlson, Wisconsin Department of Natural Resources

---

Prepared through the cooperation of the

U.S. Geological Survey

Wisconsin Department of Natural Resources

Wisconsin Geological and Natural History Survey

Wisconsin Geological and Natural History Survey
Open-File Report 2004-27 ◆ 2005

DISCLAIMER

During the latter stages of the process of completion of the first full draft of this report, the permit applications for proposed Crandon Mine project were withdrawn by Nicolet Minerals Company. As a consequence, the report was finished only to the point of ensuring a coherent full draft. The report was not subjected to a detailed review by the authors (including verification of all calculations), other project personnel at the Wisconsin Department of Natural Resources (WDNR), or any external peers. Therefore, this document should not be considered to be "Final," and should not be construed to represent the final position of the DNR with respect to the portions of the project review described herein. Any use of this document is at the risk of the user.

Published by and available from

Wisconsin Geological and Natural History Survey
3817 Mineral Point Road
Madison, Wisconsin 53705-5100
TEL 608/263.7389 FAX 608/262.8086
http://www.uwex.edu/wgnhs/

James M. Robertson, Director and State Geologist

CONTENTS

INTRODUCTION

This report describes an assessment of issues related to the source term used for the tailings management area (TMA) and the adjacent reclaim pond (RP) for the Crandon Mine, which has been proposed by Nicolet Minerals Company (NMC; also previously known as the Crandon Mining Company [CMC]). The proposed mine site is near Crandon, Wisconsin.

The intent of this report is to provide technical information necessary to support conclusions and inferences being made by the Wisconsin Department of Natural Resources in the Environmental Impact Statement (EIS) for the proposed Crandon Mine. The report is divided into four main sections. Section I deals with the characterization of the waste materials to be placed in the TMA. Section II deals with the flow of water and leachate into, through, and out of the TMA. Section III deals with oxygen transport into the TMA. Section IV deals with geochemistry and water quality in the TMA and the associated reclaim pond.

Material for this report was contributed by Dr. Craig Benson, Dr. David Blowes, Mr. Kim Lappako, and Mr. Kenneth Markart. Lappako and Markart prepared Section I. Benson prepared Sections II and III and Benson and Blowes prepared Section IV. Blowes also provided information used in the analysis in Section II. Benson compiled the sections into this report, and Dr. Christopher Carlson provided project direction and editorial review.

I. LABORATORY WASTE CHARACTERIZATION

Critical concerns regarding the impact of mine wastes on water quality involve the release of acid and trace metals. Acid is produced by the oxidation of sulfide minerals. Neutralization can occur by the dissolution of calcium carbonate and magnesium carbonate minerals. Acidification can occur when the rate of acid production exceeds the rate of acid neutralization. Whereas acidic drainage contains elevated concentrations of trace metals, elevated trace metal concentrations can also occur in circumneutral and alkaline drainage.

Drainage will not acidify as long as neutralizing minerals are present, reactive and dissolving at a rate greater than or equal to the rate of acid production. If neutralizing minerals are depleted or their reactivity is reduced below that of acid production, drainage will acidify. Reactivity can be reduced due to coating of the mineral surface with precipitates such as iron oxyhydroxides or development of leached layer at the mineral surface.

The rates of these reactions are controlled by several solid phase factors, as well as liquid and gas phase factors and the environment in which the reactions are occurring. Key solid phase variables include the specific acid-producing and acid-neutralizing minerals present, the amounts in which these minerals are present, the chemistry of these minerals, and the surface area available for reaction. The surface area available for reaction is a function of the amount of the mineral present, the mineral surface roughness, the mineral grain size and extent of mineral liberation, both of which are influenced by the size distribution of the material, and the extent of reaction-inhibiting coatings on the mineral surface. An oxidant, typically oxygen or ferric iron,

and water are necessary for the oxidation of sulfide minerals. Water also serves as a medium for transporting the reaction products through and from the mine waste disposal facility.

Trace metals are usually present as impurities in iron sulfide minerals and as distinct sulfide minerals. Their release is dependent upon both the rate of trace metal sulfide oxidation and the extent of subsequent transport. Their transport is dependent upon numerous factors including the chemistry of the individual metal species, drainage pH, redox conditions, the potential for co-precipitation, the presence of adsorbing surfaces, and the fluid flow conditions with the material.

To assess the potential for release of acid and trace metals, waste characterization studies are commonly conducted prior to mining. The goal of these studies is to determine the quality of drainage from mine wastes after they have been placed in the field. Among the more specific objectives of waste characterization studies are to determine (i) the mass of mine waste to be generated, (2) the compositional variation of mine waste, (iii) the rates of acid production and acid neutralization, (iv) the availability of acid-producing and acid-neutralizing components, and (v) the rates of trace metal release. The first two objectives can be largely addressed through the mine plan, in conjunction with chemical and mineralogical analyses and static testing. Some chemical and mineralogical data are often available from mineral exploration and mineral processing studies, and additional analyses can be conducted on available solids. The particle size of the operational mine waste and its impact on the chemical behavior of the mine waste must also be considered. For the third through fifth objectives, laboratory weathering tests are typically conducted. To extrapolate results of the laboratory testing to field conditions, factors such as oxygen transport, water movement within the mine waste disposal facility, and geochemical equilibria must be considered.

Traditional physical and geochemical analyses include particle size and mineralogical analysis along with static and kinetic tests. The particle size distribution provides a qualitative assessment of surface area available for reaction. Solid-phase chemical analyses quantify the presence of various elements and some compounds (e.g. sulfate, carbonate) in solids. Mineralogical analyses quantify the minerals present and their composition. They can also be used to assess the availability of mineral surfaces for reaction. Consequently, they describe the solid-phase characteristics which influence water quality.

Static tests are used as a screening tool to provide an initial estimation of the acid-producing character of mine wastes. They provide a measure of the potential of a sample to produce acid and to neutralize acid. They are simplistic in that they do not consider the extent to which acid-producing and acid-neutralizing components will react nor the rates at which these components react. These are important considerations in the process of acid production. In addition static tests do not measure the potential for trace metal release.

Kinetic tests are tests in which mine wastes are subjected to weathering under controlled conditions and the quality of drainage from the wastes is determined. These tests require more time to conduct than the static tests. They are typically used to determine whether or not mine wastes are likely to generate acidic drainage. This assessment is based on the assumption that the laboratory drainage from a sample simulates that which would occur from a sample of similar composition in the field. Kinetic tests can also be used to determine rates of reaction and

mineral availabilities. The results from these tests must be interpreted and extrapolated with due consideration of the reaction environment in which tests are conducted, the compositional variability of wastes to be generated, as well as potential operational variables.

I.A REPRESENTATIVENESS

Essential to any waste characterization study is the representativeness of the materials used for characterization. Thus, an assessment was made of whether the rock and ore samples used in the waste characterization and physical testing work were likely to be representative of the waste rock and tailings to be generated at the proposed Crandon Mine. The assessment was based on documents submitted by Nicolet Minerals Company (NMC), assessments of WDNR consultants, and verification work completed by WDNR personnel. Much of the information submitted by NMC is in the document "Representativeness of Ore and Tailings Sample From the Crandon Deposit," which was prepared by Steffen Robertson and Kristen (1999b) and is in the Environmental Impact Report (EIR) as Appendix A5 (also referred to as EIR Appendix 4.2-16b) of the Groundwater Quality Performance Evaluation (GWQPE), which is located in also referred to as EIR Appendix 4.2-12 (Foth and Van Dyke, 1998a).

I.A.1 Geology of the Crandon Deposit

I.A.1.1 Ore Body

The Crandon ore body is typical of volcanogenic massive sulfide deposits known world-wide. A description is found in Erickson and Cote (1996). They describe two types of mineralization. Syngenetic laminated sphalerite-pyrite zones (massive zinc) comprise most of the ore body situated in host felsic volcanic rocks and sediments. Underlying that is an epigenetic system of altered volcanic rocks and sediments with stringer veins of quartz, pyrite and chalcopyrite (copper stringer). In portions of the ore body, this copper stringer zone over prints the sphalerite (massive zinc) zone.

Within the laminated sphalerite-pyrite zone, the mineralization consists of three distinct sub-parallel stacked lenses. These lenses appear to represent cyclic pulses. Each of the massive sphalerite-pyrite lenses has an upper enriched zinc bedded to laminated sphalerite-pyrite (±) galena facies which grades stratigraphically downward into a leaner zinc, poorly bedded pyrite facies.

The copper stringer mineralization consists of multiple stages of quartz, quartz-pyrite, quartz-pyrite-chalcopyrite, and quartz-pyrite-chalcopyrite-sphalerite veinlets cross cutting altered volcanics and sediments.

Sulfide mineralogy consists of pyrite, sphalerite, chalcopyrite, galena, and tetrahedrite with rare pyrrhotite and arsenopyrite. Galena, tetrahedrite and arsenopyrite are generally associated with the massive zinc zones, whereas pyrrhotite appears to be associated with the copper stringer zone.

As reported by Lambe and Rowe (1987), the Crandon deposit exhibits some metal zoning in the massive zinc ore. Copper is uniform throughout the massive zinc zone. Highest lead and zinc values occur where the ore is thickest. The association of galena, tetrahedrite and arsenopyrite with more massive zinc zones is recognized visually when observing drill core from these areas.

Gangue minerals associated with the ore body are dominated by quartz with lesser amounts of sericite, chlorite and carbonates. More iron-magnesium-rich silicate (chlorite) with sericite is associated with the massive zinc portion of the ore body. The copper stringer ores are dominated by quartz. This is consistent with most volcanogenic massive sulfide deposits where more iron-magnesium-rich gangue minerals are associated with the more massive portions of the ore bodies and are found to grade both laterally and vertically to lesser iron-magnesium enrichment.

The two major mineral classes of concern for waste characterization work are sulfides and carbonates. Most leachable metals of concern are associated with the sulfide minerals. The amount of sulfide minerals also has a direct relation to the acid producing potential. As discussed above, there are a variety of different sulfide minerals, but most appear to be incorporated in the more massive sphalerite (zinc) rich portions of the ore body, with the exception of chalcopyrite. Chalcopyrite is dominant in the copper stringer ore.

The type and amount of carbonate becomes critical in determining if waste rock and tailings from different portions of the ore body would react with acid and limit the release of metals. The distribution of carbonates and the variety of carbonates throughout the ore body is not well defined. However, there is some general zonation recognized. More iron-rich carbonates appear to favor the copper stringer zone versus the massive zinc zone. However, the relative amount of carbonate is less in the copper stringer zone than in the massive zinc zone.

The only reference to the distribution of carbonates within and near the ore body is found in an Exxon memorandum by Rowe (1980). Associated with the ore body in the footwall 200 meters off the east end of the ore body are calcite-altered basalts. Hanging wall tuffs, also more than 200 meters away have calcite-rich fragments. Within the ore body, small dolomite pods are reported to be scattered sparsely throughout the massive zinc ore (Rowe, 1980). The memo gave an example of only one hole, DDH #91, which averaged 40.8% dolomite over a small interval.

Thresher and Son (1998) documents a screening of 150 thin sections of the Crandon ore body that was made to determine the abundance, morphology, and species of carbonate minerals. This assessment concluded that carbonate minerals are less abundant in moderate to intensely weathered zones of the ore body. Thresher and Son (1998) also discusses the morphology of pyrite, indicating at least two generations occur, particularly in the zinc ore. The first generation consists of large pyrite grains, which are jigsawed fragments with fractures filled by chalcopyrite, sphalerite, quartz and chlorite. The second generation consists of spheroidal grains. There is no discussion of any spatial relationship of the other metal sulfide minerals.

Erickson (1994), in his report on sample representativeness, indicated the Crandon ore body has modest geologic variability within the massive zinc lenses. Isolated sporadic assays of gold, arsenic and lead are seen to vary with no significant pattern.

I.A.1.2 Host Rocks

The host rock geology of the Crandon ore body is well known. This is based upon 272 drill holes into the ore zone, which approximates to drilling on 200 foot centers. Correlation between drill holes was sufficient to identify the five major stratigraphic units which would be encountered by the proposed mine development. These units are lithologically-based and represent distinct volcano-sedimentary events prior to, during and after the genesis of the mineralization. Since all mine workings were originally proposed to be in the hanging wall above the Crandon unit, which contains the economic mineralization, all waste characterization work was restricted to those units.

Based upon the proposed mine plan, the Skunk Lake Unit, Rice Lake Unit, Upper and Lower Mole Lake Units, Crandon Unit and the upper portion of the Sand Lake Unit would be encountered by mining. The Sand Lake Unit is included because it is, in part, the host for the copper stringer ore. However, the extent to which the Sand Lake Unit would be encountered during the copper phase mining has not been detailed by NMC.

Contacts for all lithologic units are gradational, but relatively discernible by an experienced geologist. The Skunk Lake, Lower Mole Lake, and Crandon Units are reported to have higher sulfide contents. These volcano-sedimentary units represent a hiatus in volcanism and the precipitation of chemical sediments of silica, iron and sulfur. The portions of the Rice Lake and Upper Mole Lake Units encountered around the proposed mine represent more active volcanism with pyroclastic tuffs and debris flows.

The upper portion of the Sand Lake Unit in the vicinity of the ore body is the base on which the Crandon deposit formed and through which mineralizing solutions permeated up to the sea floor. This unit contains the chalcopyrite-pyrite-quartz veins of the stringer ore zone. The Sand Lake Unit has been subject to local intensive pyritization and silicification.

I.A.2 Waste Rock

I.A.2.1 Waste Rock Sample Selection

All waste rock characterization samples were collected from drill core. The location of these samples were chosen to represent material that would be encountered during main shaft and ventilation shaft sinking and drift and stope access development. Based on the examination of geologic cross sections and the location of proposed mine workings, drill holes were selected where intercepts or closely correlated intercepts would encounter proposed hanging wall mine workings. Dependent upon the location of the drill hole relative to the proposed mine workings, these intercepts varied from 1.5 to 61 m (5 to 200 ft) in length. The selected intercepts were then delineated into the Skunk Lake, Rice Lake and Upper and Lower Mole Lake Units. Based upon this delineation, a three inch core sample was randomly selected every 0.6 m (2 ft) over the intercept interval for the respective four units. By drill hole and unit, this core was bagged, crushed, and then split to generate a sample of that unit for each drill hole intercept. A master composite was then made using all the sample splits of selected drill holes for each particular unit.

The Lower Mole Lake Unit is not a distinct geologic unit, but an arbitrarily designated zone located stratigraphically out to 30 m (100 ft) from the Crandon unit geologic contact. The Lower Mole Lake Unit contains most of the hanging wall mine stope accesses and drifts. The concentration and variability in concentration of sulfide minerals in the lower most 100 feet of the Mole Lake Formation is greater than any other waste rock unit encountered (Foth and Van Dyke, 2000b).

The locations of the selected drill holes used to generate the waste rock composites were evaluated by using a plot and trace of drill holes into the ore body in Figure 3.5-3 (plan map showing drill hole trace in vicinity of Crandon Formation subcrop, EIR Section 3.5). The review of these plots showed them to be located between the proposed east and west ventilation shafts. This is the area where nearly all the proposed hanging wall mine workings would be located. The sampled holes (42) represent about one-third of all drill holes situated within this area. They appear to be selected from and representative of where most mine workings would occur.

Also, mine geologic cross sections were reviewed (Markart, 1995). These sections contained the 1994 proposed mine workings, where the forty-two drill holes were selected. The core intervals selected from these 42 drill holes were from a variety of different proposed mining elevations. This satisfied the need to sample the waste rock both laterally and vertically across the proposed mine working area to generate a representative sample. The number of core intercepts used per unit were: Skunk Lake – 7 drill holes, 25 intervals; Rice Lake – 15 drill holes, 109 intervals; Upper Mole Lake – 20 drill holes, 140 intervals; and Lower Mole Lake – 40 drill holes, 173 intervals (Table 1, EIR Appendix 3.5-31; Foth and Van Dyke, 1998f). The length of the intervals selected were variable and were based upon unit lithologic contacts and prior sulfur assay analyses (Foth and Van Dyke, 1998f).

In addition to the above master composite, a high sulfur composite was made for each unit. This sample was created using intentionally biased sampling procedures. Drill holes were selected from portions of the respective units with the highest sulfur content to form the composite. The locations of the selected holes were evenly spaced across the proposed hanging wall mine workings, but appeared to favor samples from the upper portion of these proposed workings. Table 3 of EIR Appendix 3.5-31 (Foth and Van Dyke, 1998f), designates from where these samples were taken. High sulfur samples were handled similarly as before to prepare a composite, except that the entire interval was used in the sample. This was done to acquire a sufficient sample for bench scale testing.

I.A.2.2 Waste Rock Samples

Determining the degree of variability of carbonates and sulfides in the waste rock that would be encountered during mining operations was important. During mining, waste rock would be segregated based on the presence of sulfides (Type II) or the absence of sulfides (Type I). All Type II waste rock would be disposed in the TMA. Type I material was proposed to be used for construction purposes and the grading layer for the TMA. The variability of sulfide content (acid generating potential) of all waste rock must be known to assure this material would not be a significant source of acid or metals. NMC has indicated that only the Upper Mole Lake and the

Rice Lake Units are considered Type I material (MPA Section 4.8.9-3; Foth and Van Dyke, 1995a/1998d). All other waste rock is designated Type II. The waste rock units were reviewed for representativeness and variability issues individually starting with the proposed Type I material.

I.A.2.2.1 Rice Lake Unit

The Master Composite for the Rice Lake Unit used 15 drill holes and 109 sample intervals. All drill holes were located between the proposed main shaft and the east ventilation shaft. This is the area where most Type I waste rock would be developed during shaft sinking and access drifting to the ore body. The location and selection of the drill holes and sample intervals is appropriate and representative. In Table 1 of Appendix 3.5-31 (Foth and Van Dyke, 1998f), sulfur assay values for the selected intervals were found to vary from 0.01% to 6.4% sulfur and visually estimated pyrite content ranged from less than 0.1% to 2%. Lambe and Rowe (1987) examined the lithology of the Rice Lake Unit and divided it into subunits. Most Rice Lake subunits are indicative of pyroclastic, subaqueous deposition, which would have low sulfur values. Only one subunit, the Millstream Subunit, had the presence of syngenetic sulfide up to 10% in cherty tuffs. This subunit is found in the eastern portions of the proposed mine area and increases in thickness with depth from the surface. The high sulfide Rice Lake master composite that assayed out at 3.33% sulfur most likely comes from this subunit.

The variability of sulfide is dependent upon syngenetic deposition. The highest sulfide values are stratigraphically controlled. No evaluation was completed on the variability of carbonate minerals or species for the Rice Lake Master Composite. However, Lambe and Rowe (1987) reported that the Carridge Subunit within the Rice Lake Unit has calcareous tuffs. Variability for both sulfides and carbonates are related to syngenetic mineralizing processes and are stratigraphically dependent. This implies that segregation of higher acid potential zones may be achievable by understanding the detailed stratigraphy.

I.A.2.2.2 Upper Mole Lake Unit

The Master Composite for the Upper Mole Lake Unit used 20 drill holes with 140 intervals. All drill holes were located between the main shaft and the east ventilation shaft. Thirteen of the drill holes had sample intervals contiguous with the Rice Lake Unit sampled intervals. Sulfur assays varied from 0.01% to 6.4% sulfur. Visible estimated pyrite varied from less than 0.1% to 2%.

Like the Rice Lake Unit, the Upper Mole Lake Unit represents subaqueous volcanoclastic deposition, which has a generally lower sulfide content. However, minor zones of sulfide bearing cherty tuffs, which are sygenetic in origin, are reported in the upper portions of the Unit. The variable amounts of pyrite are directly related to these syngenetic processes and are stratigraphically dependent. Higher sulfide contents in the Upper Mole Lake Unit appear more prevalent in the western portions of the proposed mine workings.

The high sulfide master composite consisted of five drill holes. Only one drill hole was located within the area between the west ventilation shaft and the east ventilation shaft (main workings).

The sulfur content for the Upper Mole Lake high sulfur composite was 4.44% (Table 1, Appendix 4.8 of Foth and Van Dyke, 1995e).

I.A.2.2.3 Skunk Lake Unit

The Master Composite for the Skunk Lake Unit used seven drill holes with 25 intervals. All drill holes were situated between the main shaft and east ventilation shaft where the Skunk Lake Unit would be encountered during mine development. Six of the seven drill holes used to generate the Skunk Lake Master Composite had sample intervals contiguous with the stratigraphically underlying Rice Lake Unit. Sulfur assay values varied from 0.01% to 9.1%. Visible estimated pyrite varied from 0.1% to 9%.

The Skunk Lake Unit represents subaqueous deposition of chemical sediments and ash into a basin that deepened eastward (Lambe and Rowe 1987). As a result, the Unit appears to thin and terminate westward across the mine area. It is composed of cherty tuffs with laminae of syngentic pyrite with minor sphalerite and chalcopyrite. The variability of sulfide minerals are directly related to these syngenetic chemical precipitates and are stratigraphically dependent. There was no information on the variability or species of carbonate present in the Skunk Lake Unit.

The high sulfide composite of the Skunk Lake Unit used two drill holes and 11 sample intervals. Most of the material came from DDH 49 located in the far eastern portion of the proposed mine workings where the Skunk Lake Unit is most prevalent. The sulfur content for the Skunk Lake high sulfur composite was 3.93% (Table 1, Appendix 4.6 of Foth and Van Dyke, 1995e).

I.A.2.2.4 Lower Mole Lake Unit

The Master Composite for the Lower Mole Lake Unit used 40 drill holes with 173 intervals. These drill holes were evenly distributed through the ore body between the east ventilation shaft and the west ventilation shaft. The Lower Mole Lake Unit Master Composite was the largest sampled unit, because most hanging wall stope access drifts would be located within this unit. By developing this large sample set and selecting drill holes spaced across the proposed mine working area, NMC appears to have generated a representative sample. Only 20 of the 40 drill holes selected for the Lower Mole Lake Unit Master Composite were contiguous with the Upper Mole Lake Master Composite sample intervals. These contiguous intervals were located around the mine shaft area where both the Upper and Lower Mole Lake Units would be encountered by the proposed hanging wall mine workings. Sulfur assays were found to vary from 0.01 to 10.8%. Visible estimated pyrite content varied from 0.1% to 5%.

The Lower Mole Lake Unit is not a distinct stratigraphic unit but an arbitrarily established zone 30 m (100 ft) stratigraphically above the Crandon Unit stratigraphic contact. The 30-m (100 ft) zone is where all mine access workings are to be located with the exception of the ventilation shafts and main shaft. Within this 30-m (100 ft) zone, the Prospect Subunit of the Mole Lake Formation occurs. The Prospect Subunit consists of siliceous volcanic debris, and varies from 11 to 20 m (35 to 65 ft) in thickness above the Crandon Unit contact.

The distribution of sulfide and carbonate minerals is stratigraphically dependent. Lambe and Rowe (1987) report the lower portion of the Mole Lake Unit has alteration and mineralization along the central portion of the Crandon ore body. This represents a continuation into the hanging wall Mole Lake Unit of the main hydrothermal event which created the Crandon mineralization. Therefore, sulfide and carbonate content and variability are assumed to increase as the Crandon Unit is approached.

The high sulfide composite of the Lower Mole Lake Unit consisted of 10 drill holes with 11 sample intervals. The length of the sampled intervals varied between 1.5 – 7.5 m (5 and 25 ft). Only one drill hole had a sample contiguous with the Upper Mole Lake Unit. The location of the drill holes used to make the high sulfide composite of the Lower Mole Lake Unit are evenly distributed across the ore body. The sulfur content for this unit was 4.44% (Table 1, Appendix 4.9 of Foth and Van Dyke, 1995e).

I.A.2.3 Waste Rock Variability

NMC conducted additional acid-base accounting and bulk chemical analysis work in 1995 on the waste rock master composites to explore the issue of variability using a two-step approach (Section 4.2 of Foth and Van Dyke, 1995e). The first approach used 46 of the same core intervals used to generate the master composites. The second method used fewer drill holes (13 of 46), but used a 2-foot continuous sample per 10 feet of core per interval.

For both procedures, the selected drill holes were situated in the zone between the east ventilation shaft and the west ventilation shaft, where most of the waste rock would be developed. In the analyses of intervals that made up the individual samples which comprised the master composites (Appendix 1 of Foth and Van Dyke, 1995e), the following variability in neutralization potential (NP) and acid potential (AP) was recognized:

	Neutralization Potential (NP)*		**Acid Potential (AP)***	
Unit	**Minimum**	**Maximum**	**Minimum**	**Maximum**
Skunk Lake	1	4	<0.3	2.8
Rice Lake	3	30	<0.3	7.5
Upper Mole Lake	9	161	<0.3	5.9
Lower Mole Lake	0	92	<0.3	10.6

*All values in kg $CaCO_3$ eq/Mg.

If the NP is assumed to be mostly from the calcium-magnesium carbonate content and that the AP present is mostly from the pyrite content, then the following conclusions can be drawn:

- the Skunk Lake Unit has a carbonate content that varies by a factor of 4 and a sulfide content that varies by a factor of 10;
- the Rice Lake Unit has a carbonate content that varies by a factor of 10, and a sulfide content that varies by a factor of 20;
- the Upper Mole Lake Unit has a carbonate content that varies by a factor of 100, and a sulfide content that varies by a factor of 20; and
- the Lower Mole Lake Unit has a carbonate content that varies by a factor of 100 and a sulfide content that varies by a factor of 30.

These results imply that the variability of both total carbonates and total sulfides seems to increase in the various units as the ore zone is approached stratigraphically. The carbonate content, however, may be somewhat more variable than the sulfide content. The above considerations do not take into account the species of the carbonates present. This also shows that the waste rock master composites do contain a variable domain of individual samples and that the variability of the entire sample set increases as the ore zone (the Crandon Unit) is approached.

These conclusions are supported by the stratigraphic relationships noted earlier by Lambe and Rowe (1987). Sulfide variability is directly related to the presence of cherty units representing a hiatus in volcanic activity and chemical sedimentation. Carbonate variability is associated with these mineralizing events, but also can be associated with the influx of carbonate-rich volcanoclastic sediments. All sulfide and carbonate variability appear to be stratigraphically controlled.

I.A.3 Tailings

All physical and chemical waste characterization work on tailings material conducted by NMC/CMC was generated from drill core from eleven drill holes constructed in 1993. The 1993 drilling was designed to confirm ore grades in the massive zinc zone and to generate a composite sample (1994 Master Zinc Composite) for metallurgical testing. The 1994 Master Zinc Composite sample needed to be representative of the ore to be mined because it would form the basis for mine economics and mill design. The master composite had to consider variability in ore mineral content, habit, grain size and associated gangue minerals. This was required to ensure the mill circuit would perform as designed and would maximize ore mineral recovery. The composite sample was not specifically designed to generate a waste sample. The resultant tailings from the metallurgical work were assumed to be representative of waste material that would be generated because ore minerals would be removed to a desired level from the mill head material which would be representative of what is to be mined. The composite sample also took into account mining procedures by taking intercepts from each particular interval which were then diluted with adjacent lower zinc grade material to compensate for mining dilution.

The intervals for the dilution of ore grade material were randomly selected. The final composite took into account ore-grade variability, mineral grain size and gangue minerals that the proposed mill would encounter on a gross scale. However, the concern with gangue minerals was only evaluated if those minerals would affect ore mineral recovery and not in terms of the generation of a representative tailings sample.

In 1998, another master zinc composite (1998 Master Zinc Composite) was generated from the 1993 drill core. This was a subset produced by using the reject splits of selected core intervals used in the 1994 Master Zinc Composite. The subset used 9 of the 11, 1993 drill holes and a smaller number of ore intercept intervals. The purpose of the 1998 Master Zinc composite was to retest metallurgical processes and to generate a tailings sample that would undergo additional metallurgical testing to remove pyrite. This generated a depyritized tailings sample and a pyrite tailings sample.

I.A.3.1 1994 Master Zinc Composite

I.A.3.1.1 Sample Location

The eleven drill holes used to generate the 1994 and 1998 Master Zinc Composites are situated within the thickest portion of the Crandon Unit, between the east and west ventilation shafts. Within the plane of the ore body, these holes intercept at a variety of proposed mining levels (Figure 1, Attachment 1, GWQPE Appendix A5) which will produce 80% of the zinc ore to be mined. The drill holes appeared to be randomly placed. As reported in Erickson (1994) (Attachment 1, GWQPE Appendix A5), 100 drill holes were used to define the zinc mineralization; 71 of these holes defined the massive ore zinc zone which the eleven holes of the 1993 program retested. The eleven drill holes were divided into 625 assay intervals, of which 209 were used to make the 1994 Master Zinc Composite used for metallurgical testing. Of the eleven initial drill holes only nine contained ore intercepts. Ten drill holes were actually used to make the 1994 Master Zinc Composite. A non-ore intercept hole was used to add dilution grade material. The average zinc mill head grade of 9.4% zinc was generated by combining weighted averages of appropriate portions of the intervals in the massive zinc zone. To assure variability, some intervals with high arsenopyrite and talc were added to the composite. To maintain the proposed mill head of 9.4%, some higher grade zinc zones were randomly removed from intervals used to make the composite and associated wall rock was added to evaluate ore dilution effects.

I.A.3.1.2 Sample Preparation

Selected assay intervals to be used for the composites were sawed in half. Half of the material was then randomly selected and placed into bags, which were subsequently shipped to Lakefield Research. This material was then combined, crushed and ground to develop the metallurgical test feed material. Upon metallurgical test removal of up to 92% of the ore minerals of sphalerite, chalcopyrite, galena, and tetrahedrite, a coarse and fine tails product was generated. The two sized tailings products were generated as a result of optimizing ore mineral recovery. Initial waste characterization testing was then completed on both the coarse and fine tails. A whole tails product was generated by proportionally adding together coarse and fine tails.

The selection of drill core intervals, bagging and shipment to Lakefield was verified by WNDR personnel (Markart, 1995). Standard practices and procedures were used. Compositing, crushing or grinding of the massive zinc metallurgical sample at Lakefield was not witnessed by WDNR staff. The last stages of the metallurgical test, the preparation of tailings material for back shipment to Foth and Van Dyke, and the re-compositing of the coarse and fine tails to make whole tailings was witnessed by WDNR personnel (Markart, 1995).

Based upon observations by WDNR personnel, the 1994 metallurgical sample, was prepared using standard procedures of the mining industry to get a representative sample of ore and subsequent tailings material. NMC reported that randomly selected higher-grade zones were not incorporated into this sample because a head grade of 9.4% zinc was required. The composite was diluted with lower zinc grade intercepts. As a result, this composite sample may not have been representative for issues of variability with regard to waste characterization. However, due

to the need to prepare a sample with the anticipated head grade for the mine/mill, no other approach was viable outside of running a series of metallurgical tests using variable head grades.

I.A.3.2 1998 Master Zinc Composite

A 1998 Master Zinc Composite was generated by compositing a subset of the sample used to develop the 1994 metallurgical sample. The 1998 composite was used as feed material to generate a metallurgical test for ore recovery and a subsequent tailings product. The tailings product underwent additional metallurgical testing to generate a depyritized tailings sample containing 0.31% sulfur and two pyrite tailings of 31% and 47% sulfur, respectively.

The 1998 sample consisted of a subset of drill core intervals used in the 1994 sample. The 1994 sample used one-half of the core from designated intervals. From selected intervals, the remaining half was halved (quartered) for the 1998 composite. Fifty (50) assay sample intervals were used from nine drill holes, but over 50% of the sample came from three drill holes, DDH 264, 268 and 263 (Attachment 2, GWQPE Appendix A5). These intervals were mostly situated around the shaft area.

The 1994 vs. 1998 composites compared as follows: 12% vs. 4% were hanging wall dilution samples; 10% vs. 1% were footwall dilution samples; 7% vs. 4% were talc zone samples; 15% vs. 8% were weathered zone samples; and 1% vs. 0% were high arsenopyrite samples.

A comparison of the assay data for the 1994 vs. 1998 composite samples were:

	Zn%	Cu%	Pb%	As%	S%	Fe%	Al%
1994	9.66	0.33	1.12	0.27	29.2	23.2	2.01
1998*	9.30	0.33	0.89	0.25	31.9	25.6	1.28

*average of sample and duplicate

Chemically, there appears to be a good similarity between the 1994 and 1998 samples, considering that the 1994 sample encompassed a greater variety of intervals and included more footwall and hanging wall material while the 1998 sample consisted mostly of massive zinc ore. This can particularly be seen in comparing the sulfur and iron analyses. The comparison implies that the 1998 sample may have had more pyrite associated with it, while the amount of sphalerite was nearly the same.

Collection of the 1998 samples, compositing, and bagging was not witnessed or verified by WDNR personnel (Markart, 1998a). At the time the selection of material seemed appropriate and used similar procedures as the 1994 Master Composite. The 1998 metallurgical work at Lakefield also was not witnessed, but charging of the depyritized tails humidity cells at Foth and Van Dyke was observed (Markart, 1998b).

I.A.3.3 1999 Copper Stringer Ore Composite

The 1999 Copper Stringer Ore Composite was generated to provide a sample for bulk chemical analyses and mineralogy to compare to the massive zinc ore characterization. Eighteen drill holes (part of the 1979 Copper Stringer Ore Study) were selected which penetrated the

geologically designated Crandon copper stringer zone (Attachment 4, GWQPE Appendix A5). Spatially, these holes were situated between the main shaft and the west edge of the ore body. Figure 1 of Attachment 4 (GWQPE Appendix A5) shows the locations of these holes in the longitudinal plane of the copper stringer zone. There is an even spatial distribution vertically and horizontally with no apparent bias.

A total of 91 sample intervals were used from the 18 drill holes. A selection process was used to generate the sample composite to develop a proposed mining grade of 1.7-1.8% Cu. To ensure variability, individual intervals were selected to represent thin edges, thick central portions and weathered zones of the copper stringer zone. The intervals selected were spatially located throughout the copper stringer zone.

Selection of drill holes and intervals was observed by WDNR personnel (Markart, 1999a). Geologic cross sections, geologic logs and assay logs were used. Samples from selected intervals were collected, provided sufficient material was available. Core was not used, but rather crushed reject split samples stored in bags. This material was randomly inspected by WDNR personnel for any signs of oxidation of sulfides. Only minor tarnish of chalcopyrites was noted. If the reject bag sample contained sufficient material it was resplit (quartered of the original interval). A total of about 300 lbs. of material was generated, rebagged and shipped to Lakefield Research.

From March 8-10, 1999, WDNR personnel were present at Lakefield Research to witness portions of the mineralogical studies (Markart, 1999b). Prior to arrival, Lakefield Research composited the material and took appropriate splits to generate a sample for bulk chemical analysis and mineralogical work. This split was crushed to –10 mesh and was used to prepare individual samples for study.

I.A.4 Sample Representativeness

I.A.4.1 Massive Zinc Ore Composites

There are two sample representativeness issues for the massive zinc ore composites. First, the metallurgical sample collected must be representative of the Crandon ore body to be mined because it is the source of waste material. Second, the tailings sample must be representative of the metallurgical process which removed the ore minerals from the gangue minerals during the milling process.

I.A.4.1.1 Metallurgical Composite Samples

For the 1994 and 1998 metallurgical composites, the drill holes used to generate the samples were from the primary area to be mined for the massive zinc ore. There appeared to be a randomly selected set of assay intervals from these ore zone intervals that was used to generate the metallurgical composite with the proposed mill head grade of 9.4% zinc. Essential to this approach is the assumption that this randomness would develop a variety of material that would include all ore mineral habits, sizes and grades. For NMC this is a critical issue, because the design of the Crandon mill is based upon this composite.

The size of the 1994 composite sample was restricted by the use of drill core as the only source material. HQ and NQ core were used which represents core diameters of 137 mm (3.9 in) and 78 mm (3.1 in), respectively. The approximate weight of the 1994 composite was 675 kg (1500 lb), which was intended to represent the 30.5 million Mg (30 million ton) massive zinc zone of the ore body. The dimensions of the massive zinc zone are 1300 m x 670 m (4260 ft x 2200 ft) by an average 30 m (100 ft) thickness. The choice by NMC/CMC to use core samples to acquire their metallurgical sample rather than developing a prospecting site has limited the size of the composite sample and resultant amount of tailings available for waste characterization work. However, the issue of representativeness is not one of size, but of encompassing all variability in the ore body. By the selection and placement of drill holes in 80% of the proposed delineated area to be mined (between the east and west ventilation shafts), NMC has tested a reasonable spatial representation of the ore body. By randomly selecting a variety of samples from assayed intervals to generate the massive zinc composite sample at the proposed mining grade of 9.4% zinc using a variety of zinc (0.05% to 31.10% Zn) and copper (0.05% to 3.76% Cu) assay results, NMC has attempted to test a variety of ore grades and types within the deposit. This variety included weathered ores, hanging and footwall zones, high talc zones, and high arsenopyrite zones. However, by the nature of this process, changes in the relative proportions of the various ore types within the zinc zone were not tested. This is an acceptable mine development practice for the general design of the mill. The variation of ore grade, mineral size, and mineral composition will be handled through ore blending and adjustment as the mill operates to optimize recovery. The adjustment to variations in the ore would be to modify milling procedures to account for recovery of ore minerals and not to account for gangue minerals. These variations in the gangue minerals due to changes in the proportion of different ore types would carry through the mill and would report to the tailings.

The 1998 metallurgical sample was a subset of the 1994 composite sample. This sample was specifically collected to test the metallurgy for removal of pyrite from the tailings material. The sample used quartered intervals from the same spatially distributed drill holes for the massive zinc zone, but used one-third of the sample intervals of the 1994 composite sample intervals. The selection of the 1998 intervals was random, but aimed at producing a similar zinc head grade as the 1994 composite. The size of the sample was 306 lbs., about 1/5 of the 1994 composite sample.

In Tables 2 and 5 of GWQPE Appendix A5, the 1994 zinc ore master composite bulk chemistry is compared to the 1998 zinc ore master composite. This can also be seen in the comparison of the heads analysis in Table A of the next section. Overall, there is a reasonable similarity. The values for zinc, sulfur, iron and copper are comparable, but the 1994 composite has higher chromium, lead and nickel. The substantially higher aluminum, magnesium and sodium concentrations in the 1994 composite versus the 1998 composite could be attributed to the presence of more mica in the 1994 composite resulting from the inclusion of more hanging wall and footwall dilution material. The reason for the higher chromium and nickel values in the 1994 composite is unknown, though it is possible that they may be more associated with gangue minerals than ore minerals. The trace elements arsenic, mercury and silver are similar for both composites. These elements could be directly associated with the presence of galena or tetrahedrite. Cadmium occurs as a substitution for zinc in the sphalerite structure and is directly

related to the amount of sphalerite present. Selenium, which is lower in the 1994 composite than the 1998 composite by a factor of two, is probably associated with the sulfide phases and may be directly proportional to the amount of sulfide present as a metal selenide substitute for a metal sulfide.

When calcium is compared between the 1994 and 1998 composites, they are similar when the average of the 1998 sample and duplicate are used. There was no explanation given for the 25% difference in calcium between the 1998 sample and its duplicate by NMC. Total carbon is similar between the 1994 and 1998 composites, varying by 13%. If total carbon is directly proportional to the carbonate content, then the 1994 composite may have had slightly more carbonate minerals associated with it than the 1998 composite.

NMC evaluated the bulk chemistry of the 1994 and 1998 composites, which are based upon the 1993 drill core, with earlier metallurgical sampling conducted by Exxon in 1978. Table 2 of GWQPE Appendix A5 shows this comparison. OMC-1 and MMC-2 composites of 1978 were taken from drill hole intercepts that tested the Crandon ore body predominantly east of the main shaft. A majority of the 1978 holes are located in the proposed ore blocks containing the 30 million tons (2.72 million Mg) of zinc ore proposed to be mined in the original Mine Permit Application (Foth and Van Dyke, 1995a). The 1978 samples tested similar zones of the Crandon ore body as the 1994 drilling and offer a means to evaluate the representativeness of the 1994 and 1998 composites.

MMC-2 represents the largest set of sampled intervals. It consisted of 21 drill holes with 1890 feet of sampled intervals throughout the Crandon ore body. The 1994 master composite set consisted of 11 drill holes with 906 feet of sampled intervals, chiefly from the central portion of the ore body. MMC-2 incorporated a larger variation by including more higher grade massive zinc ore intercepts that may be encountered when the Crandon ore body is mined. The MMC-2 composite contained about 1% less zinc, but slightly higher sulfur, copper and iron values. MMC-2 had higher trace element antimony and selenium values, but lower cadmium, chromium, lead and nickel values. The amount of aluminum was the same, but sodium was less. These differences indicate that the MMC-2 composite probably included lower grade ores with the similar compositional changes in associated gangue minerals. The lead and arsenic (galena, tetrahedrite) indicate the preference of these elements for the thicker, more massive portions of the massive zinc ore body. MMC-2 composite is comparable to the 1994 master composite.

I.A.4.1.2 Tailings Sample

Table 11 of GWQPE Appendix A5 compares tailings bulk chemistry for the 1981, 1994 and 1998 tailings material generated from the metallurgical testing. In the revised Mine Permit Application, (Foth and Van Dyke, 1998d) waste characterization work is based upon the 1994 and 1998 tailings material. A comparison of these two tailings products to the 1981 product is difficult because not only was different head material used but there also may have been different metallurgical processes used. NMC staff believes that the 1994 and 1998 tailings were generated using the same metallurgical testing procedures (e.g., grind, flotation; B. Arthur, personal communication, July 11, 2000). The only difference was that an additional step in 1998 was instituted to depyritize the whole tails. Therefore, the only chemical difference between the

1994 and 1998 tailings samples was due to the head material used. The whole tails for the 1994 sample actually had two components, coarse and fine tails as a result of the metallurgical testing. These were kept as separate tailings products. The ratios of coarse to fine tails was 60/40. The 1998 tails were not segregated based on size. For an estimate of the bulk chemistry for the 1994 tails, a proportional combination of the results of coarse and fine tails on a 60/40 basis would be necessary.

In general, comparing the 1994 tails to the 1998 tails indicates a degree of similarity. The 1994 whole tails had slightly higher aluminum, arsenic, calcium, carbon, magnesium, and phosphorus values than the 1998 tails. Lower concentrations of chromium, copper, iron, lead, potassium, selenium, sodium, and zinc were present in the 1994 tails. Elements with greater than 20% difference were Ca, C (Total), Cr, Cu, K, Mg, and Se. The above differences in composition should represent differences in head materials used in the 1994 versus 1998 ore composites. In particular, the increased amount of wall rock used as a dilution factor in the 1994 composite may have contributed significantly to this difference.

Table I.A.1 is a comparison of the 1994 and 1998 heads and tails chemical analyses. These data are taken from Tables 2 and 11 of GWQPE Appendix A5. In general, both ore composites reacted similarly to the metallurgical testing. Cadmium, copper, lead, mercury, silver, sodium, sulfur and zinc values decreased indicating that these elements are reporting to the ore concentrate. In contrast, calcium, carbon (total), iron, magnesium and selenium are reporting to the tails. The trace elements antimony, arsenic and cobalt show a slight affinity for the tailings. Considering that the 1998 composite is a smaller subset of the 1994 composite, there is a relatively good comparison for most constituents of the tailings product. This implies that the 1998 whole tailings sample appears to be representative of the 1994 composite which contained a greater variety of sample.

I.A.4.2 Copper Stringer Zone Material

NMC has not undertaken detailed waste characterization studies of the copper stringer ore. They have indicated they will defer these studies until later in the project, if it is permitted, when they can better access the copper stringer zone. For permitting, they have proposed a comparison to the massive zinc ore, suggesting that the copper stringer ore tailings would present a lesser case as a source term. Only comparative bulk chemical analysis and the mineralogical study of carbonate minerals was completed and presented.

I.A.4.2.1 Copper Stringer Ore Composite Sample

As reported by NMC, the 1999 Copper Stringer Ore Composite was prepared using existing bagged split reject assay material from drilling conducted during the initial Exxon mining proposal. The drill holes selected show good spatial distribution across the ore body and with depth (Figure 1, Attachment 4, GWQPE Appendix A5). They appear to have sampled most of the delineated copper stringer zone on an estimated 700 foot center basis both horizontally and vertically. This represents 18 of 100 drill holes which penetrated the copper stringer zone. Ninety-one (91) sample intervals were selected from this zone. Approximately 135 kg (300 lb) of sample were collected to generate an average grade of 1.7-1.8% Cu. This 300 pound sample

was intended to be representative of the proposed 25.5 million Mg (25 million ton) copper stringer zone which would be mined after the massive zinc zone. Copper assays varied in the 91 selected sample intervals from 0.04 to 7.9%.

The analysis prepared by NMC compares the 1999 Copper Stringer Ore Composite to the overall stringer composite of 1979 for bulk chemistry (Table 4, GWQPE Appendix A5). In addition, a number of subsets of the 1979 composite are reported and compared to the 1999 chemical data. Of these composites, only the master stringer composite (MSC-2) provides sufficient spatial distribution and chemical analyses to be useful for comparison to the 1999 composite. The 1979 stringer composite used a larger drill hole base, but has chemical analyses for only copper, zinc, lead, silver and sulfur. Master stringer composite (MSC-1) used only eight drill holes (Table 1, Attachment 3, GWQPE Appendix A5). The pilot plant stringer composite (STRPP) had no documentation to indicate which drill holes were used to generate this sample or the number of sample intervals used. This makes the STRPP composite tenuous to compare for representativeness; rather, it may offer a sample showing degree of variability.

A comparison of the 1979 master stringer composite No. 2 (MSC-2) to the 1999 copper stringer ore composite shows good correlation for the chemical data (Table 4, GWQPE Appendix 5). The MSC-2 sample used 17 drill holes versus 18 for the 1999 sample and its 247 intervals represent 385 m (1263 ft) of drill core versus 91 intervals from 139 m (456 ft) of drilling for the 1999 sample. The MSC-2 sample tested a larger population of intervals, but incorporated different cut-off grades. For this reason, the zinc, copper, lead and silver values are higher in the 1979 sample. With these higher ore values, cadmium, antimony, arsenic and mercury would also be higher. The amount of sulfur and associated selenium are the same, while calcium, iron, magnesium, potassium and sodium are lower in the 1979 versus 1999 sample. The reason for these differences between the two can mostly be attributed to differences in ore mineral head grades between the two composites. Only three drill holes (13, 54, and 25) are common to both sets.

The 1979 composite spatially tested more of the western and upper portions of the copper stringer zone versus the lower and eastern portions for the 1999 composite sample. Due to sample availability, the 1999 sample was restricted in the amount of commonality with the 1979 sample. In comparing the two, there is good correlation and the only differences may be attributable to potential variation within the copper stringer zone.

I.A.4.2.2 Copper Stringer Tailings

No copper stringer tailings were produced from the 1999 composite sample. NMC presented a chemical analysis of a depyritized stringer tails (Test 369P) in Table 12, a stringer pyrite concentrate (Test 369P) in Table 13, and a 1979 stringer ore zinc tails in Table 11 of GWQPE Appendix A5. Figure A5-1 of GWQPE Appendix A5 indicates that the 1979 depyritized tails and pyrite concentrate are from the 1979 stringer ore composite (MSC-3, Table 4, GWQPE Appendix A5). This is assumed to be the results of test 369P (Table 12 - Depyritized Tails and Table 13 - Pyrite Concentrate). Understanding what constituted the "1979 stringer ore "zinc" tailings" from GWQPE Appendix A5 (Table 11) and GWQPE Section 3.2 is difficult, except that the tailings product was from the zinc flotation circuit. If this is the case then no comparison

should be made from Table 11 of GWQPE Appendix A5 to any tailings product from the copper stringer tailings.

I.A.5 Variability in Tailings

I.A.5.1 Massive Zinc Tailings

An evaluation of the expected variability of the tailings is required by Section NR 182.08(2)(be), Wisconsin Administrative Code, to predict potential impacts to the environment during storage or disposal. The dilemma of generating only one ore composite containing most of the potential ore variation found in the ore body for purposes of designing a metallurgical process is that by its nature such a composite may not generate a tailings product which encompasses all the potential variability that may be encountered during the life of the mine.

The most logical approach to resolving this dilemma would be to look at the variations seen in tailings generated from other metallurgical testing of the ore body, for example the 1979 work. Of most concern is the evaluation of the acid/neutralizing potential and the potentially soluble trace element contents.

NMC did not undertake detailed waste characterization studies (e.g., humidity cell, etc.) on a variety of tailings products generated from different ore composites or metallurgical tests. Essentially all of the detailed waste characterization analyses are based upon the 1994 and 1998 metallurgical products derived from the 1994 master zinc ore composite. As was discussed earlier, a number of comparisons were made by NMC to the earlier metallurgical work by Exxon. If the assumption is made that all tailings samples were generated under similar metallurgical processes, then the chemical values from a comparison of the 1979, 1981, 1994 and 1998 (subset) bulk samples (Table 11, GWQPE Appendix A5) should provide an indication of the variability in the tailings that may occur when the massive zinc ore body is mined. This is because different subsets of drill holes from different parts of the massive zinc ore body were used to make the head composite for each sample.

In evaluating the data in Table 11 of GWQPE Appendix A5, no judgment can be made as to what represents the worst case scenario, but only what the potential variability might be. Furthermore, no estimate can be made for the quantities of tailings that may contain these different constituent concentrations. The final tailings variability will be related to two factors. The first factor will be the carry through of variability in mill head feed material resulting from mining different portions of the ore body and mixing those portions in different ratios. Some aspect of this variability can be seen in Table 2 of GWQPE Appendix A5. The variation seen in composites is directly related to the subset of sample intervals and the cutoff grade and dilution material used. There appears to be distinct variability in tailings material developed by using lower grade versus higher grade zinc zones. Second, the most significant factor that could affect variability in tailings will be the recovery factors in separating the ore minerals from the gangue minerals in the metallurgical processes. For the depyritized tailings, this includes the separation of pyrite from the massive zinc tailings product.

There appears to be some direct relationship of trace metals to particular mineral phases. These are cadmium with sphalerite; lead, arsenic, antimony, silver and mercury with galena-tetrahedrite; selenium with all sulfides, particularly pyrite; and aluminum and sodium with mica minerals. The amount and variation of these trace metals in the tailings would likely be directly proportional to the amount of the original minerals that remained in the tailings. Therefore, for the trace elements associated with ore minerals, the variability of those elements in the tailings appears directly related to the efficiency of the metallurgical processes.

The composition of other elements of interest showed some significant variability. The calcium and magnesium contents of the massive zinc tails were seen to vary by a factor of 3. Magnesium is associated with carbonate, but for the most part, magnesium content is directly proportional to the amount of mica minerals present. Total carbon content varied by a factor of 4 and sulfur content varied by a factor of 5. While calcium, magnesium, sulfur and carbon do not indicate the actual variation in any particular acidifying or neutralizing mineral phase, they do indicate that carbonates which carry through the metallurgical, and possibly the depyritization, processes will vary based upon the variability of the ores mined and milled. The variation of sulfide is also directly related to the metallurgical processes and depyritization processes.

I.A.5.2 Copper Stringer Ore

The potential variability of the elemental components of the copper stringer ore can be seen in Table 4 of GWQPE Appendix A5. Each composite represents a subset of drill holes which intersect the copper stringer zone. As discussed previously, MSC-2 and the 1999 stringer ore composite are similar and appear representative of the ore body. However, these two subsets tested different areas of the copper stringer zone. Elements that appear to have varied the most are arsenic, calcium, iron, magnesium, mercury, potassium and zinc. These variations are most likely due to the selection of different ore cutoff grades as reported by NMC. However, arsenic has a greater variation than lead and is possibly associated more with variability in arsenopyrite content in the copper ore than its association with lead ore minerals. Similarly, while aluminum does not seem to vary, the calcium and magnesium contents do vary significantly. Possibly this variability reflects a wider variation in calcium-magnesium carbonate content than the association of these elements with the micas. The selenium content variability is low and follows the trend in the zinc ore by being directly proportional to the pyrite content.

I.A.5.3 Massive Zinc Ore Compared To Copper Stringer Ore

NMC has proposed to defer waste characterization studies of the copper stringer ore until operation of the mine allows access to those materials. The copper stringer zone would likely be mined after the massive zinc zone. Though not mentioned by NMC, alterations to the mill circuit may potentially be required to handle the copper stringer ore. This could affect the nature of the tails produced.

NMC has compared the 1999 copper stringer composite to the 1994 and 1998 massive zinc ore composite and proposed that the massive zinc ore represents a worst-case scenario. They argue that the copper stringer ore will have lower sulfide and trace metal contents and that the resultant

copper stringer tailings should pose less of an environmental threat than the massive zinc ore tailings. Table 5 of GWQPE Appendix A5 certainly indicates that trace metal constituents of concern are lower in the copper stringer zone than the massive zinc zone, when bulk chemistries are compared.

In considering the variability of the copper stringer ores, the potential variability recognized is less than that seen in the massive zinc ore composites, except for aluminum, cobalt, copper, magnesium, manganese, and selenium (see previous discussion; Table 4, GWQPE Appendix A5). As previously discussed, aluminum is mostly associated with micas. Magnesium is associated with both the micas and carbonates. Cobalt would be associated with the ore concentrate minerals. The selenium, being associated with pyrite, would probably report to the pyrite concentrate. Manganese, as noted from the mineralogical studies, probably would largely report with the carbonates.

The variations in chromium are more likely to be associated with the primary ferro-magnesian silicates or subsequent alteration products (e.g., diopsides, chlorites, etc.). If this is the case, then any variable amounts of chromium would report to the tailings and possibly the depyritized tailings product.

Considering the above, the only trace metal component which would not be worst-case represented by the massive zinc ore is selenium. The association of selenium with the pyrite remains valid, but the possibility of increased concentrations of selenium in the pyrites of the copper stringer ore is distinctly possible. The repercussions of this could be increased selenium values in the pyritic concentrates which would report to the backfilled mine.

I.A.5.4 Carbonate Speciation

To address the issue of tailings neutrality, NMC undertook geochemical analyses of the carbonate minerals. The carbonate mineral analyses were conducted on both ore composites and tailings material for the massive zinc ore. For the copper ore, carbonate mineral analyses were only conducted on the copper stringer ore composite. NMC reported in Sec. 2.3.3 of GWQPE Appendix A5 that geochemical analysis of the carbonates showed, "…the zinc ore has a higher proportion of ferroan dolomite/calcite and….less siderite." Intuitively this makes sense, because in the syngenetic deposition of the volcanogenic massive sulfide, iron would preferentially occur with sulfide in the more massive sulfide zone (massive zinc). In the depleted sulfur zones (copper stringer ore), excess iron would incorporate with carbonates and the ferro-magnesian minerals.

A customary geologic principle states that what is commonly seen on a large scale can usually be found at a lesser scale. In the case of carbonates, the gross distinction noted between the massive zinc and copper stringer zones, may be present on a smaller scale within each portion of the ore body. In particular, as carbonates become more distant laterally or stratigraphically from more sulfide-rich zones, their compositions may become more iron rich. Similarly, as was reported, the metallurgical process will concentrate more iron rich carbonates with the pyrite concentrate because the metallurgical collector works on the iron of either the sulfide or carbonates when separating them from less iron-rich minerals.

NMC has determined the variety of carbonate species and relative proportions in the massive zinc and copper stringer composites. Since the composites appear to be representative of the ore body, the range of carbonate compositions is known (Table 8, Attachment 4, GWQPE Appendix A5, EIR Appendix 4.2-16b). The issue then becomes one of distribution of the amounts of carbonate species, given the assumption that iron and manganese carbonates offer no net neutralization capacity to the tailings. That leaves the Ca-Mg carbonates, primarily ferroan dolomite, to handle the neutralization demand. In assessing the bulk chemical analyses and recognized mineralogy of the ore composite and tailings material, magnesium is found both in carbonates and the pervasive micas. Calcium is found dominantly in ferroan dolomite and calcite. Therefore, elemental calcium in the various ore composites would likely be most indicative of carbonates that would neutralize acid because calcium would only be associated with the neutralizing dolomite carbonate structure. If this correlation is demonstrated to be consistent, then NMC has unknowingly developed some data on Ca-Mg carbonate variability. As observed from Table 4 of GWQPE Appendix A5, the elemental calcium content was seen to range from 572 to 2000 ppm - a variation of a factor of 4 in the copper stringer ore. In Table 2 of GWQPE Appendix A5, the calcium value varies between 500 and 5100 ppm, or a factor of 10, in the massive zinc ore.

Since the dominant carbonate phase is ferroan dolomite (Table 8, GWQPE Appendix A5) the best guess for the degree of variability of this carbonate phase should be on the order of 10x for the massive zinc ores and 4x for the copper stringer ores. This seems to be substantiated by the discussion in Section 5 of GWQPE Appendix A5, when analysis of a number of single core section samples revealed variations in the distribution of carbonate species from 0 to 10% for the massive zinc ore. This is also recognized in Table 2 of Attachment 7 of GWQPE Appendix A5, where NMC reports the results of electron microprobe analyses to determine carbonate species variability in the massive zinc ore. In Table 2, the estimated carbonate content varied between nil and 10%. The location of those samples was restricted by availability of material. In evaluating the samples used, all drill holes were in the vicinity of the main shaft to the east ventilation shaft. The ore intercept intervals evaluated spanned stratigraphically across the massive zinc ore zone. While the spatial extent was restricted, the stratigraphic extent was not. Because the zinc mineralization occurred in phases, the poor lateral extent of the sample appears to have been compensated by better stratigraphic extent to develop good representativeness for this small sample population used to determine carbonate variability.

The amount and degree of carbonate variability can only be ascertained with confidence during mining. Recognizing the degrees of variability, the neutralization potential that the Ca-Mg carbonates offer might best be judged by the amount of calcium present in the ores rather than total carbon values which consider both ferroan dolomite and siderite. If this is the case, then actual carbonate neutralization variability for the massive zinc zone could vary by a factor of 10 (Table 2, GWQPE Appendix A5). Carried through to the tailings, a variation of a factor of 3 could be expected because of ore blending (Table 11, GWQPE Appendix A5). This implies that the mining and metallurgical process may reduce variations in Ca-Mg carbonate neutralizing potential by about a factor of 3.

I.A.6 Implications

The following conclusions are reached based on the assessment of representativeness that was conducted:

1. Waste rock composite samples used in the waste rock characterization evaluation are representative of the types of waste rock that would be encountered by the proposed mine for the massive ore zone and hanging wall. However, no waste characterization was conducted on the footwall rocks. All waste rock composite samples were collected from drill core. The location of the drill core holes and their selected intervals are correlatable to the locations where proposed mine workings would occur.

2. Variability of carbonate and sulfide minerals in waste rock are stratigraphically-dependent and increase as the Crandon Formation is approached. Carbonate mineral content appears more variable than sulfide mineral content.

3. Review of drill hole locations and sample intervals used for the 1994 and 1998 massive zinc composites for waste characterization studies indicate a representative portion of the massive zinc ore body was sampled. The selection of drill holes and sample intervals was made in an unbiased manner. Sampling and compositing procedures followed accepted mining-exploration industry practices for evaluating an ore body.

4. The 1994 and 1998 massive zinc composites were specifically designed to encompass variabilities in zinc ore and zinc ore grades for metallurgical testing to determine ore mineral recoveries. The 1994 and 1998 massive zinc composites were not designed to encompass variabilities of the gangue minerals (tailings), including variations in carbonate content and carbonate species.

5. Review of drill hole locations and sample intervals used for the 1999 copper stringer zone composite indicate a representative sample has been collected. The sample was collected in an unbiased manner following standard mining-exploration industry practices. Waste characterization studies were not conducted on the copper stringer ore.

6. The 1994 and 1998 tailings samples used for waste characterization studies of the massive zinc zone are representative of the tailing materials which would be generated by the current (1998) proposed metallurgical processes.

7. Comparison of the copper stringer ore composite to the massive zinc ore composite indicates potential tailings from the copper stringer ore would have a lower sulfide and trace metals content than massive zinc tailings. However, the pyrite concentrate generated from the copper stringer ore could have higher selenium values than pyrite concentrate of the massive zinc tails.

8. Trace metal variability can be recognized in the massive zinc ore and between the massive zinc ore and the copper stringer ore by evaluating the different ore composite samples generated through the course of the different economic and waste characterization studies of

the Exxon and CMC/NMC mine proposals. Different ore composites tested different portions of the ore body by using different drill holes and core intervals. By applying different cut-off grades, more variable ore types were generated.

9. Variability in metals and trace metals in the tailings are dependent upon original variations in the ore. The efficiency of recovery of ore grade minerals by metallurgical processes and depyritization processes would affect variability in tailings products. Original variations in nonferrous gangue minerals would carry through to tailings products regardless of the metallurgical processes.

10. The 1994 and 1998 tailings, depyritized tailings and pyrite concentrate are representative of the material which would report either to the tailings management area or the pyritic paste backfill. Variations of these materials can be ascertained by evaluating previous tailings products which used different ore composites and metallurgical processes.

11. Metals variability in the tailings material would be controlled by the efficiency of recovery of ore minerals. Most trace metals are associated with the ore minerals sphalerite, galena, chalcopyrite, and tetrahedrite. Arsenopyrite would split between ore concentrate and pyritic tailings. The elements antimony, cobalt, mercury and silver with some arsenic would follow the galena-tetrahedrite minerals. Cadmium would follow the sphalerite. Therefore, the varieties and concentration of these metals in the tailings would be more dependent upon the recovery rates of the ore minerals than on the variation expected in the ore body itself.

    Selenium appears to be associated with the pyrite. The variability of selenium in the depyritized tailings is dependent upon the efficiency of separation of pyrite in the depyritization process. The variability of selenium in the pyritic tails would be directly related to the original variation in the ore body.

12. The variation of the neutralizing carbonate minerals (Ca-Mg carbonate) in the depyritized tailings would be directly proportional to any variation encountered in the ore body. This essentially is the spatial variation of the ferroan dolomite in the ores to be mined. The range of variation could be by a factor of 10. This variation and the actual amounts of material with different compositions would only be recognized by detailed ore delineation drilling and chemical evaluation when the ore is mined. By ore blending and metallurgical process, the Ca-Mg carbonate content variability could be reduced to a factor of 3 in the tailings.

13. Elemental calcium content (only found in carbonates) of the ore is proposed as a better guide for assessing the expected neutralizing ability of the carbonates in tailings rather than the total carbon content.

I.B DEPYRITIZED TAILINGS

I.B.1 Methods for Depyritized Tailings Tests

I.B.1.1 Physical and Mineralogical Tests

Particle size analysis of the depyritized tailings was "done in accordance with ASTM procedures" by Steffen Robertson and Kirsten (1998e). A subsequent communication indicated that the procedure used was ASTM D-421 (NMC, 2000d).

Solid-phase chemical analyses were conducted by Lakefield Research Limited in Lakefield, Ontario, Canada. The laboratory is "certified by the Standards Council of Canada, the Canadian Association of Environmental Analytical Laboratories, and has been accredited at the ISO/IEC Guide 25 level for various inorganic and organic parameters" (NMC, 2000d). The methods are presented in Table 2.3 of GWQPE Appendix A1 (Steffen Robertson and Kirsten, 1998f), with additional details provided in NMC (2000d).

I.B.1.2 Static Tests

Methods for the static tests (acid-base accounting) are presented in GWQPE Appendix A1 (Steffen Robertson and Kirsten, 1998f), with details in Attachment B of that document. Duplicate samples were used for all determinations. The potential for acid production of duplicate samples was calculated based on total sulfur content, which was determined by LECO furnace. Sulfide and sulfate contents were also determined. The method of neutralization potential (NP) determination is unclear. In GWQPE Appendix A1, the method is referred to as both the Sobek and modified-Sobek technique, although no citation was provided for the latter method. Neutralization potential was also determined based on carbonate content. The carbonate content was determined by LECO furnace.

Lakefield Research Limited Mineralogical Services of Lakefield, Ontario conducted the following analyses. Mineralogical examinations were conducted on the depyritized tailings using binocular microscopy, X-ray diffraction (XRD), reflected and transmitted light microscopy, and scanning electron microscopy coupled with energy dispersion x-ray analysis (SEM-EDS). Standardless semi-quantitative (SSQ) analyses of carbonate grains were conducted. The methods used are described in Attachment A of GWQPE Appendix A1. In addition, CANMET Laboratories quantitatively analyzed the chemistry of carbonate using an electron microprobe. These analyses are described in GWQPE Appendix A4 (Steffen Robertson and Kirsten, 1999a).

Three different leach extractions were performed on the depyritized tailings as described in GWQPE Appendix A1 (Steffen Robertson and Kirsten, 1998f). The objective of these extractions was to determine the composition of iron oxyhydroxides. A dithionate extraction (Fuller et al., 1996) was intended to leach weakly crystalline iron oxyhydroxides using a moderate reductant at pH 8.5. Hydrochloric acid was intended to leach weakly crystalline iron oxyhydroxides and siderite at pH 3.5 to 4.0. A hydroxylamine hydrochloride extraction (Ribet et

al., 1995) was conducted with a strong reductant at pH 4.3 for 24 hours at 90 ^{o}C to leach high levels of crystalline ferric hydroxides and trace metal sulfides containing ferric iron.

Net acid generation (NAG) tests were conducted as described in GWQPE Appendix A1. The objectives of these tests were to (i) obtain an initial indication of whether and how much alkalinity is required to ensure the depyritized tailings would remain neutral and (ii) indicate a target NP:AP ratio for maintaining neutral conditions in the TMA. Six different mixtures of depyritized tailings, pyritic tailings, and limestone were subjected in duplicate to testing, as well as a control containing limestone alone and a blank containing only the hydrogen peroxide solution (Table 2.6, GWQPE Appendix A1). The target CO_3 NP:AP ratios ranged from 1.16 to 6.02. For each test, 2.5 g of sample was reacted with 125 mL of 35% peroxide solution for 96 hours, at which time the solution pH was recorded. The solution was filtered through a 0.45 Φm filter, heated to 100 degrees Centigrade, and deionized water was added to return the volume to 125 mL. The resulting solution was analyzed for pH, acidity, and alkalinity. The solid residues, along with a sample of each of the starting materials, were submitted to Lakefield Research. For each duplicate pair of residues, one was analyzed for total sulfur, sulfate sulfur, and carbonate content. The second residue from each pair was examined using optical microscopy.

Multiple step batch tests were conducted as described in Section 2.3.7 of GWQPE Appendix A1. Two multiple batch tests, each run in duplicate, were conducted on the depyritized tailings. In the first pair of tests, 10 g of depyritized tailings was subjected to six 1.14-L volumes of leachate at pH 4 and 50 mg L^{-1} ferrous iron. In the second tests the tailings mass was 50 g and the leachate volume, pH, and ferrous iron concentrations were 0.99 L, 4.1, and 300 mg L^{-1}, respectively. One test was conducted on a mixture of limestone and depyritized tailings, and the conditions are described in Table 2.7 of GWQPE Appendix A1 (in addition, two tests were conducted on the pyritic paste backfill and one on pyrite concentrate). The procedure was described as follows (pp. 4.2-15-17–19 of GWQPE Appendix A1):

> "The exact amount of solids was weighed out and placed in a 2-L narrow mouth vessel. Two holes were augured through the stopper through which glass tubes were inserted. The first was short and only passed through the stopper so that the end within the vessel was not in contact with the solution and was used to control the atmosphere inside the vessel with argon. The second tube was longer and extended to the bottom of the vessel and was used to extract samples, or replace solution as required.
>
> Once the sample was placed in the vessel and the atmosphere had been displaced with argon gas, the de-aerated leachant was introduced into the vessel. The vessel was then sealed and placed on a shaking table to agitate the slurry.
>
> Every second day, the vessel was removed from the shaker, and the solids were allowed to settle for a period of 4 - 6 hours. A small aliquot of sample was then extracted from the vessel while maintaining anoxic conditions. The sample pH, Eh, temperature, alkalinity/acidity and conductivity were obtained, and a total iron analysis was completed. Each stage of the tests was continued for a minimum period of 10 days. At the end of each stage, taking care not to extract

> solids, the leachate was extracted by vacuum. The extracted leachate was sampled and preserved as required for analysis. The leachate was replaced with fresh leachant by pumping the fresh leachant back into the system. This process was repeated until all six stages of the tests had been completed."

The addition of acidity was calculated to be adequate to dissolve all available neutralization potential during the six stages. The NP (Sobek) and CO_3 NP of the residues were determined and the residues were subjected to analysis by optical microscopy and SEM-EDS. The extent of neutralizing minerals reacted during the six leaching stages was calculated by (i) comparison of the unleached tailings and the residues using both Sobek NP and CO_3-NP measurements, (ii) based on neutralization of solution acidity during the six (and in some cases five) leaching stages, and (iii) based on the release of calcium and magnesium during the six (and in some cases five) leaching stages (GWQPE Appendix A1).

I.B.1.3 Kinetic Tests

Humidity cell tests were conducted as described in GWQPE Appendix A1 with additional information in Steffen Robertson and Kirsten (1998b, 1998c). Six humidity cells, each containing 200 g depyritized tailings, were run. The inside diameter of the cylindrical cells was approximately three inches and the height was three to four inches. The tailings rested on a nylon filter placed on a perforated plate. An inlet tube, for introduction of humidified air, and an outlet tube were located approximately two inches above the base plate. WDNR personnel observed loading of the cells (Markart, 1998b). At the beginning of the test, samples were rinsed with 0.9 liters of distilled-deionized water (GWQPE Appendix A1). Duplicate cells were run for short term (600 mL/week rinse for 22 weeks), intermediate term (150 mL/week rinse for >90 weeks), and long term (150 mL/week rinse for >> 90 weeks). To enhance rinse water flow and water removal from the solids, vacuum was applied to the receiving vessel until flow ceased.

The drainage volume collected was determined and drainage was analyzed for pH, Eh, and conductivity. Samples were preserved according to protocols described in Table 6.1 of Foth and Van Dyke (1994). Samples initially were sent to Northern Lake Service, Crandon, WI (K. Markart, Wisconsin DNR, personal communication, 2003) and subsequently to EnChem, Inc., both of which are Wisconsin Certified Laboratories (NMC, 2000d). Parameters measured at the analytical laboratory were pH, alkalinity, acidity, sulfate, total sulfur, Cl, Al, Sb, As, Ba, Be, Cd, Ca, Cr, Co, Cu, F, Fe, Pb, Mg, Mn, Hg, low level Hg, Ni, K, Se, Ag, Na, and Zn. The methods of analysis, as well as the limits of detection and quantification (LOD and LOQ, respectively) are presented in Table 2.4 of GWQPE Appendix A1. The references for the numbered methods are presented in U.S. Environmental Protection Agency (1983), with numbers preceded by SM in Joint Editorial Board of the American Public Health Association, American Water works Association, and Water Pollution Control Federation (1992) (NMC, 2000d). Low level mercury determinations were performed by Battelle Marine Science (Sequim, WA) using the method published in U.S. Environmental Protection Agency (1999) (NMC, 2000d).

Between rinses, humid air was introduced into the cell. Upon termination of the short term tests, residues were dried under anoxic conditions and representative splits were submitted for determination of bulk chemistry and ABA, as well as mineralogical examination and leach

extraction testing. The methods used for these analyses were the same as those used to analyze the unleached depyritized tailings.

I.B.2 Results of Depyritized Tailings Tests

I.B.2.1 Physical and Mineralogical Characteristics

The depyritized tailings were 100% finer than 0.297 mm, with 52.6% finer than 0.0287 mm, 24.2% finer than 0.0119 mm, 11.7% finer than 0.0062 mm, and 2.2% finer than 1.3 μm. The specific gravity was reported as 2.81, and a hydraulic conductivity of 1.4 x 10^{-4} cm/s was reported for a dry density of 12.8 kN/m^3 (81.4 pcf). Hydraulic conductivities of 2.6 x 10^{-6} to 7.2 x 10^{-7} cm/s were reported for dry unit weights of 14.5 to 15.1 kN/m^3 (92.2 to 96.1 pcf) (Tables 1, 2, 4 of Steffen, Robertson and Kirsten, 1998e).

Mineralogical analyses of the depyritized tailings by optical microscope, XRD, and SEM-EDS are presented respectively in Tables 3.1, 3.2, and 3.3 of GWQPE Appendix A1. More refined analysis of the carbonate mineral chemistry was conducted using electron microprobe. The mineralogical composition of the depyritized tailings, as determine by reflected and transmitted light microscopy, is presented in Table 3.1 of GWQPE Appendix A1 and is discussed in greater detail in Attachment A of that document. The predominant mineral phase was reported as quartz (72 wt%), with lesser amounts of carbonates (17 wt%), muscovite/illite (6.9 wt%), and chlorite (3.4 wt%). Sulfide minerals, iron oxyhydroxides, and hematite are reported present in trace quantities (<0.2 wt%).

The description of the pyrite grains provided in Attachment A of GWQPE Appendix A1 is as follows (p. 4.2-15-73):

> "Pyrite grains were typically present as inclusions in, or attachment to silicates (primarily quartz). Minor liberated pyrite grains were noted up to 100 μm in length. Trace pyrite fines (<10 μm) were noted. The De-pyritized Tails contained minor mineral aggregates up to 400 μm in diameter composed of angular pyrite and lesser silicates up to 150 μm in diameter. A moderate proportion of the pyrite in this samples (sic) is hosted within these high-sulphide aggregates."

Subsequent electron microprobe analysis (Table 1 of Steffen, Robertson and Kirsten, 1999a) indicated the carbonate mineral phases consisted of 90% ferroan dolomite (50% Ca, 38% Mg, 9.6% Fe and 2.5% Mn), 8.5% magnesian siderite (0.36% Ca, 35% Mg, 60% Fe, 4.0% Mn), and 1.7% ferroan magnesite (0.048% Ca, 84% Mg, 14%Fe, 1.75% Mn). The aforementioned values indicate that 83.4 atomic percent of the carbonate is associated with calcium and magnesium, while 16.6 atomic percent is associated with iron and manganese. Using and average carbonate content of 5.38% (Table 3.4 of GWQPE Appendix A1) yields an NP[(Ca+Mg)CO_3] of 74.7 kg $CaCO_3$ eq/Mg.

The carbonate minerals were reported to be "present as liberated grains to 250 μm in length, but typically <100 μm, and intergrowths with silicates" (p. 4.2-15-73, Attachment A of GWQPE Appendix A1).

Abbreviated duplicate bulk chemistry results are summarized in Table 3.6 and detailed results are presented in Table C-1 of Attachment C of GWQPE Appendix A1. The total sulfur content was reported as 0.755 percent (Table 2-3 of the GWQPE) and the sulfide content as 0.60 percent (Table C-1 of Attachment C of GWQPE Appendix A1). Trace metal contents exceeding 25 mg/kg were barium (85 mg/kg), copper (89 mg/kg), arsenic (100 mg/kg), lead (600 mg/kg), and zinc (1250 mg/kg).

I.B.2.2 Static Tests

The acid-base accounting (ABA) results for duplicate samples indicate total sulfur contents of 0.82% and 0.75%, with an average of 0.78% (Table 2-4 of the GWQPE). The average yields an average AP(S_T) of 24.5 kg $CaCO_3$ eq/Mg. The NP values reported were determined both by the Modified Sobek method (as opposed to the Sobek method, as reported in Table 2-4 of the GWQPE) and assuming 100% of the carbonate was associated with calcium and magnesium.

For the Modified Sobek method, the fizz rating was reported as 2 and acid additions were 47.70 and 47.85 mL 0.1 N HCl. Solution pH values prior to titration for the duplicate samples were 1.51 and 1.50 and a titration endpoint pH of 8.3 was used (Table B-1 of Attachment B of GWQPE Appendix A1). This method yielded NPs of 76.1 and 74.4 kg $CaCO_3$ eq/Mg for the duplicate samples, with an average of 75.2 kg $CaCO_3$ eq/Mg. The average value based on the carbonate content of 5.38% (individual values of 5.37% and 5.38%) was 89.6 kg $CaCO_3$ eq/Mg (Table 2-4 of the GWQPE).

Results of the NAG-3A test, which was conducted on depyritized tailings with a total sulfur content of 0.71%, showed a Modified Sobek NP of 61 kg $CaCO_3$ eq/Mg, and a carbonate NP of 87 kg $CaCO_3$ eq/Mg (Table 3.13 of GWQPE Appendix A1). Following the test, the residue was characterized with a sulfur content of 0.04% and a carbonate NP of 56 kg $CaCO_3$ eq/Mg (Table 3.14 of GWQPE Appendix A1). This indicates changes in AP of 20.9 kg $CaCO_3$ eq/Mg and carbonate NP of 31 kg $CaCO_3$ eq/Mg. Mineralogical examination indicated that the pyrite present in the residue "consisted of minute inclusions in quartz (~65% dist.) up to 10 μm in diameter and as liberated grains (~35% dist.) up to 30 μm in diameter" (p. 4.2-15-88, Attachment A of GWQPE Appendix A1). This suggests that a sulfur content of 0.026% (0.65 x 0.04 = 0.026) is present as pyrite inclusions in quartz. This represents about 4% of the sulfur originally present in the sample. For the NAG-1A residue sample, it was noted that roughly "one third of the pyrite inclusions in quartz exhibited rimming by iron oxyhydroxides, indicating some permeability of solutions into the quartz grain, with resulting pyrite oxidation" (p. 4.2-15-88, Attachment A of GWQPE Appendix A1). Thus, the extent of sulfur occurring as pyrite inclusions in quartz is small, and even these inclusions were subject to oxidation in the NAG tests. Iron staining of carbonate minerals in the residues ranged from minor to intense, the intensity generally increasing with the sulfur content of the mixture. With the higher sulfur contents (NAG-51, NAG-6A), replacement of carbonates by iron oxyhydroxides (and possibly jarosite) was also reported (Attachment A of GWQPE Appendix A1).

Values of pH, Eh, acidity and total iron concentrations for various stages of the multiple step batch tests is presented in Table 3.10 of GWQPE Appendix A1. The reaction conditions in only one test (2A) remained reducing. Relative to the other three tests, Eh values for test 2A were lower (-265 to -172 mV vs. -146 to 24 mV) and iron concentrations were markedly higher (130 to 190 mg/L vs. less than 0.5 mg/L for the first five stages).

For the anoxic multiple step batch test (2A), the pH remained above 6.0 only during the first stage, with subsequent pHs ranging from 4.9 to 5.8. Comparative analyses of the initial solids and residues indicated a Sobek NP depletion of 32% and a CO_3-NP depletion of 43% (Table 3.11 of GWQPE Appendix A1). Calculations based on neutralization of solution acidity and the release of calcium and magnesium indicated approximate depletions of 35-50% for Sobek NP and 30-40% for CO_3-NP (summarized in Table I.B.1, with more detail in Table 3.12 of GWQPE Appendix A1). Calculations based on the sum of calcium and magnesium release yielded lower NP availabilities (29 and 35%).

For the three remaining multiple step batch tests (1A, 1B, 2B), reaction conditions were described as "anoxic to mildly oxidizing conditions" (p. 4.2-15-29, GWQPE Appendix A1). For these three tests, Eh ranged from -134 to 24 mV and the pH remained above 6.0, with iron concentrations less than 0.5 mg/L for four or five of the six stages. Comparison of the initial solids and residues indicated Sobek NP availabilities of 86% to 96% and CO_3 NP availabilities of 88% to 97% (Table 3.11 of GWQPE Appendix A1). The two methods based on the water quality (acidity consumption and the sum of calcium and magnesium release) were applied for all six stages and for the first five stages only (Table 3.12 of GWQPE Appendix A1). For all six stages the two methods of calculation indicated a Sobek NP availability of about 70-90% and a CO_3 NP availability of 60-75% (see Table I.B.1). The corresponding approximate ranges for the first five stages were 60-80% Sobek NP availability and 50-70% CO_3 NP availability. The pH was 5.8 in stage five for one of the tests (DPT-1B).

Residues from multiple step batch tests 1A, 2A, and 2B were subjected to mineralogical analysis (Attachment A of GWQPE Appendix A1). Sample 1B was not analyzed. The carbonate phase of the residues from tests 1A and 2B indicated dissolution of calcium and magnesium carbonates. In contrast, the carbonate mineralogy of the residue from test 1B was "typical of primary / unaltered De-Pyritized Crandon tailings" (p. 4.2-15-62, GWQPE Appendix A1). Minor amounts of iron sulfate minerals were reported in all three residues. Iron oxyhydroxide replacement of carbonate minerals ranged from "nil" for sample 1A to "trace" for sample 2A to "extensive" for sample 2B (p. 4.2-15-95, Attachment A of GWQPE Appendix A1).

I.B.2.2 Kinetic (Humidity Cell) Tests

Detailed results of the humidity cell tests are presented in GWQPE Appendix A3 (Steffen, Roberston and Kirsten, 1998d). Leachate volume, field pH, field Eh, and field conductivity were reported through November 17, 1999, in the update – the first 71 weeks ("field" measurements are those made on site after the humidity cell drainage was collected.) Sulfate analyses are reported through week 67 and other parameters through week 65 (lab pH (measured at the analytical laboratory), alkalinity, acidity, total sulfur, Cl, Al, Sb, As, Ba, Be, Cd, Ca, Cr, Co, Cu,

F, Fe, Pb, Mg, Mn, Hg, low level Hg, Ni, K, Se, Ag, Na, Zn). Detectable concentrations of Sb, As, Be, B, Cd, Cr, Co, Cu, Pb, Hg, Ni, Se, Ag and Zn were reported in at least one sample.

I.B.2.2.1 Drainage Quality Summary

Result of the short-term humidity cell tests are described in GWQPE Appendix A3. The results indicate that the drainage pH was near neutral and increased slightly over 22 cycles. Concentrations were elevated over the first 5 cycles due to the removal of reaction products generated prior to the inception of the test. Ion balances using sulfate concentrations were close to one while those using total sulfur concentrations averaged much greater than one (see Table I.B.2). Consequently, the sulfate concentrations were deemed a more accurate indicator of sulfide mineral oxidation. The sulfate concentrations reported for cycle 9 were inconsistent with field conductivity values and considered erroneous.

The molar ratio of the sum of calcium and magnesium concentrations to sulfate concentration generally exceeded one, leading to the conclusion that "carbonate dissolution occurs readily and exceeds acid production." Moreover, "the molar ratio of the net alkalinity consumed, (i.e., total alkalinity calculated from the (Ca + Mg) release less the free alkalinity), to the acidity produced (calculated from the sulfate release rate), averages 1:1 when obvious outliers are excluded" (p. 4.2-16-21, GWQPE Appendix A3).

The molar ratio of calcium to magnesium release rates during steady state (1.5:1, 1.4:1) approximates the ratio of calcium to magnesium in the dissolving carbonate phase. This indicates that calcium rich carbonates dissolved preferentially, since the ratio of calcium to magnesium in the carbonate minerals was 0.85:1. The dissolution of iron and manganese carbonates could not be traced in a similar manner due to their low solubility. That is, iron and manganese released from carbonate minerals would precipitate from solution and not be detected in the humidity cell drainage.

Initial concentrations from the intermediate and long-term humidity cell tests indicated that sulfate and some trace metals (including zinc and manganese) were elevated, as was the case in the short-term tests. Anomalously high metal concentrations were observed for the initial flush of test DPT-IT2. These concentrations were assumed to be erroneous based on the ion balance, as well as the marked difference from other cells. Concentrations decreased over time and stabilized, and the pH increased slightly after removal of sulfate salts that had accumulated prior to the test. Ratios of anions to cations were reported to vary substantially in the initial stages of the test and stabilize at values near unity in the later stages. In particular, ratios "based on sulfate tend to be slightly deficient in anions, while those based on total sulfur show an excess of anions" (p. 4.2-16-32, GWQPE Appendix A3).

The rate of sulfate release from the intermediate and long-term tests was close to that of the short-term tests during the steady state period through cycle 22, despite the difference in rinse volumes (600 mL/week for the short-term tests and 150 mL/wk for the intermediate and long-term tests) (GWQPE Appendix A3). Based on sulfate concentrations, the rate of sulfate release from the intermediate and long-term cells decreased after cycle 22. In contrast, calculations based on total sulfur release "do not show significant differences between the two periods",

leading to the conclusion that the "oxidation rate is considered to be constant" over the duration of the test (p. 4.2-16-33, GWQPE Appendix A3).

Whereas the rate of sulfate release was not affected by the rinse volume, alkalinity release in tests using the 600 mL rinse was roughly half that for the 150 mL weekly rinse used in the short-term tests (Table 3.8 of GWQPE Appendix A3). Thus, the conclusion was drawn that "loss of $(Ca+Mg)CO_3$-NP from the humidity cell cannot be extrapolated directly to field conditions" (p. 4.2-16-33, GWQPE Appendix A3).

I.B.2.2.2 Chemical and Mineralogical Analysis of Short Term Cell Residues

Bulk chemistry of the residues was not greatly different from the unleached depyritized tailings. In particular, there was little difference in the sulfur content (the reported sulfur content of the residue from cell ST2 was higher than that from the unleached sample). This finding was inconsistent with the sulfate release in the humidity cell tests; the residue analyses were "from a single subsample of the humidity cell residue, which is subject to sample variability and analytical error" (p. 4.2-16-26, GWQPE Appendix A3). The Sobek NP values for residues from the two cells were in close agreement, as were the CO_3-NP values.

Iron oxyhydroxides were the only secondary mineral phases detected in the humidity cell test residues. The lack of secondary mineral phases was attributed to the "low sulfide content and low oxidation rate" (p. 4.2-16-24, GWQPE Appendix A3). Optical microscopy indicated some iron staining on carbonates, noting that "carbonate grains consisted of both clear particles and particles with patchy, discontinuous iron-staining at rims, along fractures and cleavages (30%)" (p. 4.2-16-275, GWQPE Appendix A3). These effects were inferred to be due to precipitation of iron released as a result of sulfide mineral oxidation. Moreover, "10% of the pyrite was present as inclusions within quartz grains, suggesting the availability of pyrite to oxidation is reduced" (p. 4.2-16-25, GWQPE Appendix A3). Nonetheless, for determination of AP, pyrite was assumed to be 100% available.

I.B.2.2.3 Oxidation Rates

Oxidation rates reported for the humidity cell tests ranged from 5.6×10^{-10} to 30×10^{-10} mol O_2/kg-s and were calculated by two methods (GWQPE). Steady-state oxidation rates were calculated based on sulfate release for cycles 6-22 (short term cells) and for cycles 10-65 (intermediate and long-term cells). These periods were referred to as "steady-state periods" and excluded removal of reaction products generated by sample dissolution prior to the inception of the experiment. This removal contributed to initially elevated sulfate concentrations.

The aforementioned values were determined by dividing the total sulfate release over the steady state period by the duration of the steady state period. The oxygen consumption was calculated by multiplying sulfate release rates by 1.875, a value determined based on the stochiometry of the oxidation reaction. The oxidation rates determined based on sulfate release from the six depyritized tailings during the steady-state period ranged from 5.6×10^{-10} to 12×10^{-10} mol O_2/kg-s (see Table I.B.3). For cycles 6 through 22 of the two short term cells, oxidation rates were 9.9×10^{-10} and 12×10^{-10} mol O_2/kg-s. These rates were also determined for cycles 10

through 65 of the duplicate intermediate (5.6 x 10^{-10}, 7.6 x 10^{-10} mol O_2/kg-s) and long-term cells (7.0 x 10^{-10}, 6.2 x 10^{-10} mol O_2/kg-s) (Table 3.9, GWQPE Appendix A3). These total sulfate releases and rates are reproduced in Table I.B.3.

Changes in solid-phase sulfate content were also considered for rate calculations regarding the short term cells. Sulfate which was lost from or accumulated within the tailings was determined as the difference between that on the residue and that on the unleached samples. Hydroxylamine hydrochloride leach extractions were used to determine labile sulfate contents.

These rates were at the upper end of the reported range. The two values were 26.2 x 10^{-10} and 30.1 x 10^{-10} mol O_2/kg-s (see Table I.B.4). The leachate assays from the hydroxylamine extractions indicated the sulfate content of the tailings residuals (after the short-term tests) were very low, with reported values of 33 and 34 mg/kg. In contrast, the sulfate content of the unleached depyritized tailings was determined as 2155 mg/kg (Tables C1-2 and C1-3 of Attachment C of GWQPE Appendix A3).

I.B.2.2.4 Rates of Trace Metal Release

The objective of the leach extractions and associated calculations was to adjust the observed metal release to humidity cell drainages for components that were released from primary minerals and accumulated in iron oxyhydroxides. The accumulation (or depletion) of components was quantified by subtracting leach extraction values for the depyritized tailings from those for the humidity cell residues. The leach extraction results for a given component were used only if there was a calculated accumulation of the component in soluble solid phases (that is, only if the mass present in a phase increased, based on data from the leach extraction tests). Consequently, release rates only increased when the leach extraction data were considered.

Release rates (humidity cell release plus accumulation in solid phase) for the three extractions were averaged (Table C1-4 of Attachment C of GWQPE Appendix A3). The HCl extraction for the ST-1 residue was not used due to attrition of the stirring bar in the extraction. The average sum was then divided by the period of record (22 weeks) to determine a modified rate of release. The modified rate was converted to units of mol/kg-s and divided by the modified sulfate release rate (mol/kg-s) to express metal release rate as a fraction of the sulfate release rate (Table 2.6 of the GWQPE and Table 3.7 of GWQPE Appendix A3). The fractions presented ranged from 4.5 x 10^{-6} for mercury to 4.2 x 10^{-2} for sodium.

I.B.2.2.5 AP and NP Consumption and Calcium and Magnesium Carbonate Availability

AP consumption was calculated by three methods: (i) comparison of unleached depyritized tailings and residues leached during the short term tests, (ii) sulfate release during the humidity cell tests (short - 22 cycles, intermediate and long term - both 65 cycles), and (iii) sulfate release during the short-term humidity cell tests in conjunction with sulfate accumulation in the solid phase as determined by leach extraction tests on the unleached tailings and the leached residues from the short term tests.

Sobek NP consumption was calculated based on analysis of unleached depyritized tailings and residues leached during the short term tests. CO_3-NP consumption was calculated based on (i) analysis of unleached depyritized tailings and residues leached during the short-term tests, (ii) calcium and magnesium release during the humidity cell tests (short, intermediate, and long term), and (iii) the sum of sulfate and alkalinity release during the humidity cell tests (short, intermediate and long term).

Comparison of analyses of unleached depyritized tailings and residues leached during the short-term tests yielded AP releases of 3.9 and -2.6 kg $CaCO_3$ eq/Mg (16% and -11%, respectively, of the initial AP) (see Table I.B.5; Table 3.4 of GWQPE Appendix A3). The result from the latter sample was considered in error resulting "from analysis of a single subsample of the humidity cell residue, which is subject to sample variability and analytical error" (p. 4.2-16-26, GWQPE Appendix A3). Sulfate release during the 22 cycles of the short-term tests indicated AP depletions of 4.08 and 4.36 kg $CaCO_3$ eq/Mg (17% and 18%, respectively, of the initial AP) (Table 3.5 of GWQPE Appendix A3). Corresponding calculations for the 65 cycles of the intermediate and long-term tests yielded AP releases of 5.2 to 6.4 kg $CaCO_3$ eq/Mg (21% to 26% of the initial AP) (Table 3.10 of GWQPE Appendix A3). Using the sulfate release during the short-term test, in conjunction with the leach extraction test results for these two cells, yielded AP releases of 7.2 and 9.3 kg $CaCO_3$ eq/Mg (29% and 38%, respectively, of the initial AP) (Table 3.5 of GWQPE Appendix A3).

Comparison of analytical results from unleached depyritized tailings and residues from the short-term tests indicated Sobek NP releases of 17 and 18 kg $CaCO_3$ eq/Mg (23% and 24%, respectively, of the initial values) and CO_3-NP releases of 12 and 14 kg $CaCO_3$ eq/Mg (14% and 16%, respectively, of the initial values). The sum of calcium and magnesium release during the 22 cycles of the short-term tests indicated CO_3-NP depletions of 5.9 and 6.5 kg $CaCO_3$ eq/Mg (6.6% and 7.3%, respectively, of the initial CO_3-NP) (see Table I.B.6; Table 3.5 of GWQPE Appendix A3). Corresponding calculations for the 65 cycles of the intermediate and long-term tests yielded CO_3-NP releases of 7.5 to 9.1 kg $CaCO_3$ eq/Mg (8.3% to 10% of the initial NP) (Table 3.10 of GWQPE Appendix A3). Using the sum of sulfate and alkalinity release during the 22 cycles of the short-term test, yielded CO_3-NP releases of 5.6 and 6.1 kg $CaCO_3$ eq/Mg (6.2% and 6.8%, respectively, of the initial CO_3-NP) (Table 3.5 of GWQPE Appendix A3). Corresponding calculations for the 65 cycles of the intermediate and long-term tests yielded CO_3-NP releases of 7.2 to 8.8 kg $CaCO_3$ eq/Mg (8.1% to 9.9% of the initial CO_3-NP) (Table 3.10 of GWQPE Appendix A3).

The conclusion was drawn that "approximately 16 to 38% of the AP has reacted, but neutral pH conditions are maintained by reaction of only 6 to 16% of the CO_3 NP" (p. 4.2-16-27, GWQPE Appendix A3).

I.B.3 Discussion of Depyritized Tailings Tests

I.B.3.1 Chemical and Mineralogical Composition

Solid-phase analyses were conducted by an accredited laboratory (Standards Council of Canada, Canadian Association of Environmental Analytical Laboratories, ISO/IEC Guide 25 level for

various inorganic and organic parameters). These tests are "non-routine" and are not required to be conducted by a Wisconsin Certified Laboratory (s. NR 182.135, Wisconsin Administrative Code). The analytical methods are presented in Table 2.3 of GWQPE Appendix A1 and are described further in Attachment A of NMC (2000d).

Abbreviated duplicate bulk chemistry results are summarized in Table 3.6 and detailed results are presented in Table C-1 of Attachment C of GWQPE Appendix A1. Although methods for carbonate and ferric iron are provided in Table 2.3, no results are reported in Table 3.6 or Table C-1 of GWQPE Appendix A1. The duplicate results (with analyses performed on different sub-samples per NMC, 2000d) are in good agreement, generally within a few percent of the mean. The total sulfur content was reported as 0.755% (Table 2-3 of the GWQPE), and the sulfide content as 0.60% (Table C-1 of Attachment C of GWQPE Appendix A1). These contents are slightly lower than the 0.785% total sulfur and 0.63% sulfide reported for acid-base accounting in Table 3.4 of the GWQPE.

I.B.3.2 Mineralogy

The mineralogical analyses were conducted using appropriate methods by personnel experienced in mineralogical analyses and observed by a geologist from the Wisconsin DNR (Markart, 1999b). The mineralogical results presented for optical microscopy indicate a carbonate mineral content of 17 wt%. Sulfide minerals, iron oxyhydroxides, and hematite are reported present in trace quantities (<0.2 wt%).

The pyrite content of less that 0.2% reported for optical microscopy is less than that determined based on the reported sulfide content of 0.63% (Table 2.4 of the GWQPE). This sulfide content implies a pyrite content of 1.2% [(32.06 x 2 + 55.85)/(2 x 32.06)]. The chemical analysis provides a more accurate determination, and the discrepancy is likely due to quantitative limitations of optical microscopy.

Subsequent electron microprobe analysis indicated the carbonate mineral phases consisted of 90% ferroan dolomite (50% Ca, 38% Mg, 9.6% Fe and 2.5% Mn), 8.5% magnesian siderite (0.36% Ca, 35% Mg, 60% Fe, 4.0% Mn), and 1.7% ferroan magnesite (0.048% Ca, 84% Mg, 14% Fe, 1.75% Mn) (Table 1 of GWQPE Appendix A4). The aforementioned values indicate that 83.4 atomic percent of the carbonate is associated with calcium (44.9%) and magnesium (38.5%), while 16.6 atomic percent is associated with iron and manganese. The percent of carbonate associated with calcium and magnesium is in good agreement with the 83% value calculated for ferroan dolomite in the earlier SSQ-EDS analyses (Table 3.3 of GWQPE Appendix A1).

Using the electron microprobe values in conjunction with the 5.375% CO_3 content yields individual carbonate contents of 4.03% $CaCO_3$, 2.92% $MgCO_3$, 1.45% $FeCO_3$, and 0.27% $MnCO_3$. This is a total carbonate content of 8.7 wt%, which is roughly half the value reported by visual analysis (Table 2-5 of the GWQPE).

The chemical analytical results for calcium, magnesium and manganese are not inconsistent with the mineralogical analyses of the carbonates. The calcium, magnesium and manganese contents

of the depyritized tailings are 1.6%, 2.0%, and 0.23%, respectively (Table C-1 of Attachment C of GWQPE Appendix A1). Using and average carbonate content of 5.38% (Table 3.4 of GWQPE Appendix A1), 45.0% of which is associated with calcium and 38.4% of which is associated with magnesium, requires calcium and magnesium contents of 1.6% and 0.84%, respectively. Thus the reported calcium and magnesium contents are adequate to account for the calcium and magnesium carbonates reported in the mineralogical analysis (Table 1 of GWQPE Appendix A4). The manganese content implies a maximum manganese carbonate content of 0.23%. This is fairly close to the 0.27% $MnCO_3$ determined by microprobe analysis and CO_3 content, and suggests that virtually all manganese is present in carbonate minerals.

I.B.3.3 Acid-Base Accounting

The sulfur content was determined using LECO furnace, an accepted method (GWQPE Appendix A1). Results for duplicate analyses were within five percent of the average, which is acceptable replication. The use of total sulfur to determine the potential for acid generation is conservative, since it may include phases that do not produce acid (e.g., gypsum).

The AP(S_T) was calculated based on an average total sulfur content of 0.78%. This indicates the tailings have a total sulfur content less than the target sulfur content of 0.85% (GWQPE Appendix A1). Furthermore, the sulfur in the depyritized tailings may be present entirely as sulfide. Therefore, the AP(S^{2-}) of the depyritized tailings would be 26.5 kg $CaCO_3$ eq/Mg, as opposed to the 19.7 kg $CaCO_3$ eq/Mg of the tailings subjected to characterization and dissolution testing. Both the sulfur and sulfide contents reported for the ABA analyses were slightly higher than associated contents reported for the chemical analysis (total sulfur: 0.78% vs. 0.76%; sulfide: 0.63% vs. 0.60%).

The NPs were calculated both using a Modified Sobek method and by assuming 100% of the carbonate was associated with calcium and magnesium. The duplicates were within 1.2% of the mean, which is acceptable replication. The NP is reported to be determined by the Sobek method, whereas the Modified Sobek method was actually used (Table B-1 of Attachment B of GWQPE Appendix A1). This discrepancy in method identification needs to be rectified. A final digestion pH in the range of 1.5 to 2.0 was used, although the pHs for the pyrite concentrate were below this range (Table B-1 of Attachment B of GWQPE Appendix A1). Since the technique used determined acid neutralization under acidic conditions, the neutralization potential available to maintain a circumneutral pH is overestimated.

The determination of carbonate content by LECO furnace is an acceptable method of analysis for carbonate content. The duplicate determinations were in close agreement (5.37% and 5.38%), and the NP-CO_3 based on the average value (5.375%) was 89.6 kg $CaCO_3$ eq/Mg (Table 2-4 of the GWQPE and Table 3.4 of GWQPE Appendix A1). This exceeded the NP[$(Ca+Mg)CO_3$] since some of the carbonate is associated with iron and manganese. Whereas the dissolution of iron and manganese carbonates initially neutralizes acid, the ultimate oxidation of the iron and/or manganese and metal hydroxide precipitation produces an equal amount of acid. These minerals provide no net neutralization since the acid produced by oxidation of these metals and subsequent metal hydroxide precipitation equals that neutralized by the carbonate mineral dissolution. Whereas NP determinations by the modification of the Sobek method and based on

CO_2 content may be subject to error, the error is of limited consequence if the NP[(Ca+Mg)CO_3] is used for analysis.

I.B.3.4 NAG Tests

The NAG test was not designed to address the objectives stated in GWQPE Appendix A1 (Steffen, Robertson and Kirsten, 1998f). Rather, NAG tests are intended as static test to assess the balance of acid producing and acid neutralizing components present without conducting sulfur analyses. The NAG test was not developed to quantify the alkalinity required to ensure mine waste drainage remains neutral nor to indicate a target NP:AP ratio for maintaining neutral conditions. The rapid oxidation of pyrite and consequent acid generation create acidic conditions that readily dissolve calcium and magnesium carbonates. This does not simulate the potential for carbonate mineral coating that would occur under conditions of slow acid generation at circumneutral pH conditions.

Steffen, Robertson and Kirsten (1998f) states that "the alkalinity data indicate there is a clear excess of neutralization potential in samples with CO_3 NP:AP ratios of 2.4 or higher" (i.e., NAG-1 to NAG-4) (p. 4.2-15-229, Attachment H). However, this discounts the implications of excess acidity reported for the leachate analyses. At best, these tests corroborate the excess NP of the samples relative to the AP. The test results will not be used as part of the decision making process. NP availability and appropriate NP:AP ratios will be determined based on humidity cell testing. The NAG test results will be used herein only for subsequent comparison, with the intent of determining their potential application for subsequent work. The NAG test results should not be extended beyond this application.

In addition, the AP reported for duplicates of NAG-6 (Table 2 of Attachment H of GWQPE Appendix A1) were 68 and 63 kg $CaCO_3$ eq/Mg, while the sulfur content of both splits was reported as 2.00%. The reason for the difference in AP values is unclear since the 2.00% sulfur content yields an AP of 62.4 kg $CaCO_3$ eq/Mg. The percent CO_3 reacted in Table 3 of Attachment H (GWQPE Appendix A1) also appear to be erroneous (see Table I.B.7).

I.B.3.5 Multiple Step Batch Tests

The objective of the multiple step batch tests was to determine the degree to which slightly acidic (pH 4.0 with two different iron concentrations) leachates affect the availability of calcium and magnesium carbonate minerals to neutralize acid under anoxic conditions at depth in the TMA (GWQPE Appendix A1). The reason for undertaking the tests was to assess the implications of acidic water migrating downward through the TMA, with a potential for contacting tailings under anoxic conditions. If this were to occur, a question of greater interest would be the affect that anoxic conditions would have on the availability of calcium and magnesium carbonates to neutralize acid in slightly acidic leachates. The availability of NP was calculated by comparison of the initial solids and solids residues, and based on changes in water quality during the individual stages. A modification of the method of Sobek and others (1978) apparently was used, and this issue needs to be clarified.

Anoxic conditions were clearly not maintained in three of the four runs (as is noted in GWQPE Appendix A1). Consequently, the applicability of the results for the intended purpose is questionable. In the fourth test (DPT-2A, in which anoxic conditions were maintained), the pH remained above 6.0 only in the first stage, and pHs for the first five leachings were 0.6 to 1.8 su lower than for the paired test (DPT-2B) (Table 3.10 of GWQPE Appendix A1). This is occurred even though less acid was generated by ferrous iron oxidation and ferric hydroxide precipitation in test 2A. For the test that was retained in a fairly anoxic condition, the extent of NP depletion by all measures was considerably less. These NP ranged from 32.8 to 50.2% of the Sobek NP and CO_3-NP. However, these NP depletions occurred largely when the pH was less than 6.0 and do not, therefore, indicate the availability to maintain pH of at least 6.0. This indicates that any acidic water which migrates to anoxic zones of the TMA will be neutralized less effectively, and emphasizes the importance of maintaining neutral pH conditions in the TMA.

The release of calcium and magnesium provided the lowest value for available NP. Mineralogical analysis of the leached solids indicated that some of the acidity removed from solution was "stored" as solid-phase acid sulfate minerals as opposed to being neutralized by dissolution of calcium and magnesium carbonate minerals. Consequently, calculation of calcium and magnesium carbonate minerals available for neutralization based on acidity consumed overestimates the carbonate mineral dissolution.

The carbonate availabilities determined under the conditions of the test may differ from those observed in the field. The availability of calcium and magnesium carbonate may have increased under test conditions due to the short term exposure to a relatively large amount of acid. In the field, carbonate minerals will likely be exposed to smaller amounts of acid over a long period of time. These conditions may be more conducive to the formation of precipitate coatings on the carbonate mineral surface, with a consequent suppression of mineral dissolution and acid neutralization. These values should not be used to determine neutralization potential availability.

I.B.3.6 Humidity Cell Tests

The tailings bed in the humidity cells was 25 mm deep (Table A-1.2 of Attachment A of GWQPE Appendix A3; this dimension is omitted in Tables A-1.1, A-3.1, A-4.1, A-5.1 and A-6.1), the bed diameter was relatively large (75 mm), and the flushing rate was reasonably high (600 or 150 mL per week). Using a bulk density of 12.8 kN/m^3 (81.4 pcf) and a specific gravity of 2.81 (Tables 1, 2, 4 of Steffen, Robertson and Kirsten, 1998e) yields a porosity of 0.54 and a pore volume of 82 mL in the bed. Thus the rinse volumes 600 and 150 mL per week represented 7.3 and 1.8 pore volumes per week, respectively. The higher pore volume would be expected to provide thorough rinsing. This was shown to be the case for sulfate in the short term cells. Sulfate contents of the tailings residuals were determined as 33 and 34 mg/kg, indicating that sulfate was not accumulating in the solids. In contrast, the sulfate content of the unleached depyritized tailings was determined as 2155 mg/kg (Tables C1-2 and C1-3 of Attachment C of GWQPE Appendix A3).

There are discrepancies between the aforementioned information and that presented in GWQPE Appendix A3 (Steffen, Robertson and Kirsten, 1998d). Table A-2.1 in Attachment A of GWQPE Appendix A3 reports a specific gravity of 2.6 for the tailings as opposed to value of

2.81 cited above. The internal consistency of the test conditions presented in Table A-2.1 is also uncertain. A specific gravity of 2.6 indicates that 200 g of tailings would occupy 77 mL. The bed volume calculated for a 75 mm diameter and 25 mm depth is 153 mL. These values yield a porosity of 0.30, which is excessively low.

I.B.3.6.1 Rates of Sulfide Oxidation

These calculations assumed that (i) sulfate release, as indicated by drainage analysis for sulfate, during the steady-state period was the result of iron sulfide oxidation during the test, (ii) all sulfate produced was released to drainage, and (iii) the release was fairly constant over the steady state period. The last assumption is supported by the cumulative sulfate release graphs presented in Figures A-1.1 through A-6.1 (sulfate concentration vs. time) and A-1.3 through A-6.3 (cumulative sulfate release vs. time) of Attachment A (GWQPE Appendix A3). These graphs indicate that the weekly variations in sulfate release, which were substantial (e.g., Table A-1.2 of Attachment A, which is not correctly numbered), tended to be more constant over longer time periods.

Two additional considerations should be made regarding the steady state rate calculations. First, total sulfur concentrations during the steady-state periods were less variable than those of sulfate, which was more consistent with variations of other parameters. Furthermore, for the steady-state periods of the intermediate and long-term cells, total sulfur determinations provided a closer charge balance than sulfate concentrations (see Table I.B.2; Tables A-3.4, A-4.4, A-5.4, A-6.4 of Attachment A of GWQPE Appendix A3). Although the charge balance for the short-term cells was closer to 1.0 for sulfate concentrations, the anomalous variation in sulfate concentrations and the better charge balance for the intermediate and long term cells indicate rate calculations should also be made using total sulfur data. The steady-state rates using total sulfur are 17 to 82% higher than those determined using sulfate. Steady state period rates based on total sulfur release were 16.8×10^{-10} and 22.0×10^{-10} mol O_2/kg-s for the short term cells and ranged from 6.48×10^{-10} to 12.2×10^{-10} mol O_2/kg-s for the intermediate and long-term cells (see Table I.B.4). Second, the sulfur released was the result of oxidation of depyritized tailings containing 0.63% sulfide. The target sulfur content for the depyritized tailings is 0.85%, and virtually all sulfur could be present as sulfide. Assuming the sulfide mineral oxidation rate is proportional to sulfide content, rates for 0.85% sulfide tailings would be 1.35 times those at 0.63% sulfide (0.85/0.63 = 1.35). This yields a range of 8.74×10^{-10} to 29.7×10^{-10} mol O_2/kg-s for the steady state periods (see Table I.B.4).

The correction for potential sulfide content in the TMA relative to that used in the humidity cell tests should also be applied to the rates for the short term cells, which considered changes in the solid-phase sulfate content. The values cited in the previous paragraph were multiplied by 0.85/0.63, yielding values of 35×10^{-10} and 41×10^{-10} mol O_2/kg-s for rates based on sulfate release and 81×10^{-10} and 94×10^{-10} mol O_2/kg-s for rates based on total sulfur release. Thus, the previous calculations yield oxidation rates ranging from 8.7×10^{-10} to 94×10^{-10} mol O_2/kg-s (see Table I.B.4).

The oxidation rates may have been more rapid during the early weeks of the experiment. Assuming all sulfate was removed from the solids in the initial period yields sulfide oxidation

rates markedly higher than the steady state rates. This more rapid release was most likely the result of removal of reaction products generated during sample storage prior to the experiment.

I.B.3.6.2 Calcium and Magnesium Carbonate Availability

Mineralogical examination of the humidity cell residues indicated the "carbonate grains consisted of both clear particles and particles with patchy, discontinuous iron staining at rims, along fractures and cleavages (30%)" (p. 4.2-16-275, Attachment B of GWQPE Appendix A3). If iron staining were to become extensive, the availability of the calcium and magnesium carbonate mineral for acid neutralization could be limited.

The extent to which calcium and magnesium carbonate minerals have dissolved in the humidity cells presents a lower bound of their availability. For the intermediate and long-term cells, this extent was calculated as 7.2 to 9.1 kg $CaCO_3$ eq/Mg (Table 3.10 of GWQPE Appendix A3). This represents 8% to 10% of the CO_3-NP (89.6 kg $CaCO_3$ eq/Mg) and 9.6% to 12% of the calcium and magnesium carbonate present (74.7 kg $CaCO_3$ eq/Mg).

It should be noted that some of the sulfate, calcium, magnesium, and alkalinity release used in these calculations may have been from reaction products generated prior to experimentation. For example, some of the initial calcium release may have been the result of dissolution of gypsum generated prior to the experiment. Assuming all calcium and magnesium release in the initial period was of this nature reduces the calcium and magnesium carbonate dissolution to a range of 3.28 to 3.93 kg $CaCO_3$ eq/Mg. This represents 3.7% to 4.4% CO_3-NP and 4.4% to 5.3% of the calcium and magnesium carbonate present.

The "low release of manganese" is mentioned as support for the hypothesis that "calcium rich carbonates are preferentially reacted and/or dissolved" (p. 4.2-16-22, GWQPE Appendix A3). Since manganese concentrations may be controlled by solubility of manganese oxyhydroxides, inferences on its low release (as calculated based on drainage quality) can not be drawn.

I.C WASTE ROCK

A detailed description of the waste rock is presented in Section IA on waste rock sample representativeness. Waste rock master composite samples of the Skunk Lake, Rice Lake, Upper Mole Lake, and Lower Mole Lake formations were constructed to provide samples representative of the waste rock to be generated from the formations. Each master composite consisted of drill core intervals from several borings (Table 3 of EIR Appendix 3.5-31 of Foth and Van Dyke, 1997). The Skunk Lake master composite was developed from 11 intervals from two borings. A similar approach was used for the Rice Lake (six intervals from three borings), Upper Mole Lake (18 intervals from 10 borings) and Lower Mole Lake (12 intervals from 11 borings).

Large-scale humidity cell tests were conducted on waste rock master composites and high sulfur composites from the Skunk Lake, Rice Lake, Upper Mole Lake, and Lower Mole Lake formations. Sulfate and metals concentrations in drainage from these tests were determined. Rates from both the master composites and high sulfur composites are presented.

The mass of solute released in each drainage sample was determined as the product of solute concentration and the volume of drainage. For sulfate, these masses were summed to determine cumulative sulfate release. Cumulative sulfate release was divided by the time over which sulfate release occurred to determine sulfate release rates. These rates were converted to rates of oxygen consumption based on the stoichiometry of pyrite oxidation.

Metals were determined less frequently. The long-term rates of metal release were usually determined as the average release for cycles 17, 33 and 54. Short-term release rates were determined based on release during cycles 1 through 9. For values reported as less than detection, the detection limit was used to determine the rate of release. Because the rock particle size distribution in the field may be finer, and the cells were not designed to remove all solutes from the solids, these rates were multiplied by 10 to provide an upper bound estimate. Uncertainties introduced by laboratory procedures and analyses, as well as uncertainties in operational conditions are identified for extrapolation of laboratory data to field conditions.

I.C.1 Methods for Waste Rock

I.C.1.1 Particle Size

Large-scale humidity cell tests were conducted on waste rock master composites and high sulfur composites from the Skunk Lake, Rice Lake, Upper Mole Lake, and Lower Mole Lake formations. The particle size distributions of the samples subjected to large-scale humidity cell testing were determined by methods presented in CMC (1994a, 1994b). The data are summarized in Table I.C.1 (Section 3.5.5 and EIR Appendix 3.5-31 of Foth and Van Dyke, 1995b). The master composite samples from the Skunk Lake, Rice Lake, Upper Mole Lake, and Lower Mole Lake formations were all less than 38 mm (1.5 in) in diameter. From 36 to 44% of the samples were finer than 7.0 mm (0.28 in), 12 to 15% finer than 2.0 mm, and 1.5 to 1.9% finer than 0.074 mm.

Since no waste rock has been generated, there are no detailed data for the waste rock particle size distribution in the field. For Type II waste rock, NMC indicated that the hoisted rock would range from approximately 24-inch size to sand sized particles, with the gradation depending on the rock type (Foth and Van Dyke, 1999). NMC (2000b) further notes that operational Type II waste rock will have a D_{80} of 8 inches (200 mm). Additional background discussion of waste rock particle size distribution is presented in NMC (2001b).

I.C.1.2 Chemical and Mineralogical Composition

The master composites and high sulfur composites from the Skunk Lake, Rice Lake, Upper Mole Lake and Lower Mole Lake formations were analyzed for S, C, Ag, Al, As, Au, Ba, Be, Bi, Ca, Cd, Co, Cr, Cu, Fe, Ga, Ge, Hg, K, Mg, Mn, Mo, Na, Ni, Pb, Sb, Se, Si, Sn, Te, Ti, Tl, U, and Zn. Chemical analyses of the 46 drill core intervals from which the master composites were formed were also conducted (Appendices 2.2-2.5 of Foth and Van Dyke, 1995e). The components were slightly different. For example, phosphorous and carbon dioxide contents of the intervals were determined. Chemical analyses were conducted by Lakefield Research Limited in Lakefield, Ontario, Canada. The laboratory is “certified by the Standards Council of

Canada, the Canadian Association of Environmental Analytical Laboratories, and has been accredited at the ISO/IEC Guide 25 level for various inorganic and organic parameters" (NMC, 2000d).

The data for the master composites and high sulfur composites are summarized in Table I.C.2 (Tables 3.5-17 and 3.5-18 of Foth and Van Dyke, 1995b/1998e). The bulk chemistry of the waste rock composites is presented in EIR Appendix 3.5-32 (Foth and Van Dyke, 1997) and summarized by sample in EIR Appendix 3.5-34 (Tables 2, 9, 16, 23, 30, 37, 44, 51 of Foth and Van Dyke, 1997).

The sulfur contents presented in Table 3.5-17 (Foth and Van Dyke, 1995b/1998e) for the Skunk Lake, Rice Lake, Upper Mole Lake and Lower Mole Lake formation master composites were 0.01, <0.01, 0.04 and 0.22% (converted from mg/kg). The corresponding sulfur contents presented in Appendices 1.5-1.8 of Foth and Van Dyke (1995e) were 0.14, 0.05, 0.10, and 0.34%. Sulfur contents presented for the high sulfur composites were only slightly different than values previously presented (Table 3.5-18 of Foth and Van Dyke, 1995b/1998e). The reason for the differences between the values reported in the two documents is unclear.

No mineralogical characterization was conducted on the waste rock composites subjected to kinetic tests.

I.C.1.3 Static Tests

ABA values for the eight samples subjected to kinetic tests are presented in Table 3.5-20 (Foth and Van Dyke, 1995b/1998e). The sulfur contents vary from those presented previously, as noted above in Section I.C.1.2. The Net NP of the master composites ranged from -4.4 to +45 kg $CaCO_3$ eq/Mg rock. The corresponding range for the high sulfur composites was -133 to -102 kg $CaCO_3$ eq/Mg rock.

I.C.1.4 Humidity Cell Tests

Large-scale humidity cell tests were conducted on master composites and high sulfur composites of Skunk Lake, Rice Lake, Upper Mole Lake, and Lower Mole Lake formations, with one cell being run for each of the eight samples. The cells were denoted WD-05 through WD-12. The physical dimensions and test conditions are described in Table 1a of EIR Appendix 3.5-33 (Foth and Van Dyke, 1997). In summary, the large scale humidity cells were constructed from polyethylene containers (120 L) with a conical base. A spigot was installed at the lowest part of the base. The cell diameter was 457 mm, yielding a cross sectional area of 0.164 m^2. This area is erroneously reported as 1.64 m^2 in Table 3.5-22 of Foth and Van Dyke (1995b/1998e).

From 84.55 to 133.18 kg of rock was placed into the master composite cells, yielding depths of 305 to 508 mm (Table 1a of EIR Appendix 3.5-33 of Foth and Van Dyke, 1997). The rock volumes ranged from 50 to 83 L and the porosities were reported as 0.36 to 0.42 (Table 3.5-22 of Foth and Van Dyke, 1995b/1998e). From 73.64 to 81.14 kg of rock was placed into the high sulfur composite cells, yielding depths of 267 to 292 mm (Table 1a of EIR Appendix 3.5-33 of

Foth and Van Dyke, 1997). The rock volumes ranged from 44 to 48 L and the porosities were reported as 0.29 to 0.35 (Table 3.5-22 of Foth and Van Dyke, 1995b/1998e).

The experimental procedure is summarized in Section 3.5 of Foth and Van Dyke (1995b/1998e). For two periods a day (0400-0800, 1600-2000) saturated air was introduced to each cell from two ports on opposite sides of the cell, slightly above the base. Deionized water was added to each cell twice a day (at 1200 and 2400) for six days of each one-week cycle. The total amount of water introduced weekly by these additions (4.8 L) was equal to the average weekly precipitation in the Crandon area (Table 3.5-22 of Foth and Van Dyke, 1995b/1998e; Table 1 of EIR Appendix 3.5-34 of Foth and Van Dyke, 1997). A volume equal to the average weekly precipitation in the Crandon area was also added on the seventh day, simulating a storm event.

Drainage from the cells was collected weekly prior to the simulated storm event. The leachate volume, pH, conductivity, and temperature were measured weekly at Foth and Van Dyke. Samples were also collected and submitted to an analytical laboratory for determination of alkalinity, acidity, aluminum, antimony, arsenic, barium, beryllium, bismuth, cadmium, calcium, chromium, cobalt, copper, gallium, germanium, iron, lead, magnesium, manganese, mercury, molybdenum, nickel, potassium, selenium, silver, sodium, sulfate, tellurium, thallium, tin, titanium, uranium, and zinc.

The test duration for master composites of the Skunk Lake and Rice Lake formations was 106 weeks, while that for the Upper and Lower Mole Lake formations was 70 weeks (Table 1 of EIR Appendix 3.5-34 of Foth and Van Dyke, 1997). The test duration for high sulfur composite of the Skunk Lake formations was 106 weeks, while that for the Rice Lake, Upper and Lower Mole Lake formations was 65 weeks.

I.C.2 Results of Tests on Waste Rock

I.C.2.1 Static Tests

Static tests were conducted in 1994 on 91 samples from the Skunk Lake (17 samples), Rice Lake (31 samples), and Mole Lake (43 samples) Formations (Table 4 of EIR Appendix 3.5-32 of Foth and Van Dyke, 1997). Eleven samples from the Crandon Formation and two tailings samples were also subjected to static testing. The samples were from drill core intervals (7.5 m to 61 m or 25 to 200 ft long) which intersected areas of potential pre-production waste rock. Richard Cote of Rio Algom conducted the initial geological description of the core. John Thresher, Jr. of Thresher and Son and Ken Markart of the WDNR examined the core subsequently, and were largely in agreement with Cote's description. Based on the consensus description of the core, about 75% of the samples selected for analysis were from segments with the highest sulfur content. As a result, these samples tend to overestimate the acid-producing potential of the waste rock. Of the 91 samples analyzed, 22 had net neutralization potentials below 0.

In 1995 static tests were conducted on 102 samples from the Skunk Lake (16 samples), Rice Lake (32 samples), Upper Mole Lake (23 samples), and Lower Mole Lake (31 samples) Formations. Of the 102 samples analyzed, five had net neutralization potentials below 0 (Tables 5 – 8 of EIR Appendix 3.5-32 of Foth and Van Dyke, 1997).

The Net NP values of rock used in kinetic tests indicate that potential acid producing waste rock samples are Skunk Lake Master Composite (Net NP = -4.4 kg/Mg $CaCO_3$) and the high sulfur composites from the Skunk Lake (-112 kg/Mg $CaCO_3$), Rice Lake (-102 kg/Mg $CaCO_3$), Upper Mole Lake (-134 kg/Mg $CaCO_3$), and Lower Mole Lake (-109 kg/Mg $CaCO_3$) formations (Tables 5 – 8 of EIR Appendix 3.5-32 of Foth and Van Dyke, 1997).

I.C.2.2 Humidity Cell Tests

I.C.2.2.1 Drainage Quality

The test duration for master composites of the Skunk Lake and Rice Lake formations was 106 weeks, and that for the Upper and Lower Mole Lake formations was 70 weeks (Table 1 of EIR Appendix 3.5-34 of Foth and Van Dyke, 1997). During this time, 10 to 18 pore volumes of drainage were collected from the cells (Table 3.5-22 of Foth and Van Dyke, 1995b/1998e). The test duration for the high sulfur composite of the Skunk Lake formations was 106 weeks, and that for the Rice Lake, Upper and Lower Mole Lake formations was 65 weeks. During this time, 17 to 32 pore volumes of drainage were collected from the cells (Table 3.5-22 of Foth and Van Dyke, 1995b/1998e). Drainage quality data for the cells are presented in EIR Appendix 3.5-34 (Foth and Van Dyke, 1997).

The four master composites produced drainage with circumneutral pH. The Skunk Lake Master Composite produced the lowest pHs, typically ranging from 6.3 to 7.3. Alkalinities were approximately 30 mg/L as $CaCO_3$ during the first nine cycles, decreased gradually, and reached a plateau near 10 mg/L as $CaCO_3$ after cycle 78. Sulfate concentrations were fairly constant and near 20 mg/L between cycles 9 and 104.

The remaining three master composites produced drainage with pH in the range of 7.8 to 8.3 after cycle eight. Alkalinity and sulfate concentrations tended to decrease over time. Initial alkalinities ranged from 80 to 100 mg/L as $CaCO_3$ and decreased to the range of 60 to 70 mg/L as $CaCO_3$. Sulfate concentrations initially ranged from 40 to 100 mg/L and decreased to the range of 5 to 14 mg/L.

The high sulfur composites produced drainage with pH below 6.0 and pHs as low as 2.5 to 3.0. Maximum reported acidities ranged from approximately 400 to 900 mg/L. No acidities were reported for the Rice Lake High Sulfur Composite. The maximum sulfate concentration reported for the Rice Lake High Sulfur Composite was 470 mg/L. Maximum sulfate concentrations reported for the Skunk Lake and Upper Mole Lake High Sulfur Composites were in the neighborhood of 1400 mg/L, and the maximum reported for the Lower Mole Lake sample was 2300 mg/L.

I.C.2.2.2 Sulfide Oxidation and Oxygen Consumption Rates

Oxidation rates for the waste rock were calculated using the mass sulfate release subsequent to cycle 9. Data were taken from Tables 3, 10, 17, and 24 of EIR Appendix 3.5-34 (Foth and Van Dyke 1997, 2000c). The cumulative sulfate releases from cycle 9 to cycle 54 and from cycle 9 to

the end of the period of record (mg SO_4 per kg rock) were divided by the respective durations and converted to moles sulfate per kg rock per second. Sulfate release rates calculated for the Skunk Lake, Rice Lake, Upper Mole Lake, and Lower Mole Lake Master Composites ranged from 4.9 x 10^{-12} to 2.4 x 10^{-11} mol SO_4/kg-s (see Table I.C.3). These release rates were multiplied by 1.875 to determine rates of oxygen consumption for the master composites. Oxygen consumption rates ranging from 9.2 x 10^{-12} to 4.5 x 10^{-11} mol O_2/kg-s (see Table I.C.3) were computed. Rates for the high sulfur composites were roughly 40 to 50 times higher (see Table I.C.4).

The waste rock humidity cell tests were not designed to remove all reaction products (Section 3.5, Foth and Van Dyke, 1995b/1998e). In particular, the fraction of sulfate generated by oxidation that was in the drainage from the cell is unknown. Consequently, the oxidation rate for each sample may have been higher than that implied by the rate of sulfate release. Since the leached solids were not analyzed after testing, quantifying the fraction of reaction products that remained in the cell is not possible. The oxygen consumption rates were multiplied by ten to account for inefficient rinsing. This factor also accounts for potential errors in sulfate determination (CMC, 1997). The adjusted rates of oxygen consumption determined for the master composites ranged from 9.2 x 10^{-11} to 4.5 x 10^{-10} mol O_2/kg-s (see Table I.C.3). Rates for the high sulfur composites were roughly 40 to 50 times higher (see Table I.C.4).

I.C.2.2.3 Metal Release Rates

Effluent chemistry data from the waste rock humidity cells are presented in EIR Appendix 3.5-33 (Foth and Van Dyke, 2000c). The data are also summarized and assessed by sample in EIR Appendix 3.5-34 (Foth and Van Dyke 2000c). Drainage volumes are summarized in Table 1 of EIR Appendix 3.5-34. Release rates for the Skunk Lake and Lower Mole Lake Master Composites are presented in NMC (2000c).

NMC used three different methods for determining metal release rates. For waste rock stored on the surface prior to disposal in the TMA, the average release for cycles 17 and 33 was used. These results are incorporated into calculations presented in NMC (2001a). A description of the method is not included in any of the reports. The second method determined release from cycles 10 through 54 (Foth and Van Dyke, 2000d). During this period the only cycles for which drainage was analyzed for metals were cycles 17, 33, and 54. Concentrations in other samples apparently were determined by linearly extrapolating between measured values, although no citation is available regarding the method of extrapolation. The third method used the observed release for cycles 1 through 54 (Steffen Robertson and Kirsten, 2000d).

Release rates for the master and high sulfur composites are summarized in Tables I.C.5 and I.C.6, respectively. Calculations for the individual humidity cells are presented in Tables I.C.7 through I.C.14. Release rates for the first cycle in the tests are also presented in Table I.C.15. These rates were often much higher than those observed in latter rinses. The higher initial release may have implications with respect to some extrapolations of the laboratory data.

I.C.3 Discussion of Release Rates for Waste Rock

I.C.3.1 Applicability of Humidity Cell Tests

The kinetic waste rock humidity cell tests were developed "to determine the ability of the material to produce acidic drainage and specifically to determine oxidation rates, neutralization rates, metal leaching rates, and water quality as a function of time" (p. 2, Foth and Van Dyke, 1995e). There are several problems associated with using these humidity cells for determination of rates, which makes the tests ill-suited to achieve the objectives.

First, the cells are much larger than cells commonly used for waste rock testing. The cells contained roughly 74 to 133 kg as compared to 1 kg in more commonly used cells (e.g., White and Lappako, 2000). The flow path through larger cells is long relative to that in smaller cells used more commonly. As mentioned previously, the rock depths in the large cells ranged from 270 to 510 mm as compared to approximately 75 mm in the smaller cells. The longer flow path increases the probability of preferential flow paths, which reduces the efficiency of reaction product transport.

Second, the amount of water added relative to the amount of rock is relatively small. The water addition to the waste rock humidity cells was not designed to remove all reaction products. Rather "deionized water was added to each column to simulate precipitative inputs in two different ways" (p. 3.5-159, Foth and Van Dyke, 1995b/1998e). As mentioned previously, the water added to the cells was 4.8 L/week, which represents 0.16 to 0.36 pore volumes per cycle. More commonly used protocols apply 500 mL of water to a 1 kg sample (White and Lappako, 2000), representing approximately 1.5 to 3.0 pore volumes per cycle. Despite the higher water application in smaller cells, removal of reaction products is less than 100%. The lower rinse water application rate in the larger cell provides less efficient transport of reaction products from the cell. Both the longer flow path and the lower rinse water addition contribute to an underestimation of chemical reaction rates based on drainage quality.

Third, there were no analyses conducted on the leached solids to determine the extent of reaction products that were not transported from the waste rock cells. Consequently it was not possible to quantify the rinsing efficiency. Such analyses were conducted on leached solids from other tests.

The two short-term humidity cell tests designated HC-DPT-ST1 and HC-DPT-ST2 were conducted on depyritized tailings. The pore volume reported for cell HC-DPT-ST2 was 33.5 mL (Table A-2.1 of Attachment A of GWQPE Appendix A3). These cells yielded approximately 600 mL of drainage per cycle (Tables A-1.2 and A-2.2 of Attachment A of GWQPE Appendix A3), representing an approximate average drainage of 18 pore volumes per cycle. Leached products from the short-term humidity cell tests on depyritized tailings were examined. Rates considering the accumulation of sulfate in the solids were roughly 2.5 times steady state rates based on drainage quality alone (Table 4.1 of GWQPE Appendix A3).

The average pore volumes drained per cycle for the short-term depyritized tailings cells was 50 to 120 times that in the waste rock tests. Consequently, less efficient removal of reaction

products would be expected for the waste rock tests. However, quantifying the degree to which reaction products accumulated in the waste rock tests is difficult.

Fourth, measurements of sulfate concentrations in the laboratory were subject to error (CMC, 1997). This problem was identified after the waste rock humidity cells were terminated. Therefore, no data are available to assess the potential degree of this error. Examination of data from the depyritized tailings humidity cells indicates that some reported concentrations were half of those expected based on a charge balance.

Fifth, the frequency of trace element analysis was very low. From cycle 10 to cycle 54, trace metals were analyzed only on cycles 17, 33, and 54. This represents only three samples over a period of 45 weeks. No samples were analyzed for trace metals from cycle 55 to the end of the tests.

Sixth, cells were not replicated and, consequently, the variability in drainage quality for a given solid-phase composition cannot be determined.

Seventh, due to the small number of samples tested, there are no empirical data describing the variation of drainage quality with solid-phase composition. This applies to the rate of sulfide oxidation and the rate of acid neutralization, as well as the resultant drainage pH. These relationships can not be quantified nor can, more generally, the type of functional relationships between the solid-phase and chemical behavior be empirically determined. The type of testing required to determine these relationships for individual lithologies has been described in the literature (Lappako and Antonson, 1994, 2002).

Eighth, the lack of mineralogical characterization of the solids further complicates the interpretation of the drainage quality data.

I.C.3.2 Extrapolation to Field Conditions

The problems with the laboratory tests described above in Section I.C.3.1 introduce uncertainty when extrapolating laboratory rates to field conditions. Additional uncertainty is caused by differences in specific surface area between the laboratory samples and waste rock in the field and differences in the degree of spatial concentration of high sulfur rock between the laboratory samples and waste rock in the field.

In particular, the specific surface area of waste rock in the humidity cells may be lower than that in the field. For example, the -200 fractions in the laboratory tests were 1.9 and 1.5% for the Skunk Lake and Lower Mole Lake Master Composites, respectively (EIR Appendix 3.5-31 of Foth and Van Dyke, 1997). In contrast, the -200 fraction of rock from an underground exploration shaft in the Duluth Complex is reported as 3.1% (Lappako, 1993). Since most of the surface area, as well as much of the liberated sulfides, may be associated with this fraction, release from the humidity cell tests may underestimate release in the field.

The rock in the laboratory cells also was relatively well mixed. As a result, high sulfur rock in the master composites was in close proximity with the more abundant low sulfur rock.

Consequently, acid generated by high sulfur rock would be readily neutralized by the surrounding low sulfur rock. In both waste rock piles and in the underground mine, high sulfur rock will tend to be concentrated. Consequently, there will be greater potential for development of acidic zones associated with high sulfur rock in the field. Due to the low pH in these zones, the rate of sulfide mineral oxidation will accelerate and trace metals will reach higher concentrations. For example, at least 6% and as much as 20% or more of the Lower Mole Lake Unit can be categorized as acid producing (Markart, K., Wisconsin DNR, personal communication, 2003). This rock could create acid producing zones in a deposit of waste rock that would yield higher release of some trace elements. For example, rates of copper and zinc release from the Lower Mole Lake High Sulfur Composite were roughly 100 and 900 times, respectively, those from the Lower Mole Lake Master Composite. In a waste rock pile, the acid could also migrate and create acidic conditions in surrounding rock.

Quantifying the fraction of acidic rock, with attendant elevated metals release, is difficult. As a result, several fractions of acidic rock can be considered. NMC has calculated releases without using data from the Lower Mole Lake High Sulfur Composite. As a lower bound for acidic zones, 6% of the Lower Mole Lake rock can be assumed to be represented by the high sulfur composite. Additional cases to consider would be 20 and 40%. The last case assumes acid from the Lower Mole Lake high sulfur rock has migrated and affected rock that would otherwise be neutral. The use of 100% high sulfur composite would clearly represent an upper bound.

To account for the aforementioned uncertainties, the following extrapolation is proposed. For extrapolation of laboratory rates to broken rock, rates of sulfate and metal release may be multiplied by factors of 20 and 10, respectively. If rock with high sulfur content is likely to be present, rates from the high sulfur composites should be used. Furthermore, the possibility of drainage from high sulfur rock creating acidic environments in surrounding rock must be considered. For application of laboratory rates to mine walls, release rates for sulfate and metals should be multiplied by factors of 5 and 10, respectively. If rock with high sulfur content is likely to be present, rates from the high sulfur composites should be used.

II. WATER MOVEMENT INTO, WITHIN, AND OUT OF THE TMA

II.A. INTRODUCTION

The tailings management area (TMA) and the reclaim pond (RP) at the proposed Crandon Mine are conventional engineered containment facilities to be constructed with conventional materials and methods. As such, both the TMA and RP include a liner system designed to limit leakage to groundwater. The TMA also includes a cover that will limit ingress of precipitation and oxygen into the waste after the TMA is filled. Schematic diagrams of the liner and cover designs for the TMA are shown in Fig. II.A.1. A schematic diagram of the liner for the RP liner is shown in Fig. II.A.2

.

In this review, an independent set of estimates was made regarding flow in the TMA and leakage from the liner. Because the TMA and RP are conventional engineered containment facilities, conventional engineering methods representing the state of practice were used to make these

estimates. Conservative but realistic assumptions were used when making the calculations. Thus, the leakage rates reported herein probably are higher than would actually occur provided the facility is constructed and operated as planned. Most of the analyses employed analytical equations to compute leakage rates. NMC also used analytical equations, as well as the USEPA's **H**ydrologic **E**valuation of **L**andfill **P**erformance (HELP) Model. Leakage rates computed by NMC are summarized in Tables II.A.1 and II.A.2. A detailed description of the calculations can be found in Benson and Grefe (2002).

II.B. HYDROLOGIC PERIODS OF THE TMA

Hydrologic conditions in the TMA are divided into four sequential hydrologic periods for this report: (i) operations, (ii) drain down and closure, (iii) post-closure transition, and (iv) post-closure steady state. The operations period consists of the time following construction of the TMA during which the TMA is being filled. Leachate will be pumped from the TMA regularly during the operations period. This period is followed immediately by drain down and closure, which commences once a TMA cell is filled (i.e., tailings discharge into the cell has ceased). During drain down, liquid in the tailings drains into the leachate collection system and the degree of saturation in the tailings decreases. The final cover is also placed during drain down. Drainage from the tailings decreases continually during drain down until ultimately the drainage rate equals the inflow rate from the surface (i.e., percolation rate from the final cover). After capping and near the completion of drain down, pumping from the TMA will cease and the post-closure transition period begins. During the post-closure transition period, percolation from the cover flows down through the tailings, and accumulates on the surface of the liner. The depth of liquid on the liner increases until leakage from the liner equals the percolation rate from the cover. This final condition of balanced flows is referred to herein as the post-closure steady-state period.

Leakage rates from the TMA were calculated for each of these periods. During operations, drain down, and transition, the leakage rate was computed using the amount of liquid pooled on the liner due to discharge from the tailings. Computing the leakage rate during these three periods required computations regarding flow from the tailings, flow through the leachate collection system, the depth of liquid pooled on the liner, and the leakage rate corresponding to the depth of liquid pooled on the liner. In contrast, the steady-state leakage rate was assumed to equal the long-term percolation rate from the final cover.

II.C. METHODS TO COMPUTE FLOWS AND LEAKAGE RATES

A variety of methods exist to predict the hydrologic behavior of containment facilities. The most common method is to use USEPA's HELP Model (Schroeder et al., 1994 a,b). HELP is a quasi-two-dimensional, deterministic, water-routing model used to describe the water balance of waste containment facilities. HELP uses a set of analytical equations to route water through a vertical profile. Key advantages of HELP include its speed, its climatic and weather databases, and the ease with which default inputs can be selected. Comparisons with field data have also shown that predictions made with HELP generally are conservative (Khire et al., 1997).

A disadvantage of HELP is that calculations made by the program are not readily apparent. Thus, for well-defined scenarios, analytical expressions are sometimes used that provide the designer or analyst with a direct means of assessing exactly how input parameters are affecting outputs. Additionally, HELP is not well suited for some scenarios, such as maintaining saturated conditions in a waste mass (e.g., ponded conditions in the TMA during operations) or simulating unsaturated flow under non-uniform conditions (e.g., drainage in the TMA tailings). HELP also is not applicable for predicting leakage rates from ponds and lagoons (e.g., leakage from the RP).

Where possible, the computations described in this report were made using analytical expressions from the refereed literature that have been shown to provide accurate or conservative predictions. This approach is justified by the relatively stable hydrologic conditions anticipated to exist during the operations and post-closure steady-state hydrologic periods. However, some unsaturated flow analyses required special models that properly account for the underlying physical processes. For these analyses, a numerical model common in practice (HYDRUS-2D, Simunek et al., 1996) was used as needed.

II.C.1. Liner System

A liner system consists of a hydraulic barrier (liner) overlain by a more permeable layer (leachate collection layer). The function of the liner is to limit discharge of contaminated water (i.e., leachate) to an acceptable amount. The leachate collection layer is used to remove leachate accumulating on the liner. Reducing the depth of liquid on the liner reduces the leakage rate from the liner.

The liner systems planned for the TMA and RP include a composite liner as the hydraulic barrier. A composite liner consists of an earthen component overlain by a polymeric (plastic) sheet, referred to as a geomembrane. The earthen component of the liners proposed for the TMA and RP consists of a sieved till layer overlain by a geosynthetic clay liner (GCL). A GCL is a factory manufactured clay liner consisting of a layer of bentonite clay sandwiched between two geotextiles. A high-density polyethylene geomembrane is to be placed directly on top of the GCL.

In principle, a geomembrane should preclude all leakage from a composite liner. However, some defects in the geomembrane inevitably exist once a liner is placed. Thus, leakage from composite liners is generally anticipated. Leakage rates for composite liners can be estimated using analytical expressions. The most common analytical expressions were developed in a series of publications by J.P. Giroud and his colleagues (Giroud and Bonaparte, 1989; Khatami et al., 1989; Giroud et al., 1992; Giroud, 1997). Some of these expressions have been incorporated into the HELP Model. The most recent equation described by Giroud (1997), referred to herein as the 'Giroud's equation,' was used for making the leakage rate calculations in this report pertaining to composite liners. Giroud's equation for leakage from a circular defect in a geomembrane is:

$$Q = \xi\left[1 + 0.1\left(\frac{h_w}{H_s}\right)^{0.95}\right] a^{0.1} h_w^{0.9} k_s^{0.74} \qquad \text{(II.1)}$$

where Q is the leakage rate per hole (m^3/s), ξ is a contact factor, h_w is the average depth of leachate on the liner (m), H_s is the thickness of the low-conductivity soil component of the liner (m), a is the cross-sectional area of the hole from which leakage is occurring (m^2), and k_s is the saturated hydraulic conductivity of the underlying earthen component (m/s). Giroud's equation is a semi-empirical equation, and must be used with the stated units. The contact factor ξ represents the degree of contact between the geomembrane liner and the underlying earthen liner. For geomembranes placed on compacted clay liners, Khatami and others (1989) recommend that $\xi = 0.21$ for 'good' contact and 1.15 for 'poor' contact.

Assessing the accuracy of Giroud's equation using field data is difficult because the input parameters to the equation are never known in an actual facility. However, Foose and others (2001) did evaluate whether Giroud's equation captured the key processes controlling flow in composite liners. Foose and others (2001) concluded that Giroud's equation provides conservative estimates of leakage rate; i.e., leakage rates estimated using Giroud's equation are higher than would be predicted based on hydraulic theory. A limitation of Giroud's equation is that the contact factors apply to composite liners where the earthen component is compacted clay rather than the GCL proposed for the TMA. However, the findings in Foose and others (2001) can be used to define a contact factor for composite liners where a geomembrane is placed against a GCL. Analysis of the results in Foose and others (2001) indicates that a suitable contact factor for a geomembrane-GCL interface is 0.007, provided the liner is surcharged with overburden (e.g., the tailings provide such a surcharge in the TMA). This contact factor (ξ=0.007) was used for the computations described in this report that are related to leakage from the TMA liner. A similar contact factor is recommended by Thiel and others (2001). They indicate that contact factors for composite liners with GCLs fall between 0.00015 and 0.0005, and have conservatively recommended using a contact factor equal to 0.01 for leakage calculations.

Inspection of Giroud's equation shows that the depth of leachate on the liner is needed to compute the leakage rate. The depth of leachate can be computed using the HELP Model, or using analytical expressions. The Giroud-Houlihan equation (Giroud and Houlihan, 1995) was used to compute the depth of leachate for this review:

$$T_{max} = jL_p \frac{\sqrt{4\frac{q_i}{K_L} + \tan^2\beta} - \tan\beta}{2\cos\beta} \qquad \text{(II.2)}$$

where T_{max} is the maximum depth of liquid in the leachate collection layer, j is a correction factor ranging between 0.88 and 1.0, L_p is the distance to the leachate collection pipe in the leachate collection layer, q_i is the rate at which liquid enters the leachate collection layer from the overlying material (i.e., tailings for the TMA), K_L is the saturated hydraulic conductivity of the leachate collection layer, and β is the slope of the leachate collection layer. The parameter q_i is often referred to as the impingement rate. The average depth in the leachate collection layer (h_w), which is used in Eq. II.1, is approximately $T_{max}\cos\beta/2$. Eq. II.2 was used in lieu of Moore's

equation (which is more common), because Eq. II.2 provides a greater depth of leachate, which results in a more conservative estimate of the leakage rate from the liner (Giroud and Houlihan, 1995). Giroud and others (2000) also indicate that the derivation of Moore's equation is not documented and that the Giroud-Houlihan equation more closely matches predictions made using numerical methods.

When using Eq. II.2, K_L is assumed to remain constant over time. In a waste containment facility, however, K_L may decrease if the pores in the leachate collection layer become clogged by materials such as suspended solids in the leachate, biological matter, or mineral precipitates. NMC evaluated whether changes in K_L were likely to occur in the TMA as a result of migration of tailings or precipitation of minerals. A physical test was used to evaluate the potential for clogging by tailings (J&L Testing, 1998). Geochemical analyses employing the computer program MINTEQA2 were used to evaluate the potential for clogging by mineral precipitation (Steffen, Robertson and Kirsten, 2000 a, b). NMC also indicated that physical tests were to be conducted to evaluate the potential for mineral clogging (NMC, 2000a), but no reports on tests of this sort have been submitted to date.

The physical tests were conducted by J & L Testing (1998). A vertical column was used that contained materials simulating the profile expected in the TMA (drainage layer, the P40 filter layer, tailings). Till from the site was used for the drainage layer and the filter layer. The tailings were obtained from previous testing of Crandon ore. Tests were conducted for three levels of overburden pressure and hydraulic gradient to assess whether fines in the tailings would migrate through the filter and into the drainage layer during various filling conditions in the TMA. Results of the tests showed that the tailings were immobile for all conditions that were evaluated. No noticeable build up of tailings in the drainage layer occurred.

The geochemical analyses were set up to evaluate conservative cases. Upper range estimates for the concentrations were used, CO_2 in the gas-phase was assumed to be at atmospheric conditions, and Eh was set for oxidizing conditions. In each case, the fraction of the pore space calculated to be occupied by mineral precipitates was less than 0.1% and the calculated effect on hydraulic conductivity was negligible. Additional analyses were conducted where all of the precipitate mass was assumed to form within 1 m from the leachate collection pipes. Even in these analyses the calculated change in porosity was very small (< 0.02%) and the calculated effect on the hydraulic conductivity was negligible (Steffen, Robertson and Kirsten, 2000 a, b).

II.C.2. Final Cover

The final cover planned for the TMA is a resistive cover design that is widely used for waste containment facilities in seasonal humid climates. Many of the elements in the cover design (Fig. II.A.1a) are similar to the elements in the liner design (Fig. II.A.1b). A composite liner is used as the hydraulic barrier, and a drainage layer is provided to remove water that accumulates on top of the hydraulic barrier. Protective and vegetative layers are placed above the drainage layer. Percolation from the final cover controls the rate of leakage from the TMA during the steady-state period.

Methods used to predict percolation from final covers with composite barriers are less precise than those used for liners. The reason for the lack of precision is that final covers are subjected to more complex hydrological conditions. Unsaturated conditions generally exist in the soil layers overlying the barrier layer, water is extracted from the cover by plants and evaporation, and water pools on the geomembrane only intermittently. In addition, a cover is exposed to thermal cycles that drive flow upward and downward. To date, models have not been developed that accurately simulate all of these processes. As a result, calculations are generally made conservatively to ensure that percolation rates are not under-estimated. The USEPA is currently conducting a study to develop a more thorough understanding of the hydrology of final covers (Bolen et al., 2001).

There are two common methods for predicting percolation rates from resistive final covers that contain geomembranes. One method is to use the HELP Model. The other is to use a combination of Giroud's equation (Eq. II.1) and the Giroud-Houlihan equation (Eq. II.2). The impingement rate in the Giroud-Houlihan equation is assumed to equal a fraction of the annual precipitation. The latter approach was used in this report because it provides more conservative percolation rates, and reduces the impact of uncertainty on the estimated percolation rate.

Field data describing the hydrology of final covers with composite barriers are limited. One long-term study was conducted by Melchior (1997) on a final cover similar in design to that proposed for the TMA and located in a similar climate. The cover consisted (from bottom to top) of a 600-mm-thick compacted clay layer, a 1.5-mm-thick HDPE geomembrane, a 250-mm-thick sand drainage layer, and a 750-mm-thick layer of soil used for protection and vegetation. Melchior recorded percolation rates ranging between 0.1 and 3.0 mm/yr during an eight-year monitoring period, with an average rate of 1.3 mm/yr. Dwyer (2002) reports a similar average percolation rate for a comparable final cover test section located in a semi-arid climate.

The final cover for the TMA will include a GCL instead of compacted clay, a more permeable drainage layer than used in Melchior's study, and the geomembrane will be tested with a leak location survey during installation (see Benson and Grefe 2002 for more detail on the cover design). Leak detection surveys were not implemented by Melchior (1997) or Dwyer (2002). For these conditions, an upper range estimate forn the percolation rate from the TMA cover can be realistically assumed to be 1 mm/yr. Much lower rates may be realized. For example, USEPA's ACAP program is currently monitoring a composite cover with a GCL that has discharged no percolation to date (Benson et al., 2002).

NMC has predicted a percolation rate for the final cover using the HELP Model (0.0005 mm/yr, Foth and Van Dyke, 2001c) that is appreciably lower than the percolation rates reported by Melchior (1997) and Dwyer (2002). Thus, NMC has agreed to field test the cover design and to construct a double composite cover if the field test shows that the proposed cover transmits percolation at a rate higher than NMC has anticipated based on HELP Model analyses. The double composite final cover profile is assumed to consist of two composite barrier layers and two drainage layers. The lower barrier layer and drain consists (from bottom to top) of a soil barrier layer, a GCL, a geomembrane, and a geocomposite drainage layer. The upper barrier layer and drain consists of a GCL, a geomembrane, and a gravel drainage layer. Protective layers similar to those shown in Fig. 2b would be placed on top of the upper gravel drainage

layer. Percolation rates estimated for the proposed cover (single composite design) and the double composite cover are presented in this report.

II.C.3. Tailings

Flow within the tailings is governed by the same principles that control flow of water in soil and other porous media. During filling of the TMA, operation of the decant pond at the surface of the tailings is assumed to result in one-dimensional vertical saturated flow through the tailings. After filling, the tailings will desaturate, and unsaturated flow will occur. Flows during these conditions can be estimated using analytical expressions, the HELP Model, and numerical models.

Flow rates during the saturated flow condition can be estimated with acceptable precision using the one-dimensional form of Darcy's Law:

$$q = K_{st} i \qquad \text{(II.3)}$$

where q is the flow rate per unit area (also known as the discharge velocity, or Darcy velocity), K_{st} is the saturated hydraulic conductivity of the tailings, and i is the hydraulic gradient. Because the TMA is broad and the tailings are deep relative to the depth of water in the decant pond, flow in the tailings will be predominantly vertical. Thus, nearly unit gradient (i=1) flow will occur. For this condition, the flow rate per unit area (discharged from the tailings to the leachate collection system) is approximately equal to the saturated hydraulic conductivity of the tailings (i.e., $q \approx K_{st}$).

Flow rates in a continuously saturated waste mass are not readily estimated using the HELP Model. However, the model can be manipulated (albeit using unrealistic inputs and assumptions) to simulate saturated flow. These manipulations include increasing the precipitation rate above the saturated hydraulic conductivity of the tailings, reducing the runoff coefficient, and raising the relative humidity of the atmosphere to 100%. When the HELP Model is manipulated in this manner, discharge from the tailings will be approximately equal to that predicted using Eq. II.3.

For clarity, Darcy's Law was used for all calculations presented herein regarding discharge rates from the tailings during saturated flow conditions. A unit hydraulic gradient was assumed. Manipulations of the HELP Model were not used.

Eq. II.3 cannot be used to calculate the discharge rate during drain down because the flow occurs under unsaturated conditions. Unsaturated flow can be simulated with the HELP Model, but is more precisely and directly described using numerical models that solve Richards' fundamental equation describing unsaturated flow. Models based on Richards' equation incorporate the effects of capillarity, whereas HELP assumes that flow always occurs under unit gradient conditions. To simulate the physical processes occurring during drain down properly, discharge rates from the tailings were computed using the numerical model HYDRUS-2D, which solves Richards' equation using the finite element method (Simunek et al., 1996).

II.D. LEAKAGE RATES FOR THE TMA

A summary of the physical properties used to describe the liner proposed for the TMA is in Table II.D.1 The GCL used in the liner was assumed to have a hydraulic conductivity of 6.9×10^{-11} m/s, which was measured by NMC at low effective stresses (35 kPa) using a synthetic liquid simulating the non-acidic leachate expected from the TMA. This hydraulic conductivity is believed to be representative and yet conservative, because the tailings are to be de-pyritized and will impose a large effective stress on the liner (>400 kPa when the TMA is filled). The hydraulic conductivity of the leachate collection layer was assumed to be 0.003 m/s. This hydraulic conductivity conservatively assumes that the geocomposite drainage layer on the slope is no more permeable than the gravel on the base. A frequency of 2.5 defects/ha was assumed for the geomembrane. These frequencies are based on recommendations in the literature (e.g., Giroud and Bonaparte, 1989), with consideration that the electrical leak location survey combined with accepted construction quality control (CQC) methods will result in a very high level of quality assurance. This defect frequency corresponds to the residual condition after defects identified by the electrical leak location survey are repaired. The electrical leak location technology has been demonstrated to be very effective at locating defects in installed geomembranes (Darilek et al., 1995; Rollin et al., 1999; Phaneuf and Peggs, 2001).

Sizes for the defects were based on recommendations in Giroud and Bonaparte (1989) for design computations. Giroud and Bonaparte (1989) recommend that circular defects with a diameter of 11 mm be used for computing design flows and that a diameter of 1 mm be used for computing expected flows. The objective of this analysis was to determine an expected leakage rate. Thus, the 1-mm-diameter defect is the appropriate size to use for computations. However, to be conservative, each defect was assumed to consist of one 11-mm-diameter hole and one 1-mm-diameter pinhole.

Properties assumed for the TMA cover are summarized in Table II.D.2. Two conditions were simulated for the cover: (i) design and (ii) reduced performance. Parameters for the design condition are comparable to those proposed for the TMA by NMC. The reduced performance case simulates partial clogging of the drainage layer, as well as a reduction in slope of the drainage layer due to settlement. The hydraulic conductivity of the GCL was not changed because the GCL will be protected by a geomembrane that is surcharged by overlying cover soils.

A reduced performance scenario was considered for the cover, but not the liner, because the cover may have a service life of hundreds of years, which is appreciably beyond the experience record for engineered facilities. The final cover is expected to be replaced at intervals of a few hundred years, or when its performance declines, using a monetary mechanism to be funded by NMC and administered by the Wisconsin DNR. Although the experience record for geosynthetic-based containment facilities is only a few decades long, the lifetime of HDPE geomembranes is estimated to be on the order of several hundreds of years (Hsuan and Koerner, 1998; Bonaparte et al., 2002).

II.D.1 Operations Period

The leakage rate during operations was computed using Eq. II.1. The depth of liquid pooled on the liner was computed using Eq. II.2 assuming an impingement rate equal to the saturated hydraulic conductivity of the tailings ($7x10^{-8}$ m/sec or 2.2 m/yr). The contact parameter ξ was assumed to be 0.007. Other parameters that were used as input are in Table II.D.1. Leakage rates of $5.5x10^{-6}$ mm/yr and $3.3x10^{-4}$ mm/yr were obtained for the side slope and base, respectively.

II.D.2 Drain-Down and Closure Period

The leakage rate during drain down and closure was assumed in this analysis to vary linearly between the leakage rate during operations and the leakage rate at the end of the drain down period. The duration of the drain down period was estimated by conducting an unsaturated flow simulation using the numerical model HYDRUS-2D. A description of the modeling is in Benson and Grefe (2002). The numerical analysis showed that the rate of drainage diminishes rapidly, and then tails off slowly to a negligible amount about 50 years after drain down begins. The approximately exponential drop in drainage rate from the tailings indicates that the assumption of a linear reduction in leakage rate during the drain down period is conservative.

Leakage from the liner system at the end of the drain down period was computed assuming an impingement rate of 1 mm/yr (i.e., the percolation rate from the final cover) and continued operation of the leachate collection system. All other parameters were the same as those used in computations for the operations period. These calculations yielded a leakage rate of 5.2×10^{-9} mm/yr on the side slope and 1.3×10^{-7} mm/yr on the base.

II.D.3 Duration of Post-Closure Transition Period

The duration of the transition period was computed based on a simulation conducted with HYDRUS-2D. Details of the analysis are in Benson and Grefe (2002). This analysis showed that the transition period is relatively small and can be ignored. Accordingly, the steady-state leakage rate was assumed to begin as soon as the drain down period ends.

II.D.4 Post-Closure Steady-State Period

The steady-state condition is when leachate is no longer being pumped from the leachate collection system and the depth of liquid on the liner has accumulated sufficiently so that the leakage rate from the liner equals the percolation rate from the cover (i.e., balanced flows). Thus, the leakage rate during the steady-state period is obtained by estimating the percolation rate from the cover. A separate calculation of leakage from the liner is not required.

Percolation rates were estimated for the final cover design proposed by NMC in the feasibility report (FR; Foth and Van Dyke, 1998g), which employs a single composite barrier layer) and the conceptual double composite cover that would be used if field tests show that the percolation rate from the proposed final cover exceeds the rate predicted during design. The percolation rate for the final cover design in the FR was estimated by conservatively assuming that approximately one-half of the annual precipitation (specifically 400 mm/yr) will infiltrate the surface of the

final cover and ultimate reach the drainage layer. The depth of liquid in the drainage layer corresponding to this impingement rate was computed using Eq. II.2 assuming the parameters in Table II.D.1 and a contact factor of 0.21. A larger contact factor was used for the cover computations because the effective stress on the surface of the barrier layer will be much lower in the cover than on the liner. These computations yield a percolation rate of 0.0016 mm/yr.

Percolation from the double composite final cover was computed using Eqs. II.1 and II.2. Leakage from the upper barrier was conservatively assumed to occur at 1 mm/yr (Benson and Grefe, 2002). Input parameters corresponding to design and reduced performance conditions (Table II.D.2) were used in the computations. The defect frequency for the geomembrane in the lower composite barrier was assumed to be twice that in the upper composite barrier to account for difficulties associated with a leak location survey of a double lined system after construction of the upper composite barrier. The depth of liquid on the lower barrier was computed using Eq. II.2 assuming that the leakage rate from the upper barrier (conservatively estimated at 1 mm/yr) was the impingement rate for the lower drainage layer. Percolation rates between 6.6×10^{-6} and 1.0×10^{-4} mm/yr were obtained using this approach, depending on the input parameters used for Eq. II.1.

In summary, percolation rates for three scenarios were assumed or computed for the final cover: (i) 1 mm/yr (upper range), (ii) 0.0012 mm/yr (proposed design scenario), and (iii) 1.0×10^{-4} mm/yr (largest percolation rate computed for the double barrier scenario). The areal extent of the cover is approximately 3.1 times larger than the areal extent of the base of the TMA. Thus, the steady-state leakage rate from the bottom of the liner will be 3.1 times larger than the percolation rate from the cover (assuming the sideslope drains continue to function as designed, resulting in negligible sideslope leakage). Accordingly, the three estimates of the steady-state leakage rate are (i) 3.1 mm/yr (upper range), (ii) 0.0037 mm/yr (design), and (iii) 0.00031 mm/yr.

II.E. LEAKAGE RATES FOR THE RP

The Reclaim Pond (RP) is a proposed composite lined lagoon used to store leachate and decant water pumped from the TMA (Benson and Grefe 2002 and Foth and Van Dyke 1995a/1998d). A summary of the physical parameters for the RP liner is in Table II.E.1. Two cases were assumed for the upper GCL: design and reduced performance. For the design case, the hydraulic conductivity of the upper GCL was assumed to be 6.9×10^{-11} m/s. The reduced performance condition assumed that the upper GCL has a hydraulic conductivity of 6.9×10^{-10} m/s. This higher hydraulic conductivity reflects that the GCL in the upper liner will be in direct contact with process water in the pond at locations where defects exist in the geomembrane, and will not be prehydrated because it is installed in the upper composite liner. The lower GCL was assumed to have a hydraulic conductivity of 6.9×10^{-11} m/s in both cases because the lower GCL is expected to prehydrate via contact with the subgrade. The defect frequency for the geomembrane in the lower composite liner is assumed to be twice that in the upper composite liner to account for difficulties associated with a leak location survey of a double lined system after construction of the upper composite barrier. As was assumed for the TMA liner, the upper composite liner in the RP was assumed to have 2.5 defects/ha, and each defect was assumed to consist of an 11-mm-diameter hole and a 1-mm-diameter pinhole.

Leakage rates were computed for two conditions: operations and post-closure of the TMA. Operations corresponds to the operations period of the TMA when leachate is being pumped from the decant pond and the leachate collection system. Post-closure corresponds to the period when the TMA is capped and leachate is being pumped from the leachate collection system. The depth of liquid is estimated to be 4.6 m (15 ft) during operations and 2.3 m (7.5 ft) during post-closure (Benson and Grefe, 2002).

Leakage rates for the upper and lower composite liners were computed using Eq. II.1. For the design condition, the leakage rate was 3.9×10^{-4} mm/yr for the operations period and 1.2×10^{-4} mm/yr for the post-closure period. For the reduced performance condition, the leakage rate is 1.1×10^{-2} mm/yr for the operations period and 3.2×10^{-3} mm/yr for the post-closure period.

II.F. SUMMARY

A summary of the leakage rates computed in this review and those predicted by NMC using the HELP model is in Table II.F.1. In general, the leakage rates predicted by NMC are comparable or larger than those predicted in this review. Thus, the leakage rates predicted by NMC should be acceptable for use in computing the source term for the TMA and RP.

The only exception is the long-term steady state case. For this case, the leakage rate depends to great extent on the cover profile that ultimately is used for the TMA. Unless reasonable assurances can be made that the cover will perform with a very low percolation rate (e.g., using a field demonstration), the most conservative estimate of the long-term leakage rate (3.1 mm/yr) should be used for the source term computations.

III. OXYGEN TRANSPORT IN THE TMA

III.A TRANSPORT MECHANISMS

Oxygen transport is a critical issue for the TMA because the rate at which oxygen is delivered to the waste will control the rate at which oxidation occurs. Oxygen may be delivered to the waste by different mechanisms and along different pathways. The primary mechanisms of oxygen transport are advection and diffusion in the liquid and gas phases. The primary access paths are the open upper surface of the TMA (during operations), the closed upper surface of the TMA (after installation of the cover), and the sideslopes and base of the TMA.

III.A.1 Liquid-Phase Transport of Oxygen

Liquid phase advection occurs when water flows into the waste due to precipitation onto the open waste surface (before closure) or by percolation from the final cover (after closure). Dissolved oxygen flows into the waste along with the water molecules (in effect, the water molecules drag the oxygen molecules along with the flow). Liquid-phase advection may also occur through the sideslopes and base of the TMA as well. However, given that these areas are covered with a composite barrier system and are appreciably below ground surface (but above the water table), ingress of water across the sideslopes and base can be assumed to be negligible.

Liquid-phase diffusion of oxygen occurs when a gradient in oxygen concentration exists in the pore water. In the TMA, gradients in oxygen concentration will exist because the waste will consume nearly all of the oxygen within the pore water, whereas water entering the waste from the surrounding environment will have a dissolved oxygen concentration consistent with the surrounding biological and geochemical conditions. In general, liquid-phase diffusion of oxygen generally is not appreciable because oxygen has very low solubility in water (nearly always less than 10 mg/L, and generally less than 4 mg/L in natural systems) and the free solution diffusion coefficient for water is small (approximately four orders of magnitude smaller than the diffusion coefficient in air).

III.A.2 Gas-Phase Transport of Oxygen

Advection of oxygen occurs when air in the atmosphere flows into the waste. Because air contains 21% oxygen, air flow is tantamount to oxygen flow. Air will only flow into the waste when the waste is unsaturated, and the only significant pathway is through the open surface of the tailings or through the final cover. Air flow is driven by pressure gradients caused by wind and changes in barometric pressure, the latter being the most significant.

Gas-phase diffusion of oxygen occurs when a gradient in oxygen concentration exists between the atmosphere and the gas-filled pore space in the waste. A concentration gradient will nearly always exist between the waste in the TMA and the atmosphere because of the preponderance of oxygen in air and the rapid consumption of oxygen by the waste.

III.A.3 Relative Importance of Transport Mechanisms

Kim (2000) conducted an analysis to determine the relative contributions of each mechanism to oxygen transport in closed mine waste containment systems comparable to the TMA. Kim's analysis showed that gas-phase diffusion always was the dominant mechanism. In particular, the flux of oxygen by gas-phase diffusion was 100-1000 times higher than the flux due to any other mechanism.

A similar analysis was prepared by NMC and reported in GWQPE Appendix C1 (Steffen, Robertson and Kirsten, 1998a) and GWQPE Appendix C2 (Steffen, Robertson and Kirsten, 1999c). Their conclusions were essentially the same as those drawn by Kim, except their calculations showed that gas-phase advection after closure contributed nearly the same flux of oxygen as gas-phase diffusion. However, the analysis of gas-phase advection in GWQPE Appendix C1/C2 ignored the soil layers above the geomembrane in the cover, and these layers cause an appreciable reduction in the advective oxygen flux (Kim 2000). Thus, an analysis based on gas-phase diffusion alone is adequate. Accounting for gas-phase advection using the approach in GWQPE Appendix C1/C2 is conservative, but unnecessary.

III.A.4 Relative Importance of Transport Pathways

GWQPE Appendix C1 (Steffen, Robertson and Kirsten, 1998a) presents an analysis to determine the relative importance of various pathways for oxygen transport into the TMA. Fluxes were

computed for the transport through the surface of the exposed waste, the final cover over the closed TMA, the sidewalls of the TMA, and the base of the TMA. The analysis showed that the exposed surface of the waste is the dominant pathway prior to placement of the final cover on the TMA. After the cover is in place, the analysis showed that the flux across the cover was comparable to that across the sidewalls of the TMA. In all cases, the flux from the base of the TMA was very small relative to the fluxes along other pathways. The analyses presented in GWQPE Appendix C1 ignored oxygen transport through appurtenances such as leachate collection lines and clean out lines. Although appurtenances can be sources of oxygen, their small area and the use of sumps to maintain saturated conditions render their overall effect on oxygen transport as negligible.

The analyses presented in GWQPE Appendix C1/C2 used very conservative assumptions when computing the flux across the sidewall and base of the TMA. A very high diffusion coefficient was assumed for the geomembrane, and the soil outside the TMA was assumed to be completely dry. Neither of these conditions will be realized for the TMA, and the flux across the sidewalls almost certainly will be much lower that that across the cover.

An analysis evaluating the relative contributions of diffusive oxygen flux through the intact geomembrane and defects in the geomembrane was also presented in GWQPE Appendix C1/C2. The geomembrane was conservatively assumed to have an oxygen diffusion coefficient of 10^{-12} m^2/s. This analysis showed that the oxygen flux through defects is appreciably larger than the oxygen flux through the intact geomembrane. Kim (2000) draws a similar conclusion, and indicates that oxygen transport across a final cover comparable to that proposed for the TMA can be computed assuming that transport only occurs through the defects in the geomembrane.

The analyses presented in GWQPE Appendix C1/C2 and Kim (2000) show that the primary pathway for oxygen transport is the exposed waste (during operations and consolidation) and the final cover (after closure). Moreover, the primarily pathway through the final cover is through defects in the geomembrane. Including the flux across the sidewalls of the TMA and through the intact geomembrane will make the analysis more conservative. However, incorporating these additional transport pathways is not necessary.

IIII.B TRANSPORT PERIODS AND FLUXES

Oxygen transport into the waste can be divided into three periods: (i) operations, (ii) drain down prior to placement of the final cover, and (iii) after placement of the final cover. The following discusses the operative transport mechanisms during these periods and the oxygen fluxes likely to be realized.

III.B.1 Transport During Operations

During operations, tailings will be continuously deposited into the TMA as a slurry via a series of spigots. The spigots will be operated in a sequential fashion around the rim of the TMA so that the TMA is filled in a uniform manner. Because deposition will occur as a slurry, the tailings will be saturated when deposited. After deposition, the tailings will simultaneously consolidate and dry due to evaporation. These processes will compensate each other, resulting in tailings that remain saturated or nearly saturated during operations. Moreover, tailings that

become unsaturated will remain so only for a short period due to the nature of the sequential deposition of tailings from the spigots (deposition of slurry over existing unsaturated tailings will re-saturate underlying unsaturated tailings). Consequently, oxygen transport into the tailings can be assumed to occur under saturated conditions during operations.

An exception to this assumption would occur if operations are ceased temporarily or intermittently. If this were to occur, then the tailings would desaturate due to drainage and evaporation. Oxygen fluxes under this condition would be treated using the methods appropriate during drain down, which are described in Section III.B.2.

Oxygen transport into the saturated tailings consists of liquid phase advection and liquid phase diffusion. Gas phase transport will not occur unless the tailings desaturate.

Liquid phase advection occurs due to water that flows into the pores as a result of infiltration. The advective flux of oxygen is computed as the product of the oxygen concentration in the liquid, the porosity, and the rate of infiltration. The maximum rate of water flow due to infiltration approximately equals the saturated hydraulic conductivity of the tailings (7×10^{-8} m/s, Section II.D.1). However, the actual rate of water flow will be lower because of upward flow due to consolidation. In a natural or industrial environment, a reasonable upper range estimate of the oxygen concentration is 4 mg/L. If the porosity of the tailings is assumed to be 0.6 and the oxygen concentration is assumed to be 4 mg/L, then the oxygen flux due to liquid phase advection is 0.3 moles $0_2/m^2$-yr. This flux is comparable to the liquid phase advective flux reported in GWQPE Appendix C1, which is 0.5 moles $0_2/m^2$-yr.

Liquid phase diffusion occurs due to gradients in oxygen concentration in the pore water. The liquid phase diffusive flux (J_{dl}) can be computed as:

$$J_{dl} = C_o \sqrt{rD} \qquad \text{(III.1)}$$

where C_o is the concentration of oxygen in the liquid at the surface of the tailings, r is the reaction rate, and D is the effective liquid-phase diffusion coefficient. Eq. III.1 applies to first order reactions in a semi-infinite domain with constant concentration at the surface (Crank, 1979). The effective liquid-phase diffusion coefficient can be estimated as the product of the porosity, tortuosity, and the diffusion coefficient of oxygen in water (2×10^{-9} m^2/s, Cussler, 1997). If the porosity is assumed to be 0.6, the tortuosity is assumed to be 0.5, the concentration is assumed to be 4 mg/L, and the reaction rate is assumed to be 1.5×10^{-6} s^{-1} (an upper range estimate computed using the consumption rate in Sec. I.B.3.6.1), then an upper range estimate of the liquid-phase diffusive flux is 0.18 moles $0_2/m^2$-yr. This estimate is more than an order of magnitude lower than the upper bound liquid-phase diffusive flux reported in GWQPE Appendix C1 (6.0 moles O_2/m^2-yr). However, the calculations reported here were made using a reaction rate for the depyritized tailings. No calculations for liquid-phase diffusion were provided by NMC using a reaction rate for the depyritized tailings. The oxygen flux reported in GWQPE Appendix C1 was computed using the reaction rate for the tailings before depyritization was considered.

The total liquid-phase oxygen flux can be estimated as the sum of the advective and diffusive fluxes. For this analysis, the total flux is 0.48 moles $0_2/m^2$-yr. In contrast, the upper bound estimate in GWQPE Appendix C1 is 6.5 moles $0_2/m^2$-yr. Thus, the upper bound estimate provided in GWQPE Appendix C1 should be conservative and reasonable.

III.B.2 Transport During Drain Down

Liquid and gas phase transport can occur during drain down. However, as cited in Section III.A, when both liquid and gas phase transport occur, gas-phase diffusion is by far the dominant mechanism of oxygen transport. The diffusive flux prior to placing interim cover on top of the tailings can be calculated using Eq. III.1. For this analysis, the concentration C_o is the concentration of atmospheric oxygen (8.9 moles O_2/m^3), D is the effective diffusion coefficient for the unsaturated tailings, and r is the reaction rate.

A variety of methods can be used to estimate the effective diffusion coefficient. An analysis by Kim and Benson (1999) shows that comparable estimates of flux are obtained regardless of the method used (i.e., the method selected to estimate the diffusion coefficient is not particularly important). Thus, for this analysis, the Elberling equation was used (Elberling et al., 1993):

$$D = \tau D_a [1-\Theta]^a + \tau\Theta D_w/K_H \qquad \text{(III.2)}$$

where D_a is the free diffusion coefficient of oxygen in air ($2x10^{-5}$ m^2/s, Cussler, 1997), D_w is the free diffusion coefficient of oxygen in water, τ is a tortuosity factor ($\approx$ 0.3), a is an empirical coefficient ($\approx$ 3.3), Θ is the water saturation, and K_H is Henry's constant for oxygen. The Elberling equation provides a composite effective diffusion coefficient corresponding to liquid and gas phase diffusion. However, the liquid-phase component is only significant when the tailings are nearly saturated.

The water saturation used in the Elberling equation decreases as the tailings as the tailings drain during the drain down period. To determine representative water saturations as a function of time, unsaturated flow simulations were conducted using the unsaturated flow model HYDRUS-2D. These simulations are described in Benson (2000a). Lower Range (LR) and Upper Range (UR) reaction rates for depyritized tailings were used in the analysis ($2.2x10^{-7}$ and $1.6x10^{-6}$ s^{-1}, respectively; from Tables I.B.2 and I.B.3, corrected for bulk density of the tailings). A summary of the fluxes is in Table III.A.1 along with the depth of oxygen penetration. The fluxes range between 16.6 and 313.4 moles O^2/m^2-yr depending on the reaction rate and the time during drain down.

A sensitivity analysis was presented in GWQPE Appendix C1 and determined an upper-bound estimate of the flux during the first three years of drain down. For first order reactions, they report an oxygen flux of 609 moles O^2/m^2-yr. In contrast, this analysis yielded a maximum flux during the first three years ranging between 85-229 moles O^2/m^2-yr depending on the reaction rate that was used in the analysis. Thus, the flux estimated in GWQPE Appendix C1 should be conservative.

III.B.3 Transport After Placing the Final Cover

The analysis by Kim (2000) showed that gas phase diffusion is the dominant mechanism affecting oxygen transport in mine waste containment facilities with composite caps. The primary transport pathway is through defects in the geomembrane. An analysis of gas-phase diffusion of oxygen was conducted with the finite element model developed by Kim (2000) for the final cover over the TMA. Details of the analysis are described in Benson (2000b, 2002).

The analysis showed that the steady-state oxygen flux after placing the final cover could range between 0.8 and 9.0 moles O_2/m^2-yr depending on the hydrologic conditions within the soil layers overlying the geomembrane. A similar analysis presented in GWQPE Appendix C1 yielded a steady-state oxygen flux of 1.5 moles O^2/m^2-yr.

IV. ANTICIPATED WATER CHEMISTRY WITHIN THE TMA AND THE RECLAIM POND

IV.A GEOCHEMICAL MECHANISMS AFFECTING WATER QUALITY

The primary geochemical processes that are anticipated to affect water quality within the Tailings Management Area and the Reclaim Pond are oxidation of sulfide minerals, neutralization of acid, precipitation and dissolution of secondary minerals, and adsorption and ion exchange. Each of these processes is discussed below.

IV.A.1 Sulfide Mineral Oxidation

The principal environmental concerns associated with tailings impoundments and waste-rock piles result from the oxidation of sulfide minerals within the waste materials, and the transport and release of oxidation products. The principal sulfide minerals in mine wastes are pyrite and pyrrhotite. The oxidation of pyrite can be described through the equation:

$$FeS_2 + \frac{7}{2}O_2 + H_2O \rightarrow Fe^{2+} + 2SO_4^{2-} + 2H^+ \qquad \text{(IV.1)}$$

This reaction consumes pyrite, oxygen and water, generates low pH conditions and releases Fe(II) and SO_4 to the water flowing through the mine waste. The Fe(II) released by sulfide oxidation may be oxidized to Fe(III) through the reaction:

$$Fe^{2+} + \frac{1}{2}O_2 + H^+ \Leftrightarrow Fe^{3+} + \frac{1}{2}H_2O \qquad \text{(IV.2)}$$

The resulting Fe(III) may precipitate as a ferric oxyhydroxide phase, through a reaction of the form:

$$Fe^{3+} + 3H_2O \Leftrightarrow Fe(OH)_3 + 3H^+ \qquad \text{(IV.3)}$$

Alternatively, Fe(III) may oxidize additional pyrite or other sulfide minerals through reactions of the form:

$$FeS_2 + 14\,Fe^{3+} + 8\,H_2O \rightarrow 15\,Fe^{2+} + 2\,SO_4^{2-} + 16\,H^+ \qquad \text{(IV.4)}$$

Within mine wastes, sulfide oxidation proceeds rapidly, and is catalyzed by chemolithotrophic bacteria of the *Thiobacillus* group (Boorman and Watson, 1976).

In addition to the iron-sulfide minerals, other metal-sulfide minerals are susceptible to oxidation, releasing elements such as As, Cd, Co, Cu, Ni, Pb, Zn to the water flowing through the mine waste.

The rate of sulfide oxidation in mine tailings can be described by numerical models, which couple oxygen transport mechanisms with consumption by sulfide mineral oxidation. Davis and Ritchie (1986, 1987) and Davis and others (1986) developed a series of numerical models that couple oxygen gas transport through the pore space of a tailings impoundment by diffusion, with oxygen transport through an alteration rim surrounding the primary sulfide grain. Other models couple gas transport to oxygen consumption at the mineral surface (e.g., Scharer et al., 1984). Comparison of model calculations with field data suggest that this model provides a reasonable description of sulfide-mineral oxidation in mine tailings impoundments (Blowes and Jambor, 1990; Blowes et al., 1991). Calculations conducted using these models suggest that the peak period of oxidation occurs shortly after tailings deposition, as sulfide minerals near the impoundment surface are consumed rapidly. The rate of sulfide oxidation gradually decreases as the depth to unaltered tailings increases, and as alteration rims accumulate on particle surfaces. The duration of sulfide oxidation depends on the thickness of the vadose zone and the sulfide content of the tailings, and can persist for very long periods. For example, Blowes and Jambor (1990) estimated that sulfide oxidation will continue at the Waite Amulet tailings impoundment, Noranda, Quebec, for more than 500 years.

IV.A.2 Acid Neutralization

The oxidation of sulfide minerals results in acidification of the pore water in a waste rock pile or a tailings impoundment, and releases high concentrations of dissolved metals. This acidic water reacts with the non-sulfide gangue minerals within the mine wastes. Acid-neutralization reactions consume H^+, resulting in a progressive increase in the pH along the flow path. The most significant pH-buffering reactions are the dissolution of carbonate minerals, aluminum hydroxide and ferric oxyhydroxide minerals, and aluminosilicate minerals.

The most abundant carbonate minerals in the Crandon mine wastes are dolomite ($CaMg(CO_3)_2$), ankerite ($CaFe(CO_3)_2$), siderite ($FeCO_3$) and calcite ($CaCO_3$). The dissolution of dolomite can be described as:

$$CaMg(CO_3)_2 + 2\,H^+ \Leftrightarrow Ca^{2+} + Mg^{2+} + 2\,HCO_3^- \qquad \text{(IV.5)}$$

Dissolution of these minerals has the potential to raise the pH of the pore water to near neutral. Carbonate mineral dissolution releases Ca, Mg, and cations such as Mn that are included as impurities, and increases the alkalinity of the water. At many sites, the mass of carbonate minerals contained in the mine wastes is large when compared to the mass of sulfide minerals, and the rapid dissolution of carbonate minerals is sufficient to maintain neutral pH conditions through the mine waste pile. Neutral pH conditions have been observed in tailings impoundments derived from processing of vein-type gold deposits in the Timmins and Red Lake areas of Ontario (Blowes et al., 1995; McCreadie et al., 1999).

The wastes derived from the processing of massive sulfide ores frequently contain a sulfide content in excess of the carbonate neutralization capacity. At these sites the available carbonate content is quickly consumed, with the most soluble and most reactive carbonate minerals depleted first. At many sites, calcite is depleted initially, followed by dolomite/ankerite and siderite (Blowes and Ptacek, 1994). As the carbonate content of the waste dissolves, the pH is buffered to near neutral. Under the neutral pH conditions maintained by carbonate mineral dissolution, the precipitation of crystalline and amorphous metal hydroxide phases is favored. After the carbonate minerals contained in the waste are depleted, the pH of the pore water falls until equilibrium with the most soluble of the secondary hydroxide minerals is attained. Field studies at several mine tailings impoundments have indicated that the initial hydroxide mineral to dissolve is $Al(OH)_3$, buffering the pH in the region of 4.0 to 4.5 (Dubrovsky, 1986; Blowes and Jambor, 1990; Johnson, 1993). After the secondary $Al(OH)_3$ present in the tailings has been depleted, the pH falls until equilibrium with an iron oxyhydroxide mineral, has been attained, typically ferrihydrite or goethite. Dissolution of ferric oxyhydroxide minerals typically maintains pH values in the range of 2.5 to 3.5.

Throughout the period of carbonate and hydroxide mineral dissolution, the aluminosilicate gangue minerals also dissolve, consuming H^+, and releasing H_4SiO_4, Al^{3+}, and other cations such as K, Ca, Mg and Mn to the pore water. Although aluminosilicate dissolution is generally not rapid enough to buffer the pore water to a specific pH, these reactions consume H^+. In addition, Al and other metals released from aluminosilicate minerals may accumulate in secondary minerals that act as secondary pH buffers.

The sequence of pH buffering reactions observed within mine tailings impoundments results in a progressive increase in the pore-water pH along the groundwater flow path. These changes in pH occur as long zones of relatively uniform pH, which are dominated by a single pH buffering reaction, separated by fronts or relatively sharp changes in pH as a buffering phase is depleted. Field data from the Nickel Rim mine tailings impoundment presented by Johnson (1993) illustrate a pH buffering sequence observed at a field site. At the Nickel Rim site, the pH of the pore water at the base of the impoundment is near neutral, varying from 6.5 to 7.0. Geochemical calculations indicate that the pore water in this zone approaches or attains equilibrium with respect to calcite. Overlying the calcite-buffered zone, calcite is absent from the tailings and the pH is buffered by the dissolution of the ferrous carbonate mineral siderite, and possibly by the dissolution of dolomite. The complete depletion of carbonate minerals is accompanied by a sharp decline in pH from 5.8 to 4.5. Immediately above the depth of carbonate mineral depletion, the pH is relatively uniform, varying from 4.0 to 4.5 and the pore water approaches or attains equilibrium with respect to the aluminum hydroxide mineral gibbsite ($Al(OH)_3$). Near the

surface of the impoundment, the pH falls sharply from 4.0 to 3.5, then more gradually from 3.5 to approximately 2.5. Throughout this decrease in pH the pore water is under-saturated with respect to ferrihydrite, and approaches equilibrium with respect to the crystalline iron oxyhydroxide mineral goethite.

IV.A.3 Formation of Secondary Minerals and Attenuation of Dissolved Metals

Sulfide oxidation and acid neutralization reactions occurring in mine tailings impoundments and waste rock piles generate high concentrations of dissolved constituents. At many locations throughout these wastes the concentrations of dissolved constituents exceed the solubilities of secondary minerals, which accumulate in the wastes or in underlying aquifers. The precipitation of secondary minerals limits the concentrations of dissolved major ions and dissolved metals in the waste-derived waters, and in some cases, accumulations of secondary minerals are sufficient to decrease the porosity and permeability of the waste materials or underlying aquifers (Blowes et al., 1991).

The most abundant dissolved constituents derived from sulfide oxidation and acid neutralization reactions are SO_4, Fe(II), Fe(III), and the major cations Ca, Mg, K, Na, and HCO_3^-. These dissolved constituents react in the effluent waters, resulting in the precipitation of a number of secondary minerals including gypsum ($CaSO_4 \cdot 2H_2O$), jarosite ($KFe_3(SO_4)_2(OH)_6$), geothite (FeOOH), ferrihydrite ($Fe_8(OH)_9$), siderite ($FeCO_3$), and rarely, melanterite ($FeSO_4 \cdot 7H_2O$). The precipitation and dissolution of these phases limits the dissolved concentrations of the major ions in the pore water and provides substrate for the attenuation of dissolved metals.

In addition to affecting the aqueous concentrations of the major ions, precipitation-dissolution reactions limit the concentrations of some dissolved metals. The formation of the lead sulfate mineral anglesite has been observed to limit dissolved Pb concentrations at several mine sites (Boorman and Watson, 1976; Blowes and Jambor, 1990). The formation of secondary covellite (CuS) on the surfaces of pyrrhotite and sphalerite has been observed to limit dissolved copper concentrations (Boorman and Watson, 1976; Johnson, 1993).

IV.A.4 Adsorption and Ion Exchange

The precipitation of secondary minerals limits the maximum concentrations of many dissolved elements within tailings impoundments. At concentrations that do not attain saturation with respect to secondary minerals, dissolved metal concentrations may also be limited by adsorption on the surfaces of primary minerals present in the tailings or to the surfaces of secondary iron and aluminum hydroxide minerals. Jambor and Owens (1993) indicated that goethite precipitated in the vadose zone of the Nickel Rim mine tailings impoundment contained up to 0.9 wt.% Ni. Jambor and others (1991) identified goethite as the primary host for adsorbed As in the inactive mine tailings impoundment at the Delnite gold mine near Timmins, Ontario. Adsorption on iron and aluminum hydroxide phases is strongly pH dependent with more extensive adsorption occurring as the pH increases (Dzombak and Morel, 1990). The progressive increase in pH observed along the flow path within tailings impoundments results in an increase in the potential for attenuation of dissolved metals as the pore water migrates along that flow path. Although adsorption may provide an important sink for dissolved metals within the tailings impoundment,

these mechanisms were not considered by NMC in the evaluation of the potential concentrations of dissolved elements in the leachate expected from the TMA and will not be addressed in detail herein.

IV.B. OPERATIONS PERIOD

IV.B.1 Volume and Composition of Water in the TMA and Reclaim Pond

Water present in the TMA would be derived from two principal sources, water discharged to the TMA by milling operations and water entering the TMA surface as rain and snow. Water discharged to the TMA from the mill would be derived from a number of sources, principally the differing mill circuits used for the recovery of various metals. The TMA would also receive discharge from site laboratory operations. NMC has estimated the volumes and compositions of each of these streams and has combined these estimates to prepare a prediction of the overall water composition entering the TMA. Throughout the mining operation water would be recovered from the TMA discharge and recycled through the mill. Recycling water would result in an increase in the concentration of dissolved constituents. In the analysis performed by NMC, the increase in dissolved constituents due to water recycling was not addressed. The concentrations of calcium and sulfate, however, were increased to account for the contributions from milling reagents.

Estimated concentrations of dissolved constituents contained in the water that is expected to be discharged from the mill into the TMA with the tailings solids was presented in GWQPE Appendix B (Steffen, Robertson and Kirsten, 1999d). This water was assumed to be a combination of waters derived from differing process streams within the mill. The water chemistry of these streams was weighted according to the relative volumes of water contained within the process circuits. The components included in this mass balance, and their relative volumes, are listed in Table IV.B.1 (Table 1 of GWQPE Appendix B). The values presented in Table IV.B.1 are consistent with those in Table 5.4-1 of Foth and Van Dyke (1998g).

NMC anticipates that the mill-process water will be dominated by the effluent from the Zinc Tails Thickener Overflow (ZTTO), with lesser contributions from the Depyritized Tailings Process Water (DTPW), the Zinc Concentrate Thickener Overflow (ZCTO) and the Pyrite Backfill Overflow (PBPO). Because the ZTTO stream and the ZCTO stream are assumed to have the same composition, this water is expected to comprise about 65% of the water discharged to the TMA. Combined, the lead and copper recovery circuits are expected to contribute approximately only 5% of the total discharge to the TMA.

The concentrations of the solutes in the mill-streams expected to be discharged to the TMA were estimated from the composition of water derived from different stages of the metallurgical testing program. The concentrations and weighting for each of the streams is estimated in Table 2 of GWQPE Appendix B (see Table IV.B.2). The composition of the process water streams is considered in detail below in Section IV.B.3.1.

IV.B.2 Relative Importance of Geochemical Mechanisms during TMA Operation

Tailings solids and process water will be discharged continuously to the TMA from the mill, as described previously. The mechanisms that are likely to alter the composition of the tailings pore water following deposition in the TMA are sulfide oxidation, dissolution of primary tailings minerals and precipitation of secondary minerals within the tailings mass.

Throughout the tailings deposition program the point of tailings discharge will be alternated on a regular basis, resulting in frequent deposition of fresh tailings on the exposed beaches (Section 5.4.2.1 of Foth and Van Dyke, 1998g). The continual discharge of tailings will result in burial of exposed tailings with fresh material. The constant addition of mill process water is expected to result in high moisture contents within the freshly deposited tailings. The diffusion coefficient of saturated tailings is low (approximately 5×10^{-11} m^2/s). The high moisture content of the tailings and the relatively brief period of exposure should be sufficient to limit the zone of extensive sulfide oxidation to near the impoundment surface in the beach areas during the period of active tailings deposition. Layers of oxidized sulfide materials have been observed in other tailings impoundments following the completion of tailings deposition. These layers, commonly referred to as paleosurfaces, can be identified by the partial oxidation of sulfide minerals and by the occurrence of plant detritus (Blowes and Jambor, 1990). Typically the pore water associated with these layers is similar to the water present in the bulk of the tailings mass, suggesting that increases in concentrations of dissolved constituents associated with the formation of paleosurfaces are minor.

In the absence of sulfide oxidation, the most significant changes in pore water composition following tailings deposition are likely to be associated with three sources: 1) the dissolution of primary minerals contained in the tailings as they are discharged to the impoundment, 2) the oxidation of thiosalts contained in the mill-effluent water discharged into the tailings impoundment with the tailings, and 3) the dissolution of oxidation products associated with the waste rock that will be deposited in the tailings impoundment along with the tailings.

The estimated abundances of minerals within the depyritized tailings in the TMA are listed in Table 2-5 of the GWQPE (derived from the modal analysis presented in GWQPE Appendix A2). Of the mineral phases listed in Table 2-5, those most likely to dissolve within the TMA are the carbonate and iron oxyhydroxide minerals. The most abundant carbonate minerals expected to be within the TMA are ferroan dolomite, magnesian siderite and ferroan siderite (Table 1 of GWQPE Appendix A4). The rates of dissolution of the iron hydroxide minerals and the carbonate minerals identified to be present in the tailings material are anticipated to be sufficiently rapid that equilibrium will be attained between these minerals and the tailings pore water during the residence period of pore water within the TMA.

The oxidation of thiosalts contained in the water will generate sulfate and increase the free acidity of the pond water in the TMA. The extent of thiosalt oxidation will depend on the season, with extensive oxidation occurring during warm summer months and slower oxidation occurring in the winter when temperatures are low and oxygen concentrations may be limited by ice covering the tailings. The spring season has the greatest potential for the disruptive effects of thiosalt oxidation to become most apparent. The rapid oxidation of high concentrations of

thiosalt that accumulate over the winter has the potential to result in acidic conditions within the TMA pond.

The addition of waste rock to the TMA will result in an increase in the concentrations of dissolved constituents. The waste rock will be exposed to oxygen during storage in the waste rock storage area, prior to placement in the TMA. A portion of the oxidation products accumulated on the surfaces of the waste rock will be released to water in the TMA, and will contribute to solute concentrations in the TMA pond water and the tailings pore water within the TMA.

IV.B.3 Prediction of Equilibrated Pore Water Quality

IV.B.3.1 Process Water Streams

IV.B.3.1.1 NMC Estimates of Solute Concentrations from the Process Water

The concentrations of the solutes in the mill streams expected to be discharged to the TMA were estimated from the composition of water derived from different stages of the metallurgical testing program. The concentrations and weighting for each of the streams is estimated in Table 2 of GWQPE Appendix B (see Table IV.B.2). The complete chemical analysis of the Process Water from the depyritized tailings and the pyrite concentrate process water are provided in Attachment D of GWQPE Appendix A1. Where specific water streams were not available, the concentrations were estimated using substitutes for the specific process streams. For example, the Pyrite Backfill Overflow water quality was estimated from the process water quality measured for the pyrite concentrate effluent. The effluent water from the zinc concentrator was assumed to be similar to the zinc tailings process water.

The pilot plant operation did not include components that simulated the concentrations of dissolved constituents in the Lead Hydroseparator Overflow, the Lead Concentrator Overflow, and the Copper Concentrator Overflow. The concentrations of dissolved constituents in these flow components were estimated using the equilibrated process water from the depyritized tailings testing program.

IV.B.3.1.2 Variability in the Process Water

The two principal mill water streams discharged the TMA will be water derived from the zinc tails thickener overflow (ZTTO) and the depyritized tailings process water (DTPW). Through a sensitivity analysis, NMC evaluated the effect of substantial changes in the magnitudes of the flows of these process water streams (Steffan, Robertson and Kirsten, 2000b). The sensitivity analysis extended beyond the changes that could reasonably be anticipated in the course of normal operations. One of the sensitivity cases included increasing the flow rate of the DTPW by a factor of two and decreasing the flow rate of the ZTTO to compensate. A second case included increasing the ZTTO flow rate by a factor two and decreasing the DTPW by a compensating volume. The results of these changes are presented in Table 2.1 of Steffan, Robertson and Kirsten (2000b) (see Table IV.B.3). The changes in the concentrations that arise from these unrealistically large changes in the discharge of mill water are modest. These results suggest that

day–to-day variations in the relative proportions of effluent streams discharged to the TMA are unlikely to result in dramatic changes in the composition of the process water.

The concentrations of dissolved constituents in the lead hydroseparator overflow (LHSO), the lead concentrator overflow (LCO) and the copper concentrator overflow (CCO) were estimated using the equilibrated process water from the depyritized tailings testing program. This assumption is more questionable than those noted above. The potential effects of this assumption were assessed through a sensitivity analysis. The rationale for this assumption is the similarity between the pH of the equilibrated depyritized tailings effluent water and the pH expected for the LHSO, LCTO and the CCTO. The volumes of these streams are small when compared to the overall volume of water flowing to the TMA, but the concentrations of many dissolved constituents are lower in the equilibrated depyritized tailings effluent than in the other tailings process water streams. An alternate selection of the process water stream would result in slightly higher concentrations of some dissolved metals; the greatest difference would be observed if the process water derived from the lead and copper circuits were more similar to the Pyrite Backfill Overflow water chemistry. This most significant difference would be an approximately 20% greater concentration of dissolved Zn (increase from 6.9 mg/L to 8.6 mg/L). There are no secondary phases included at this stage of the evaluation for Zn, and as a result this 20% difference would carried through to the source term estimate for the operational phase of the TMA.

In the current NMC calculations (GWQPE Appendix B), the predicted Zn concentration within the TMA is less than the Wisconsin DNR Preventative Action Limit (PAL) by approximately a factor of 100 (ch. NR140, Wisconsin Administrative Code). Consequently, an alternate choice of water chemistry for the Lead Hydroseparator Overflow, the Lead Concentrator Overflow, or the Copper Concentrator Overflow most likely would not result in a significantly different conclusion with respect to the facility compliance at the TMA or Reclaim Pond Design Management Zone (DMZ) Boundaries (see Table IV.B.4).

The analysis conducted by NMC of TMA water quality assumes that mill-discharge water will be used to convey the tailings to the TMA and that this water will form the basis for the pore water that resides in the TMA during operations and after closure. An alternative approach would be to remove the mill water from the tailings prior to discharge, and to use an alternative water source, such as mine-pumpage water or treated wastewater, for a portion of the slurry used to convey tailings to the TMA.

Through a sensitivity analysis, NMC evaluated the effect of substituting mine water for the Depyritized Tailings Process Water (DTPW) stream. The sensitivity analysis is documented in Steffan, Robertson and Kirsten (2000b). The composition of the mine water in this comparison was derived from the last five of seven flushes of the unweathered ore and waste rock columns. The comparison between the expected mill process water and the process water derived from substituting mine water for the DTPW stream suggests that the change in water quality that arises from this mixture is modest (see Table IV.B.5).

IV.B.3.1.3 Additional Sensitivity Analyses for Mill Process Water

Supplemental sensitivity analyses were conducted on the makeup of the carriage water used to pump the tailings to the TMA to evaluate additional alternatives. One sensitivity analysis conducted for NMC substituted mine water for the total DTPW stream (Steffan, Robertson and Kirsten, 2000b). Additional sensitivity analyses were conducted for this review by substituting mine water for the Zinc Tailings Thickener Overflow (ZTTO) water. Three analyses were conducted, the first compares the water chemistry assuming that 1800 L/m (475 gpm) of ZTTO water is replaced by mine water. This volume is consistent with the volume of DTPW replaced in the sensitivity analysis conducted for NMC. The second analysis assumes that 1130 L/m (300 gpm) of the ZTTO water is replaced. This volume is similar to the minimum estimate of mine water that will require pumping (Carlson, 2001). The third analysis is based on replacing 2260 L/m (600 gpm) of the ZTTO stream with mine water. This volume represents NMC's proposed maximum mine pumping rate for project operation (NMC, 2001c). The results of this comparison are presented in Table IV.B.6. These results indicate that there is no clear advantage to using the mine water to transport tailings from the mill to the TMA.

The selection of mine-water composition used in the NMC sensitivity analysis differs from the composition presented by NMC in Table 3-2 of Foth and Van Dyke (1998c). The concentrations of dissolved constituents vary between these two estimates of mine water. An analysis was conducted to evaluate the effects of these differences in mine water chemistry. The sensitivity analysis was conducted using the NMC sensitivity analysis as a base case, replacing 1800 L/m (475 gpm) of DTPW with mine water (see Table IV.B.7). The results of this comparison also indicate that there is no clear advantage to using the mine water to transport tailings from the mill to the TMA.

A sensitivity analysis was also conducted to assess the change in carriage water composition that would result from replacing a portion of the process water with treated effluent discharged from the wastewater treatment plant. This analysis assumes that 1420 L/m (375 gpm) of either the DTPW stream or the ZTTO stream is replaced by the treated effluent water from the wastewater treatment plant. A discharge of 1420 L/m (375 gpm) from the wastewater treatment plant is predicted by NMC for their "average conditions" mine pumping rate of about 400 gpm (Figure 6-1 of Foth and Van Dyke, 1995a/1998d). Regardless of actual conditions, the volume of treated water available would be limited to the maximum volume discharged from the wastewater treatment plant. The results of these analyses are presented in Table IV.B.8. These analyses indicate that the advantage of replacing the mill process water with treated effluent from the wastewater treatment plant is modest.

IV.B.3.1.4 Assessment of the Effects of Mill Water Recycling

The overall average mill water balance (Figure 6-1 of Foth and Van Dyke, 1995a/1998d) indicates that the combined mill inflow volume is 1460 L/m (3858 gpm). Of this volume, 9231 L/m (2442 gpm) is derived from the recycled water from the TMA and RP. This volume represents 63% of the volume of water entering the mill. The reclaim pond water is a mixture of water from the TMA decant and the tailings underflow. The analysis conducted for NMC accounts for recycling of water within the mill, but does not account for recycling of water from

the TMA to the mill (GWQPE Appendix B). One of the principal constraints on the extent of recycling likely will be the potential for precipitation of gypsum in the mill circuit. Gypsum saturation in the mill process water was evaluated in GWQPE Appendix B. In this evaluation, it was assumed that the approach to gypsum saturation resulted from the addition of milling reagents to the process water in the mill circuit. The approach to gypsum saturation as a result of water recycling will result in similar concentrations of Ca and slightly higher concentrations of SO_4, which will result from complexing between Mg and SO_4. Water recycling will also increase the concentrations of other ions.

An analysis was conducted to evaluate the effect of water recycling on the concentrations of solutes in the mill process water (Steffan, Robertson and Kirsten, 2000b). This analysis indicates that gypsum saturation will be attained when Ca concentrations increase by a factor of 2.24, and SO_4 concentrations increase by a factor of 2.07 (average Ca and SO_4 increase by a factor of 2.15). For this evaluation the concentration of all solutes was increased by a factor of 2.15. These concentrations are summarized in Table IV.B.9. The results suggest that the recycling of process water will increase the concentrations of dissolved constituents, and that these increases should be accounted for in the development of the TMA source term.

IV.B.3.1.5 Summary of Process Water Variability

A series of sensitivity analyses were conducted to assess the variability in process water chemistry that can be anticipated within the range of expected flows of mill-process water from various streams (see Table IV.B.2). The results of these analyses indicate that variations in process streams, over a range that is greater than expected during normal operations, can be anticipated to have a modest effect on the process water composition. In addition, the substitution of mine water for mill-process water in the slurry solution to transport tailings to the TMA, will have a minor effect on the process water composition. Furthermore, the benefit of the substitution of mine water for mill-process water is not consistent for all dissolved constituents. In both of these cases there may be potential to decrease the concentrations of target elements should the concentrations of a limited number of dissolved constituents represent an environmental concern. As anticipated, substitution of treated effluent from the wastewater treatment plant for mill-process water used to slurry the tailings from the mill to the TMA decreases the concentrations of dissolved constituents in the process water entering the TMA. The benefit of using the treated wastewater in this manner, however, is modest.

The process water concentrations estimated for NMC account for increases in concentrations of Ca and SO_4 beyond those observed in the metallurgical testing program (GWQPE Appendix B). The increases are attributed the addition of reagents in the mill process. The NMC estimates of process water chemistry do not account for increases in solute concentrations that will arise from recycling water from the reclaim pond to the mill. The extent of water recycling likely will be limited by the concentrations of Ca and SO_4 in the reclaim water and the approach to saturation with respect to gypsum. Calculations conducted for NMC indicate that gypsum saturation will be attained after solute concentrations are increased by a factor of 2.15. This increase in concentration should be accounted for in the estimate of the process water chemistry that will be discharged to the TMA. The NMC estimates of process water composition and the composition recommended by this review are summarized in Table IV.B.9.

IV.B.3.2 Addition of Waste Rock to the TMA

NMC has committed to deposit within the TMA all potentially acid generating waste rock ("Type II") that is brought to the surface. Because of differences in scheduling development of the TMA and production of waste rock in underground operations, a portion of the waste rock would be stored on surface in the Type II Waste Rock Storage Area (WRSA) prior to deposition within the TMA. The Type II WRSA would be lined, but would not include provisions to prevent the oxidation of the exposed waste rock. Oxidation of waste rock in the Type II WRSA would release dissolved constituents to the water within the pile, which would be collected and sent to the Reclaim Pond, and would result in the accumulation of soluble secondary minerals. The subsequent disposal of the waste rock in the TMA would release solutes to the water within the TMA pond and to the pore water of the tailings within the TMA.

Steffan, Robertson and Kirsten (2001) calculated the mass of solutes that will be released during the period of waste rock storage, to account for the additional solutes that will be derived from the oxidized waste rock. These calculations combined an estimate of the period of waste rock storage from the Mine Permit Application (Foth and Van Dyke, 1995a/1998d), with estimates of the solute release rates from the waste rock determined through the waste characterization studies (Foth and Van Dyke, 1995e).

The waste rock storage period was divided into two segments. The first segment extends from years 1 through 9 of the mine life. The second period extends from years 16 to 22 of mine life. These two periods were selected because they represent times during the mine life when the production of waste rock to surface would exceed the demand for Type II waste rock for construction and disposal within the TMA. Varying amounts of excess Type II waste rock would be produced each year. To account for this variability, a weighted-average storage time for each of the two storage periods was estimated. The weighted average storage times used are 4.7 years for the first period and 3.9 years for the second period.

The waste rock leaching rates were derived from testing conducted on the Lower Mole Lake Master Composite and the Skunk Lake Master Composite. The ratio of the two rock types was assumed to be 93% from the Lower Mole Lake Formation and 7% from the Skunk Lake Formation. Leaching rates derived from these tests were then used in conjunction with estimates of the exposure time to calculate the masses of solute released through sulfide oxidation during the exposure period in the TMA. Two cases were considered by Steffan, Robertson and Kirsten (2001). The best engineering judgement (BEJ) case assumes that waste rock would be deposited in the TMA at the expected average rate of 86,800 Mg/yr (95,700 tons/yr). The upper bound (UB) case assumes that waste rock would be deposited in the TMA at a rate of 120,000 Mg/yr (132,000 tons/yr). In both cases, all solutes are assumed to be released to the TMA pond water immediately upon deposition into the TMA. This assumption is conservative when considering the TMA pond water and the Reclaim Pond water, but may not be conservative when considering the liquid (leachate) accumulating in the drainage layer at the base of the TMA. The NMC estimates of incremental solute contributions to the TMA are summarized in Table IV.B.10.

The NMC solute contribution calculations assume that the solute release rates derived from the waste-rock characterization program are representative of the rates that would be observed on the Type II WRSA. Review of the waste-rock characterization program (Section I) indicated, however, that the sample size and sample preparation steps used in the program may result in underestimates of oxidation and solute release, and provided scaling factors to account for these effects. Revised incremental solute contributions computed using these scaling factors are summarized in Table IV.B.11. These increased rates should be used in subsequent analyses.

IV.B.3.3 Generation and Fate of Thiosalts

In addition to solutes derived from the milling operation, as described in GWQPE Appendix B, ore processing is also expected to release thiosalts to the mill-discharge water (Attachment H of Foth and Van Dyke, 2000d). Thiosalts are partly oxidized sulfur compounds that are intermediate between sulfide and sulfate. These compounds are released at various stages of the grinding, milling, and concentrating processes. Thiosalts are principally thiosulfate ($S\text{-}SO_3^{2-}$) and polythionates ($SO_3\text{-}S_n\text{-}SO_3^{2-}$), and are oxidized when exposed to atmospheric oxygen. Oxidation of thiosalts consumes oxygen, nitrate, or ferric iron, and releases acidity. Oxidation of thiosulfate in the TMA or the Reclaim Pond will release H^+ through the reaction:

$$S_2O_3^{2-} + 2O_2 + H_2O \Rightarrow SO_4^{2-} + 2H^+ + 2SO_4^{2-} \qquad \text{(IV.6)}$$

This reaction will also release sulfate. There is potential for thiosalt oxidation to affect water quality at three locations in the tailings disposal system, the TMA Pond, the TMA drain layer, and the Reclaim Pond. Thiosalts may also be present in the liquid that percolates through the TMA liner into the underlying geological materials. The affect of thiosalt oxidation in each of these locations was considered by NMC in Foth and Van Dyke (2001a).

Steffan, Robertson and Kirsten (2001) reviewed the results of the test work conducted for the Crandon project, including analyses conducted for the 1986 mine permit application. These test results indicate thiosalt concentrations ranged from very low values up to 1,157 mg/L in the cemented pyritic tailings testing program. Metallurgical testing conducted by NMC indicates that thiosalt concentrations of greater than 1,600 mg/L would impair zinc recovery within the mill circuit. Testing was conducted at thiosulfate concentrations of 1,600 mg/L, 3,200 mg/L, and 6,400 mg/L. Concentrations less than 1,600 mg/L were not evaluated.

Steffan, Robertson and Kirsten (2001) recommends that 500 mg/L be considered the BEJ concentration for thiosalts in the mill-discharge water, and recommends an UB concentration of 1,000 mg/L. These thiosalt concentrations are consistent with those observed at other sulfide mine sites (CANMET, 2000). Additional sensitivity calculations, conducted to evaluate the potential impacts of thiosalt concentrations of up to 1,500 mg/L, are recommended. Concentrations in excess of 1,500 mg/L are not likely to be sustained in the mill circuit because of the poor Zn recovery observed at these higher thiosalt concentrations and the financial incentive to maintain lower thiosalt concentrations in the mill.

The rate of thiosalt oxidation in the TMA decant pond depends on the availability of oxygen and the pond temperature. Thiosalt oxidation would occur in the TMA pond throughout most of the

ice-free portion of the year, with more rapid oxidation occurring during warm periods and more restricted oxidation occurring during colder periods. In the winter, when portions of the TMA pond are ice covered, the rate and extent of thiosalt oxidation would be limited and thiosalt concentrations would rise. Generation of acidic waters at tailings impoundments can arise from thiosalt oxidation, with acidification tending to occur in the spring. The association of acidification with the spring season can be attributed to two reasons. First in the winter, the rate of thiosalt oxidation is slow, and there is potential for the thiosalt concentration in the tailings impoundment water to increase. Second, as the temperature rises, and the extent of the ice cover decreases, the rate of thiosalt oxidation in the tailing impoundment pond increases. Lime additions that are sufficient to maintain neutral pH through the colder winter months are no longer adequate, and if excess lime cannot be provided to the system rapidly enough, acidification of the tailings pond water can occur.

At the Crandon site, the normal operating system for much of the year probably would include extensive oxidation of thiosalts in the TMA pond with some additional oxidation in the Reclaim Pond, necessitating the use of lime to maintain neutral pH. The oxidation of thiosalts and lime neutralization would result in increased concentrations of dissolved constituents, principally Ca and SO_4. During the winter months, less extensive oxidation of thiosalts is expected and the concentrations of SO_4 and Ca probably would be lower. The rate of thiosalt oxidation can be anticipated to occasionally exceed the rate of lime addition and that acidification of the pond water would ensue. These periods are likely to be brief and would occur more commonly in the spring than at other times of the year.

Steffan, Robertson and Kirsten (2001) conducted calculations to account for the oxidation of thiosalts in the TMA. Two conditions were simulated. Under the first condition, there is no provision for the oxidation of thiosalts. This condition is analogous to what would be expected under normal winter operations, when the rate of thiosalt oxidation is slow due to low temperatures and the presence of an ice cover. The second condition assumes that the thiosalts oxidize completely and that the increase in sulfate concentrations is offset by an increase in the concentrations of Ca and Mg derived from dolomite, which is contained in the tailings in the TMA. Under these conditions, metals present in the process water and metals released from the oxidized waste rock are assumed to remain in solution. This condition is a reasonable representation of periods when the rate of thiosalt oxidation and acidification in the tailings pond exceeds the rate of lime addition. These calculations do not simulate the condition, which can be expected to prevail over much of the ice-free period, of complete oxidation of thiosalts in the TMA with neutralization by lime addition to maintain neutral pH.

As noted previously, oxidation of thiosalts in the TMA can be conceptualized as occurring in three operational periods: the winter period, when there is little oxidation of thiosalts accompanied by effective neutralization of produced acidity by the alkalinity normally present in the system; the summer, when there is complete oxidation of thiosalts accompanied by effective neutralization using added lime; and periods of upset, when the rate of thiosalt oxidation exceeds the rate of lime addition. The NMC estimates simulate the winter period and the period of upset. A third scenario representing typical summer conditions should also be included in the calculations. This scenario should include complete oxidation of thiosalts to form SO_4 and H^+,

neutralization by lime ($Ca(OH)_2$), followed by precipitation of secondary minerals to equilibrium concentrations.

IV.B.3.4 NMC Estimates of TMA Pond Water Quality

Steffan, Robertson and Kirsten (2001) combined estimates of process water composition, waste rock leaching, and the contributions of thiosalt oxidation to forecast the concentrations of dissolved constituents in the pond water of the TMA under acidic and neutral conditions. BEJ and UB estimates of these concentrations were developed. These estimates are provided in Tables IV.B.12 and IV.B.13, respectively.

Steffan, Robertson and Kirsten (2001) used a time-weighting scheme to develop the two sets of estimates of pond water quality (BEJ and UB). These estimates of average pond water quality are summarized in Table IV.B.14 (BEJ case) and Table IV.B.15 (UB case). A review confirmed that the calculation steps outlined in the document yield the concentrations presented in these tables.

IV.B.3.5 Recommended Estimates of TMA Pond Water Quality

The preceding sections include a series of recommendations for modifications to the assumptions made in the development of the NMC estimate of the pond water quality. These recommended modifications have been compiled into a series of revised estimates of pond water quality. The Lower Range Estimate (LRE) includes increasing the process-water concentrations to simulate the effect of water recycling between the TMA-Reclaim Pond and the mill, and increasing the mass of solutes released from the waste rock to better account for the incorporation of Type II waste rock into the TMA. The Upper Range Estimate (URE) includes increasing the thiosalt concentration from 1,000 mg/L to 1,500 mg/L and incorporating three operational periods of thiosalt oxidation per year. These estimates do not account for the precipitation of $Sb(OH)_2$ from the TMA pond water.

Time-weighted estimates of the concentrations of dissolved constituents in the TMA pond water were developed using the LRE and URE concentrations. The LRE time-weighted average concentrations assume that winter thiosalt oxidation conditions prevail for 90 days of each year and that there will only be one acidic event each year. Summer thiosalt oxidation conditions are assumed for the balance of the year. The time-weighted LRE is presented in Table IV.B.16. The time-weighted URE average concentrations assume that winter conditions prevail for 90 days per year and that there are three acidic events per year. Summer thiosalt oxidation conditions prevail for the balance of the year. The time-weighted URE is presented in Table IV.B.17.

IV.B.3.6 Solute Concentrations in the "Pond Water Dominated Zone" of the TMA

During tailings deposition in the TMA, the pond water would mix with the tailings and the tailings pores will be filled with pond water. Over prolonged periods of exposure there would be sufficient time for the pond water and the tailings solids to react. During the operations period, most of the tailings in the TMA would be covered with water or freshly deposited tailings. The low oxygen diffusion coefficient of the water-saturated tailings would limit the rate of sulfide oxidation. As a result, the principal reactions between the pond water and the tailings solids

would be dissolution of soluble minerals within the tailings solids and precipitation of secondary minerals. Steffan, Robertson and Kirsten (2001) has termed the zone of tailings pore water that is derived principally from the tailings pond as the "Pond Water Dominated Zone". The composition of the water in this zone was estimated by equilibrating the predicted TMA pond water with a representative mineral assemblage. In the BEJ calculations, the BEJ TMA pond water was equilibrated with a mineral assemblage including dolomite and gypsum. Gibbsite, ferrihydrite, calcite, dolomite, barite, and $Sb(OH)_2$ were allowed to precipitate if they reached saturation. In the UB calculations, the UP TMA pond water was also equilibrated with siderite (with an equilibrium constant of $10^{-10.89}$). Precipitation of ferrihydrite was not allowed. The results of the NMC BEJ and UB calculations are presented in Table IV.B.18.

Alternate estimates of solute concentrations (LRE and URE) in the Pond Water Dominated Zone of the TMA were computed based on the aforementioned recommendations. Similar assumptions to those made by Steffan, Robertson and Kirsten (2001) in the development of estimates of solute concentrations were used, with the exception that $Sb(OH)_2$ precipitation was not allowed in either the LRE or URE cases. For the LRE case, the LRE pond water solute concentrations in Table IV.B.16 were used. For the URE case, the URE concentrations in Table IV.B.17 were used. The LRE and URE solute concentration estimates in the pond-water-dominated portion of the TMA are presented in Table IV.B.19.

IV.C. CONSOLIDATION PERIOD

IV.C.1 Prediction of Oxidation Zone Water Chemistry

During the consolidation period, the tailings are drained by the leachate collection system and atmospheric O_2 enters into the unsaturated tailings. Sulfide minerals present in the unsaturated zone oxidize releasing Fe^{2+}, SO_4, and H^+ according to the reaction:

$$FeS_2 + \frac{7}{2}O_2 + H_2O \rightarrow Fe^{2+} + 2SO_4^{2-} + 7H^+ \qquad \text{(IV.7)}$$

The mass of sulfide minerals oxidized is limited by the supply of oxygen from the tailings surface, which is described in Section III.B.

The rate of sulfide oxidation within the tailings impoundment is also dependent on the rate of oxidation at the mineral surface. As described in Section I, the sulfide oxidation rate was estimated using the results of the laboratory tailings program. Two reaction rates were selected for this analysis (see Table III.B.1.). The rates were selected to calculate the depth of oxygen diffusion and the flux of oxygen into the tailings. The lower estimate of the oxidation rate developed in Section I is 1.3 x 10^{-9} mol O_2/kg-s, which is equivalent to an oxidation rate constant of 2.19 x 10^{-2} s^{-1} for the tailings. The upper estimate provided in Section I is 9.42 x 10^{-9} mol O_2 kg^{-1} s^{-1}, which is equivalent to an oxidation rate constant of 1.58 x 10^{-6} s^{-1} for the tailings.

The effective oxygen diffusion coefficients calculated using the estimates of moisture content derived from the HYDRUS simulations and the oxidation rate values derived from the kinetic test data were used as input data to calculate the oxygen flux into the vadose zone and the depth

of oxidation in Section III.A. The resulting diffusion coefficient values, the oxygen flux into the tailings, and the depth of oxidation derived from those calculations are presented Section III.A.4.

As shown in Table III.B.1, the depth of penetration increases as the period over which the tailings are exposed increases. Accordingly, the depth of oxidation increases as the period of exposure increases. Consequently, the final cover should be placed on the tailings as expeditiously as possible. NMC has committed to placing the cover on the TMA cover as soon as possible, estimated to be three years or less. Nevertheless, unforeseen circumstances may delay placement of the cover. To account for an extended period of exposure, the consolidation period was assumed to extend for five years prior to placement of the cover. The depth of oxygen penetration after 5 years is 1.67 m (low oxidation rate case) and 0.62 m (high oxidation rate) (see Table III.B.1).

IV.C.2 Expected Leachate Water Chemistry

Pore water in the oxidation zone will originate as pond water, which infiltrates into the tailings. Precipitation that falls on the TMA surface will mix with this process water and geochemical reactions between the water and the tailings will alter solute concentrations. Calculations were conducted to estimate the water quality in the oxidation zone for two cases, a lower range estimate (LRE) case and an upper range estimate (URE) case.

An unsaturated flow and transport analysis was conducted with HYDRUS-2D to evaluate concentrations in the leachate collection system due to mixing of water draining from the oxidation zone and the process water zone during drain down and after closure. Details of this analysis are described in Benson (2000a, 2002). The analysis showed that concentrations in the leachate collection system are essentially identical to those in the process water zone for at least 500 years after closure. At approximately 500 years, the concentrations in the leachate collection zone begin to increase at a very slow rate. For the period between 500-1500 years, concentrations in the leachate collection system increased at a rate less than 1% per annum.

IV.C.2.1 Expected TMA Leachate Composition

Composition of the TMA leachate was estimated for the LRE and URE cases. The LRE was made using the pond water LRE described in Section IV.B.3.6, moisture contents obtained from the HYDRUS-2D simulations described in Benson (2000a, 2002), oxidation rates from Section I, and tailings infiltration rates provided in Foth and Van Dyke (1995d, 1998g). The URE was calculated in the same manner, except the pond water URE was used along with the upper estimate of the oxidation rate (see Section IV.C.1)

Masses of solutes released by sulfide oxidation in the unsaturated zone were calculated using the metal release rates determined through the kinetic tests. These masses were compared to the total mass of species available for release in the oxidation zone. Where the mass calculated to be released by oxidation exceeded the mass available for release, the available mass was used in subsequent calculations. The mass derived from the pond water was added to the mass released by sulfide oxidation to determine a total mass value. The total volume of water present in the oxidation zone was calculated as the sum of the volume of water determined from saturation

profiles derived from the HYDRUS-2D simulations (Benson, 2000a, 2002) and the volume of infiltrating precipitation.

The oxidation of sulfide minerals results in the release of acidity and the subsequent dissolution of carbonate minerals through acid neutralization reactions. The products of sulfide oxidation and acid neutralization combine to result in the formation of secondary minerals. The NMC estimates assumed that conversion to secondary minerals was complete and solutes were released to solution through the subsequent dissolution of these secondary phases.

The overall reaction describing sulfide oxidation, acid neutralization and secondary mineral formation was assumed to be:

$$\frac{1}{2}FeS_2 + \frac{15}{8}O_2 + \frac{21}{4}H_2O + Ca_{0.5}Mg_{0.5}CO_3 + \frac{1}{2}(0.111)FeCO_3 + \frac{1}{8}(0.111)O_2 + \frac{5}{4}(0.111)H_2O \rightarrow \frac{1}{2}CaSO_4 \bullet 2H_2O + \frac{1}{2}MgSO_4 \bullet 7H_2O + \frac{1}{2}Fe(OH)_3 + CO_{2(g)} + \frac{1}{2}(0.111)Fe(OH)_3 + \frac{1}{2}(0.111)H_2CO_3 \quad \text{(IV.11)}$$

This reaction stoichiometry assumes that the principal products of sulfide oxidation are secondary minerals.

The short-term column experiment results described in Section I indicate that the products of sulfide oxidation and acid neutralization include both solid-phase products and aqueous products. The maximum proportion of aqueous products observed in the two short-term experiments was 57%. The masses of Fe, SO_4, Ca and Mg were proportioned into aqueous components in this manner, with Fe present as $Fe(OH)_3$, Ca present as gypsum ($CaSO_4 \cdot 2H_2O$), Mg present as epsomite ($MgSO_4 \cdot 7H_2O$), and SO_4 present in both gypsum and epsomite. These mineral masses were included with the solute masses in subsequent geochemical calculations.

The solute concentrations were determined by dividing the total solute concentrations by the total water volume. MINTEQA2 was used in conjunction with the aqueous and solid-phase concentrations to determine the degree of saturation with respect to the minerals listed in Table IV.C.1. This selection of possible mineral phases is similar to that specified in Steffan, Robertson and Kirsten (2001) for simulations conducted in developing estimates of the oxidation zone water quality. One phase, $Sb(OH)_{2(s)}$ which was included in the NMC calculations, was not included in these calculations. Although laboratory studies have reported formation of this phase, $Sb(OH)_{2(s)}$ has not been reported as a direct precipitate in mine waste environments. Furthermore, high concentrations of Sb have been observed at the Giant Mine in Yellowknife, Canada (Steffan, Robertson and Kirsten, 2001). At this site, waters supersaturated with respect to $Sb(OH)_2$ have been observed, suggesting that $Sb(OH)_2$ does not act as an effective solid-phase constraint on aqueous Sb^{2+} concentrations.

The same calculation procedure was followed to estimate the masses of dissolved constituents for the URE. The resulting concentrations were equilibrated with respect to the mineral phases listed in Table IV.C.1 for the URE case.

The leachate derived from the TMA will be a combination of the water present in the un-oxidized portion and the oxidized portion of the TMA. The estimates of the ratio of oxidized zone water to unoxidized zone water are developed and presented in Section II. Based on weighting using these calculations, the concentrations of dissolved constituents in the leachate water are summarized in Table IV.C.2.

IV.C.2.2 Estimated Water Chemistry for the Reclaim Pond

The composition of the water in the Reclaim Pond was estimated for both the operations period, when a pond is retained on the TMA surface, and for the closure period (consolidation and post capping) when there is no pond present on the TMA surface and all Reclaim Pond water is derived from the TMA leachate collection system. The operations period composition was calculated by combining estimates of the TMA pond water quality and leachate water quality with estimates of the volume of water derived from the pond surface and from the TMA leachate collection system. The estimated Reclaim Pond concentrations are summarized in Table IV.C.3.

REFERENCES

Benson, C. (2000a), Solute transport during consolidation and drainage, memorandum to David Blowes with copy to Christopher Carlson of WDNR, dated 15 November.

Benson, C. (2000b), Estimate of oxygen flux from the base of the TMA's composite cap, memorandum to David Blowes with copy to Christopher Carlson of WDNR, dated 17 November.

Benson, C. (2002), Errata – memorandum on oxygen flux dated November 17, 2000, memorandum to Christopher Carlson of WDNR, dated 13 July.

Benson, C., Albright, W., Roesler, A., and Abichou, T. (2002), Evaluation of Final Cover Performance: Field Data from the Alternative Cover Assessment Program (ACAP), *Proceedings of Waste Management '02*, Waste Management Symposia, Inc., Tucson, AZ.

Benson, C. and Grefe, R. (2002), Estimates of Leakage Rates for the Tailings Management Area and Reclaim Pond Liners: Proposed Crandon Mine, Forest County, Wisconsin, report to Wisconsin Dept. of Natural Resources, dated 6 December.

Blowes, D.W., and Jambor, J.L. (1990), The pore-water geochemistry and the mineralogy of the vadose zone of sulfide tailings, Waite Amulet, Québec, Canada, *Applied Geochemistry,* 5, pp. 327-346.

Blowes D. W. and Ptacek C. J. (1994) Acid-neutralization mechanisms in inactive mine tailings, *in* Blowes, D.W., and Jambor, J.L. (eds.), *The Environmental Geochemistry of Sulfide Mine-Wastes*, Mineralogical Association of Canada Short Course Series, Volume 22, pp. 271-292.

Blowes, D.W., Reardon, E.J., Cherry, J.A., and Jambor, J.L. (1991), The formation and potential importance of cemented layers in inactive sulfide mine tailings, *Geochimica et Cosmochimica Acta*, 55, pp. 965-978.

Blowes, D.W., Lortie, L., Gould, W.D., Jambor, J.L. and Hanton-Fong, C.J. (1995), Geochemical, mineralogical and microbiological characterization of a sulfide-bearing, carbonate-rich, gold mine tailings impoundment, Joutel, Québec, *Applied Geochemistry,* 31, pp. 687-705.

Bolen, M., Roesler, A., Benson, C., and Albright, W. (2001), Alternative Cover Assessment Program: Phase II Report, Geo Engineering Report No. 01-10, Dept. of Civil & Environmental Engineering, University of Wisconsin-Madison.

Boorman, R.S., and Watson, D.M. (1976), Chemical processes in abandoned sulfide tailings dumps and environmental implications for Northeastern New Brunswick, *CIM Bulletin*, 69(772), pp. 86-96.

Bonaparte, R., Daniel, D., and Koerner, R. (2002), Assessment and Recommendations for Improving the Performance of Waste Containment Systems, Report No. EPA/600/R-02/099, Office of Research and Development, National Risk Management Research Laboratory, US Environmental Protection Agency, Cincinnati, Cincinnati, OH, USA.

Broughton, L.M., Chambers, R.W., Robertson, A. (1992), Minerock guidelines: Design and control of drainage water quality, Saskatchewan Environment and Public Safety Report No. 93301, Prince Albert, Saskatchewan.

CANMET (2000), Mines and Mineral Sciences Laboratories Thiosalt Bibliography. CANMET website: http://www.nrcan.gc.ca/es/msd/emmic/web/subjectthiosalt_e.html.

Carlson, C.P. (2001), Letter to interested parties concerning Wisconsin DNR estimates of mine pumping, dated 10 September.

Crandon Mining Company (1994a), Letter to Larry Lynch, Wisconsin DNR, from Ken Collison, dated 23 May.

Crandon Mining Company (1994b), Letter to Larry Lynch, Wisconsin DNR, from Ken Collison, dated 30 September.

Crandon Mining Company (1997), Letter to Ron Arneson, Wisconsin DNR, from Don Moe, dated 3 October.

Crank, J. (1975), *The Mathematics of Diffusion*, Oxford University Press, Oxford, UK.

Cussler, E. (1997), *Diffusion, mass transfer in fluid systems*. 2nd Ed., Cambridge University Press, Cambridge, UK.

Darilek, G., Menzel, R., and Johnson, A. (1995), Minimizing Geomembrane Liner Damage While Emplacing Protective Soil, *Proc. Geosynthetics '95*, Industrial Fabrics Assoc. International, St. Paul, 669-676.

Davis, G.B., and Ritchie, A.I.M. (1986), A model of oxidation in pyritic mine wastes, I, Equations and approximate solution, *Applied Mathematical Modelling*, 10, pp. 314-322.

Davis, G.B., Ritchie, A.I.M. (1987), A model of oxidation in pyritic mine wastes, 3, Import of particle size distribution, *Applied Mathematical Modelling*, 10, pp. 417-422.

Davis, G.B., Doherty, G., and Ritchie, A.I.M. (1986), A model of oxidation in pyritic mine wastes, II, Comparison of numerical and approximate solution,s *Applied Mathematical Modelling*, 10, pp. 323-329.

Dubrovsky, N.M. (1986), *Geochemical evolution of inactive pyritic tailings in the Elliot Lake uranium district,*. Ph.D. thesis, University of Waterloo.

Dwyer, S. (2002), Water Balance Performance of Final Landfill Covers in an Arid Environment, *Proc. Waste Management '02*, Waste Management Symposia, Inc., Tucson, AZ.
Dzombak, D.A., and Morel, F.M.M. (1990), *Surface Complexation Modeling: Hydrous Ferric Oxide*, John Wiley and Sons, 545 pp.

Elberling, B., Nicholson, R., and David, D. (1993), Field evaluation of sulphide oxidation rates. *Nordic Hydrology*, 24(5), 323-338.

Erickson, Jr., A.J. and Cote' R. (1996), Geological Summary-Crandon Deposit, *in* Laberge, E. (ed), Institute on Lake Superior Geology, Volume 42, Part 2, pp. 129-141.

Erickson, Jr. A.J. (1994), Sample Representativeness of Master Ore Composite, memorandum to K.W. Collison, Crandon Mining Company, dated July 5, *in* EIR Appendix 3.5-31, pp. 28-65.

Erickson, Jr., A.J. (1996), Crandon Deposit Hanging Wall Sulfide Content Review, memorandum *in* Appendix C, Mine Permit Application, dated July 10.

Filion, M.P., Firlotte, F.W., Julien, M.R., and Lacombe, P.F. (1994), Regulatory Controlled Design-Louvicourt Project – A Case Study, *Proceedings of the Third International Conference on the Abatement of Acidic Drainage*, Pittsburgh, PA, Volume 2, pp 22-31, US Bureau of Mines, SP06B-94.

Foose, G., Benson, C., and Edil, T. (2001), Predicting Leakage Through Composite Landfill Liners, *Journal of Geotechnical and Geoenvironmental Engineering,* ASCE, 127(6), 510-520.

Foth and Van Dyke (1994), Notice of Intent to Collect Data and Detailed Scope of Study, Crandon Project, dated February.

Foth and Van Dyke (1995a), Mine Permit Application, Crandon Project (MPA), dated May and updated through December 1998.

Foth and Van Dyke (1995b), Environmental Impact Report, Crandon Project (EIR), dated May and updated through December 1998.

Foth and Van Dyke (1995c), Project Quality Assurance Plan Updates, EIR Appendix 3-1, dated May.

Foth and Van Dyke (1995d), Crandon Project Tailings Management Area Feasibility Report/Plan of Operation (FR), dated May and updated by Addendum No. 1 dated February 1996, Addendum No 2 dated March 1996, Addendum No. 3 dated January 1997, Addendum No. 4 dated June 1998, and the response to completeness determination dated 12 December 1997.

Foth and Van Dyke (1995e), Waste Characterization Update Report, dated December.

Foth and Van Dyke (1997), update to EIR Appendix 3.5-31 through 3.5-35 through October 1996, dated August.

Foth and Van Dyke (1998a), Crandon Project Ground Water Quality Performance Evaluation (GWQPE), dated April, and updated March 2000, *in* EIR Appendix 4-12.

Foth and Van Dyke (1998b), Crandon Project Reflooded Mine Source Term, dated April, *in* EIR Appendix 4.2-13.

Foth and Van Dyke (1998c), Preliminary Engineering Report for Wastewater Treatment Facilities (PER), originally issued September 1995, updated November and revised April 1999.

Foth and Van Dyke (1998d), Mine Permit Application, Crandon Project (MPA), originally issued May 1995, substantially updated December, and updated through 2003.

Foth and Van Dyke (1998e), Environmental Impact Report, Crandon Project (EIR), originally issued May 1995, substantially updated December, and updated through 2003.

Foth and Van Dyke (1998f), Data Regarding the Preparation of the Composites used in the Master Characterization Studies, EIR Appendix 3.5-31, update dated December.

Foth and Van Dyke (1998g), Addendum No. 5 to the May 1995 Crandon Project Tailings Management Area Feasibility Report/Plan of Operation (FR), dated December 24 and updates dated July 19, 1999, and April 20, 2000.

Foth and Van Dyke (1999), Addendum No. 6 to the May 1995 Crandon Project Tailings Management Area Feasibility Report/Plan of Operation (FR), dated November.

Foth and Van Dyke (2000a), updates to GWQPE appendices, EIR Appendix 4.2-12 and associated appendices, dated February.

Foth and Van Dyke (2000b), Environmental Impact Report, Crandon Project (EIR), Section 3.5 update, dated March (Sections 3.5.5.2.1, 3.5.5.3.1).

Foth and Van Dyke (2000c), EIR Appendix 3.5-33 and 3.5-34 updated with additional parameters, dated 8 August.

Foth and Van Dyke (2000d), Addendum No. 1 to the Mine Permit Application, Crandon Project (MPA), Reflooded Mine Management Plan (RMMP) dated December.

Foth and Van Dyke (2001a), Addendum No. 1 to TMA Groundwater Quality Performance Evaluation (GWQPE), Memorandum to Gordon Reid, Nicolet Minerals Company, from Steve Donohue, dated 14 September.

Foth and Van Dyke (2001b), Crandon Project - Reclaim Pond Liner, Technical Memorandum from Dr. Paruvakat, dated 30 July and updated 26 October, *in* Appendix D, Crandon Project - Addendum No. 1 to TMA Groundwater Quality Performance Evaluation (GWQPE), dated September 14, 2001.

Foth and Van Dyke (2001c), Crandon Project-Verification/Contingency Plan for Long-Term Performance of Tailings Management Area Cap, dated 27 November.

Fuller, C.C., Davis, J.A., Coston, J.A., Dixon, E. (1996), Characterization of metal adsorption variability in a sand and gravel aquifer, Cape Cod, Massachusetts, U.S.A. *Journal of Contaminant Hydrology*, 22. p. 165-187.

Giroud, J. (1997), Equations for Calculating the Rate of Liquid Migration Through Composite Liners Due to Geomembrane Defects, *Geosynthetics International*, 4(3-4), 335-348

Giroud, J., Badu-Tweneboah, K., and Bonaparte, R. (1992), Rate of Leakage Through a Composite Liner due to Geomembrane Defects, *Geotextiles and Geomembranes*, 11, 1-28.

Giroud, J. and Bonaparte, R. (1989), Leakage Through Liners Constructed with Geomembranes – Parts I and II, *Geotextiles and Geomembranes*, 8, 27-111.

Giroud, J. and Houlihan, M. (1995), Design of Leachate Collection Layers, *Proc. Sardinia 95, Fifth International Landfill Symposium*, CISA, Cagliari, Italy, 613-640.

Giroud, J., Zornberg, J., and Zhao, A. (2000), Hydraulic Design of Geosynthetic and Granular Liquid Collection Layers, *Geosynthetics International*, 7(4-6), 285-380.

Hsuan, Y. and Koerner, R. (1998), Antioxidant Depletion lifetime in HDPE Geomembranes, *J. of Geotech. and Geoenvironmental Eng.*, 124(6), 532-541.

J&L Testing (1998), Laboratory Model Test and Performance Assessment Crandon Drainage Filter System, Report to Foth and Van Dyke, dated 11 June.

Jambor, J.L. (1994), Mineralogy of sulfide-rich tailings and their alteration products, *in* Blowes, D.W., and J.L. Jambor (eds.), *The Environmental Geochemistry of Sulfide Mine-Wastes*, Mineralogical Association of Canada Short Course Series, Volume 22, pp. 59-102.

Jambor, J.L., and Blowes, D.W. (1991), Mineralogical study of low-sulphide, high-carbonate , arsenic –bearing tailings from the Delnite minesite, Timmins area, Ontario, *in* P*roceedings of the Second International Conference on the Abatement of Acidic Drainage*, Volume 4, pp. 173-198, Mend Secretariat, Ottawa, Ontario.

Jambor, J.L., and Owens, D.R. (1993), Mineralogy of the tailings impoundment at the former Cu-Ni Deposit of Nickel Rim Mines Ltd. eastern edge of the Sudbury Structure, Ontario, CANMET Division Report, MSL-93-4 (CF), Dept. Energy Mines and Resources Canada.

Johnson, R. H., Blowes, D. W., Robertson, W. D., and Jambor, J. L. (2000), The hydrogeochemistry of the Nickel Rim mine tailings impoundment, Sudbury, Ontario, *Journal of Contaminant Hydrology,* 41, pp. 49-80.

Joint Editorial Board of the American Public Health Association, American Water Works Association and Water Pollution Control Federation (1992), *Standard Methods for the Examination of Water and Wastewater*, 18th edition.

Khatami, A., Giroud, J., and Badu-Tweneboah, K. (1989), Evaluation of the Rate of Leakage Through Composite Liners, *Geotextiles and Geomembranes*, 8, 337-340.

Khire, M., Benson, C., and Bosscher, P. (1997), Water Balance Modeling of Earthen Landfill Covers, *Journal of Geotechnical and Geoenvironmental Engineering,* ASCE, 123(8), 744-754.

Kim, H. (2000). Oxygen transport through multi-layer caps over mine waste. PhD thesis, University of Wisconsin, Madison.

Kim, H. and Benson, C. (1999). Oxygen transport through multilayer composite caps over mine waste. *Proceedings of Sudbury '99 - Mining and the Environment II*, Centre in Mining and Mining Environment Research, Laurentian University, Sudbury, Ontario, 183-192.

Kraus, J., Benson, C., Erickson, A., and Chamberlain, E. (1997), Freeze-Thaw and Hydraulic Conductivity of Bentonitic Barriers, *Journal of Geotechnical and Geoenvironmental Engineering,* ASCE, 123(3) 229-238.

Lambe, R. and Rowe, R. (1987), Volcanic History, Mineralization and Alteration of the Crandon Massive Sulfide Deposit, Wisconsin, *Economic Geology*, Vol. 82, pp. 1204-1238.

Lapakko, K.A. (1993), Field dissolution of test piles of Duluth Complex rock. Report to the US Bureau of Mines Salt Lake City Research Center on Cooperative Agreement No. C0219003. 41p. plus appendices.

Lapakko, K.A., Antonson, D.A. (1994), Oxidation of sulfide minerals present in Duluth Complex rock, *in Environmental Geochemistry of Sulfide Oxidation*, ACS Symposium Series No. 550, American Chemical Society, Washington, DC, 1993. p. 593-607.

Lapakko, K.A., Antonson, D.A. (2002), Drainage pH, acid production, and acid neutralization for Archean greenstone rock. Preprint 02-73 *in* SME Annual Meeting, February 25-27, Phoenix, AZ (CD-ROM). Soc. for Mining, Metallurgy, and Exploration, Inc. Littleton, CO.

Markart, K.D. (1995), Waste characterization study verifications, memorandum to Larry Lynch, Wisconsin DNR, dated 31 July.

Markart, K.D. (1998a), Verification of metallurgical samples "MET-98", Wisconsin DNR memorandum, dated 10 February.

Markart, K.D. (1998b), Verification of charging of depyritized tailings humidity cells - Nicolet Minerals Project, Wisconsin DNR memorandum, dated 23 July.

Markart, K.D. (1999a), Waste characterization: verification of copper stringer ore zone composite sample collection, Wisconsin DNR memorandum, dated 22 January.

Markart, K.D. (1999b), Verification of the mineralogical studies on the depyritized tailings, massive zinc ore and copper stringer ore, Wisconsin DNR memorandum, dated 18 March.

Melchior, S. (1997), In Situ Studies on the Performance of Landfill Caps, *Proceedings International Containment Technology Conference*, St. Petersburg, FL, 365-373.

McCreadie, H., Blowes, D.W., Ptacek, C.J. and Jambor, J.L. (2000), The influence of reduction reactions and solids composition on pore-water arsenic concentrations, *Environmental Science and Technology,* 34, pp. 3159-3166.

Nicolet Minerals Company (2000a), Letter to Bill Tans, Wisconsin DNR, from Gordon Reid, dated 20 April, including Section 5.45 and Appendix J of Addendum No. 5 to the May 1995 Crandon Project Tailings Management Area Feasibility Report/Plan of Operation.

Nicolet Minerals Company (2000b), Letter to Christopher Carlson, Wisconsin DNR, from Gordon Reid, dated 25 April.

Nicolet Minerals Company (2000c), Letter to Christopher Carlson, Wisconsin DNR, from Gordon Reid, dated 19 May.

Nicolet Minerals Company (2000d), Letter to Kim Lapakko from Ken Black, dated 26 July.

Nicolet Minerals Company (2001a), Letter to Bill Tans, Wisconsin DNR, from Gordon Reid, dated 14 September.

Nicolet Minerals Company (2001b), Letter to Christopher Carlson, Wisconsin DNR, from Gordon Reid, dated 30 October.

Nicolet Minerals Company (2001c), Letter to Bill Tans, Wisconsin DNR, from Gordon Reid, dated 5 December.

Petrov, R. and Rowe, R. (1997), Geosynthetic Clay Liner (GCL) – Chemical Compatibility by Hydraulic Conductivity Testing and Factors Impacting Its Performance, *Canadian Geotechnical Journal*, 34, 863-885.

Phaneuf, R. and Peggs, I. (2001), Landfill Construction Quality: Lessons Learned from Electrical Resistivity Testing of Geomembrane Liners, *Geotechnical Fabrics Report*, April 2001, 28-35.

Reardon, E.J., and Moddle, P.M. (1985), Gas diffusion coefficient measurements on uranium mill tailings: implications to cover layer design, *Uranium,* 2, pp. 111-131.

Ribet, I., Ptacek, C.J., Blowes, D.W., Jambor, J.L. (1995), The potential for metal release by reductive dissolution of weathered mine tailings, *Journal of Contaminant Hydrology*, 17, pp. 239-273.

Rollin, A., Marcotte, M., Jacquelin, T., and Chaput, L. (1999), Leak Location in Exposed Geomembrane Liners Using an Electrical Leak Location Detection Technique, *Proceedings of Geosynthetics '99*, Industrial Fabrics Assoc. International, St. Paul, 615-626.

Rowe, R.G. (1980), Exxon Coal and Minerals memorandum dated 15 April. Referenced as CMC-NOI-148 in Foth and Van Dyke (1994).

Scharer, J.M., Nicholson, R.V., Halbert, B., and Snodgrass, W.J. (1994), A computer program to assess acid generation in pyritic tailings, *in* Alpers, C.N., and Blowes, D.W. (eds.), *Environmental Geochemistry of Sulfide Oxidation*, American Chemical Society Symposium Series Volume 550, pp. 132-152.

Schroeder, P., Dozier, T., Zappi, P., McEnroe, B., Sjostrom, J., and Peyton, R. L. (1994a), The Hydrologic Evaluation of Landfill Performance (HELP) Model: Engineering Documentation for Version 3, EPA/600/R-94/168B.

Schroeder, P., Lloyd, C., Zappi, P., and Azziz, M., (1994b), The Hydrologic Evaluation of Landfill Performance (HELP) Model Users Guide for Version 3, EPA/500/R-94/168a.

Simunek, J., Sejna, M., and van Genuchten, M. (1996), *The HYDRUS-2D Software Package for Simulating Water Flow and Solute Transport in Two-Dimensional Variably Saturated Media*, US Salinity Laboratory, Agricultural Research Service, US Dept. of Agriculture, Riverside, CA.

Sobek, A.A., Schuller, W.A., Freeman, J.R., Smith, R.M. (1978), Field and laboratory methods applicable to overburden and minesoils, U.S. Environmental Protection Agency, Report No. EPA 600/2-78-054.

Steffen, Robertson and Kirsten (1998a), Crandon Project TMA Oxygen Transport Modeling, Addendum 1 to the April 1997 TMA Oxygen Transport Modeling Report, dated 7 March, *in* Appendix C1 of EIR Appendix 4.2-12, also referred to as GWQPE Appendix C1.

Steffen, Robertson and Kirsten (1998b), Crandon TMA Supplemental Waste Characterization Program Final Report, dated April.

Steffen, Robertson and Kirsten (1998c), Work Plan for Characterization of Depyritized Tailings and Paste Backfill, dated May.

Steffen, Robertson and Kirsten (1998d), Corroborative Testing of Depyritized Tailings, Pyrite Concentrate and Pyritic Paste Backfill, dated May and updated March 2000, *in* EIR Appendix 4.2-16, also referred to as GWQPE Appendix A3.

Steffen, Robertson and Kirsten (1998e), Tailings testing and density projections for the Crandon Project, memorandum to Jerry Sevick, Foth and Van Dyke, from Dave Hallman, dated 6 August, *in* Appendix B of Foth and Van Dyke (1998g).

Steffen, Robertson and Kirsten (1998f), Geochemical Characterization of Depyritized Tailings, Pyrite Concentrate and Pyritic Paste Backfill, dated November and updated in March 2000, *in* EIR Appendix 4.2-15, also referred to as GWQPE Appendix A1.

Steffen, Robertson and Kirsten (1999a), Electron Microprobe Analysis of Carbonates in the Depyritized Tailings and Pyrite Concentrate, dated May and updated March 2000, *in* EIR Appendix 4.2-16a, also referred to as GWQPE Appendix A4.

Steffen, Robertson and Kirsten (1999b), Representativeness of Ore and Tailings Samples from the Crandon Deposit, dated May and updated March 2000, *in* EIR Appendix 4.2-16b, also referred to as GWQPE Appendix A5.

Steffen, Robertson and Kirsten (1999c), Update to Oxygen Transport Estimates, dated May and updated March 2000, *in* Appendix C2 of EIR Appendix 4.2-12, also referred to as GWQPE Appendix C2.

Steffen, Robertson and Kirsten (1999d), Geochemical Modeling, dated May and updated March 2000 and revised August 2000, *in* Appendix B of EIR Appendix 4.2-12, also referred to as GWQPE Appendix B.

Steffen, Robertson and Kirsten (2000a), Crandon Project Assessment of TMA Drain Layer, memorandum to Jerry Sevick, Foth and Van Dyke, from John Chapman, dated 19 April.

Steffen, Robertson and Kirsten (2000b), Crandon Project TMA Sensitivity Analysis, dated April and received as an attachment to a letter dated 20 April.

Steffen, Robertson and Kirsten (2000c), Crandon Project Impact of Thiosalts on TMA Underdrain Permeability, memorandum to Steve Donohue, Foth and Van Dyke, from John Chapman, dated 21 December.

Steffen, Robertson and Kirsten (2000d), Reflooded Mine Source Concentrations, Crandon Project, dated November, *in* Appendix A of Foth and Van Dyke (2000e).

Steffen, Robertson and Kirsten (2001), Crandon Project Revised GWQPE Source Term, *in* Appendix A of Addendum No. 1 to the GWQPE (Foth and Van Dyke, 2001a).

Thiel, R., Daniel, D., Erickson, R., Kavazanjian, E., and Giroud, J.P. (2001), The GSE GundSeal GCL Design Manual, GSE Lining Technology, Inc., Houston, TX.

Thresher and Son (1998), Mineralogical Evaluation of the Crandon Tailings, dated January.

U.S. Environmental Protection Agency (1983), Methods for chemical analysis of water and wastes, EPA-600/4-79-020, dated March.

U.S. Environmental Protection Agency (1999), Method 1631, Revision G: Mercury in water by oxidation, purge and trap, and cold vapor atomic fluorescence spectrometry, EPA-821-R-99-005, dated May.

Vasko, S., Jo, H., Benson, C., Edil, T., and Katsumi, T. (2001), Hydraulic Conductivity of Partially Prehydrated Geosynthetic Clay Liners Permeated with Aqueous Calcium Chloride Solutions, *Geosynthetics 2001*, Industrial Fabrics Assoc. International, St. Paul, MN, 685-699.

White, W. III, and Lapakko, K. (2000), Preliminary indications of repeatability and reproducibility of the ASTM 5744-96 kinetic test for drainage pH and sulfate release rate. *Proceedings from the Fifth International Conference on Acid Rock Drainage*. Soc. for Mining, Metallurgy, and Exploration, Inc. Littleton, CO. p. 621-630.

FIGURES and TABLES

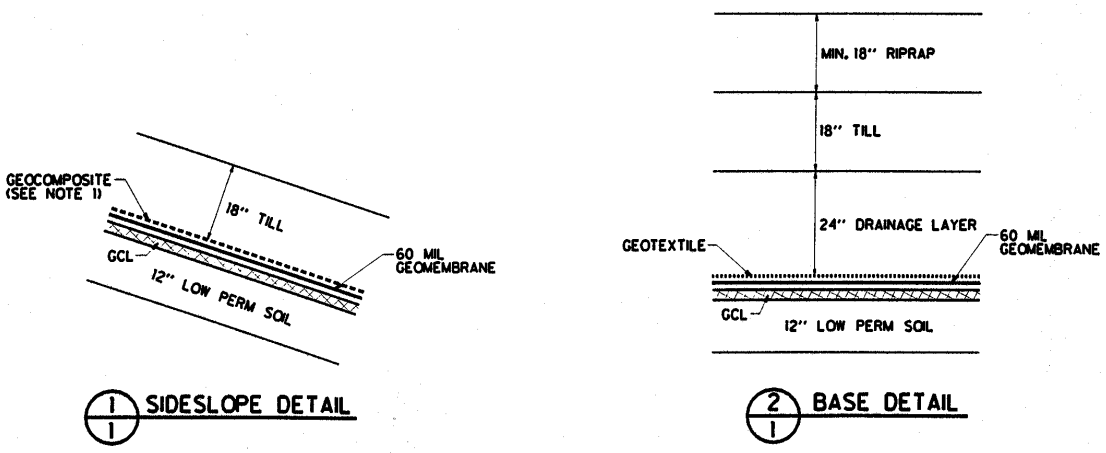

(a)

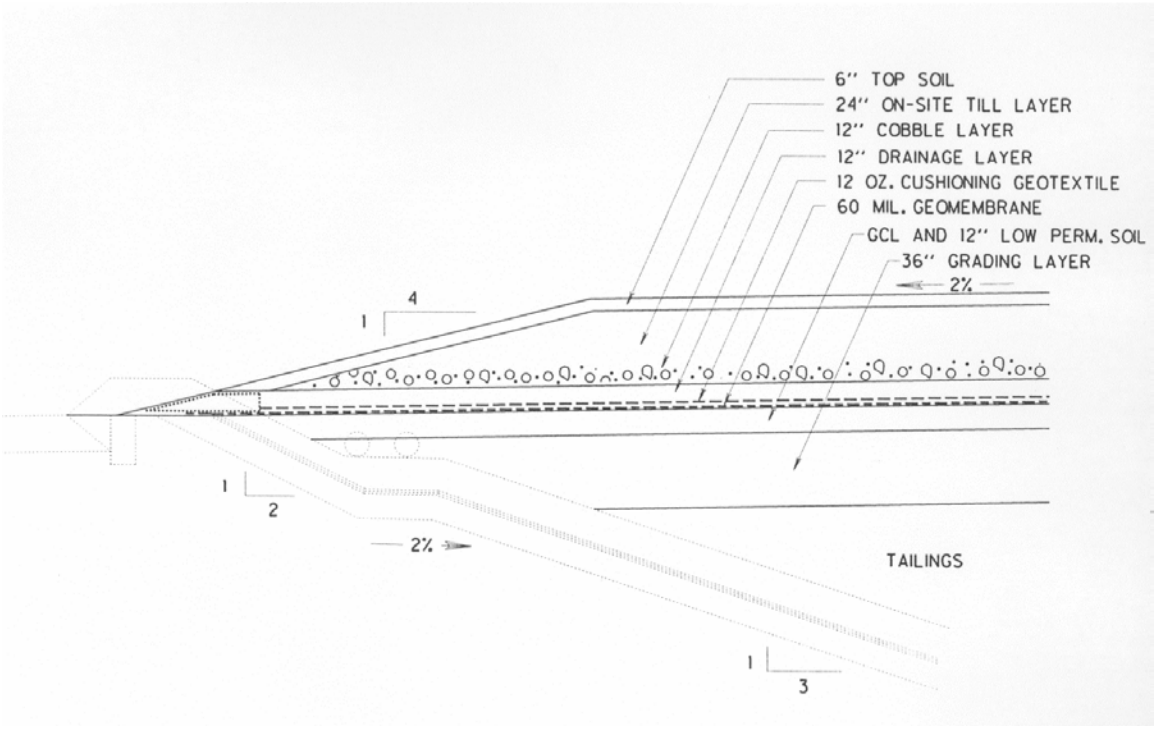

(b)

Figure II.A1. Cross-sections of the liner (a) and cover (b) for the TMA (from Foth and Van Dyke, 1998g).

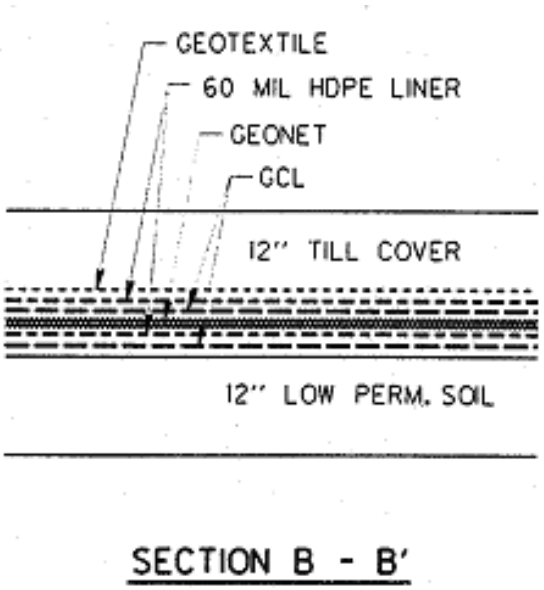

(a)

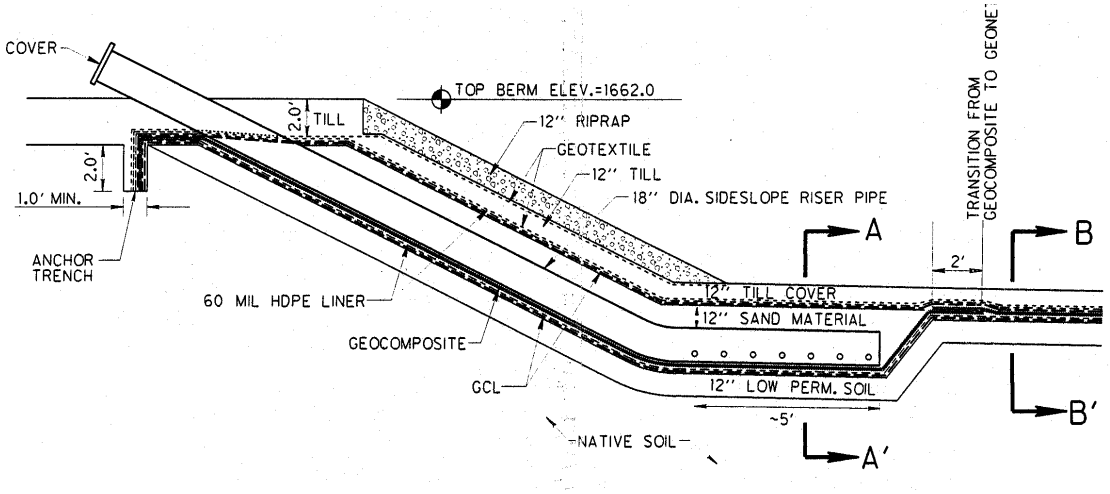

(b)

Figure II.A2. Cross-sections of the liner (a) and sump area (b) for the RP (from Foth and Van Dyke, 2001b).

Table I.A.1. Comparison of heads and tails between 1994 and 1998 metallurgical testing programs.

	1994		1998	
Constituent (g/ton)	Heads	Tails[1]	Heads[2]	Tails
Al	20,100	17,569	12,350	16,000
Sb	85	40	60	50
As	2,700	2,672	2,445	2,400
Ba	<50	<20	25	39
Cd	260	40	240	46
Ca	4,100	9,326	4,450	6,700
C (total)	4,400	4,700	3,800	4,200
Cr	70	13	27	38
Co	67	87	72	77
Cu	3,300	502	3,250	840
Fe	232,000	271,400	256,500	290,000
Pb	11,200	2,954	8,850	3,100
Mn	460	605	505	560
Mg	11,200	11,900	7,950	9,000
Hg	7	2	7.5	2.9
Ni	100	8	5.75	43
K	4,400	1,440	3,800	4,300
Se	42	93	98	140
Ag	42	17	40	25
Na	1,800	164	355	330
S	291,000	290,000	319,000	306,000
Zn	96,000	6,100	93,100	9,300

[1]Recombined using a 60:40 weighted average of coarse tails and fine tails analyses.
[2]Average of two analyses.

Table I.B.1. Summary of ratio of anions/cations using sulfate (SO_4) and total sulfur (S(T)) determinations. With the exception of the short-term cells, S(T) values provide a better anion/cation balance for the steady-state period (cycles ∃ 6). These values should be used for calculations for the intermediate and long-term cells. Calculations using these values should also be used as alternatives for the short-term cells.

Cell	n		Range for Anion/Cation Ratio		Average Ratio		Number of ratios from 0.8-1.2	
	SO_4	S(T)	SO_4	S(T)	SO_4	S(T)	SO_4	S(T)
ST1	14	14	0.81-1.33	0.94-2.34	1.05	1.38	10 (71%)	6 (43%)
ST2	14	14	0.74-1.34	0.94-1.91	1.00	1.32	11 (79%)	7 (50%)
IT1	10	11	0.75-1.23	0.78-1.75	0.92	1.04	6 (60%)	9 (82%)
IT2	13	14	0.50-1.33	0.53-1.86	0.90	1.09	10 (77%)	10 (71%)
LT1	10	13	0.66-1.10	0.79-1.78	0.86	1.14	7 (70%)	9 (69%)
LT2	13	14	0.65-1.09	0.66-1.66	0.87	1.05	9 (64%)	10 (71%)
	Cycles ∃ 6							
ST1	9	9	0.81-1.33	0.95-2.34	1.07	1.34	6 (67%)	4 (44%)
ST2	9	9	0.74-1.34	0.94-1.67	1.00	1.32	6 (67%)	5 (56%)
IT1	9	9	0.75-1.05	0.78-1.10	0.88	0.97	6 (67%)	8 (89%)
IT2	12	12	0.50-1.33	0.81-1.86	0.87	1.08	9 (75%)	10 (83%)
LT1	9	11	0.66-1.10	0.79-1.78	0.84	1.11	6 (67%)	8 (73%)
LT2	12	12	0.65-1.07	0.66-1.44	0.85	1.00	8 (67%)	9 (75%)

Table I.B.2. Cumulative release and associated release rates for sulfate and total sulfur for depyritized tailings humidity cells.

	ST1		ST2		IT1		IT2		LT1		LT2	
	SO_4	S(T)	SO_4	S(T)	SO_4	S(T)	SO_4	S(T)	SO_4	S(T)	SO_4	S(T)
Rinse off period	**Cycles 0-5**				**Cycles 0-9**							
3mass, mg kg^{-1}	3395	1778	3544	1902	3967	1802	4815	1919	4679	1925	4143	1884
3mass, mol kg^{-1}	0.0353	0.0555	0.0369	0.0593	0.0413	0.0562	0.0501	0.599	0.0487	0.0600	0.0431	0.0588
mol S $kg^{-1}s^{-1}$ x 10^{10} (1)	117	183	122	196	75.8	103	92.0	110	89.4	110	79.2	108
mol O_2 $kg^{-1}s^{-1}$ x 10^{10} (2)	219	344	229	368	142	194	173	206	168	207	149	202
Steady State Period	**Cycles 6-22**				**Cycles 10-65**							
3mass, mg kg^{-1}	520	296	638	394	963	375	1326	709	1217	695	1071	465
3mass, mol kg^{-1}	0.00541	0.00923	0.00664	0.0123	0.0100	0.0117	0.0138	0.0221	0.0127	0.0217	0.011	0.0145
mol S $kg^{-1}s^{-1}$ x 10^{10} (1)	5.26	8.98	6.50	12.0	2.96	3.45	4.07	6.53	3.74	6.40	3.29	4.28
mol O_2 $kg^{-1}s^{-1}$ x 10^{10} (2)	9.90	16.8	12.1	22.0	5.55	6.48	7.64	12.2	7.01	12.0	6.17	8.03
(85/63) x mol O_2 (3)	13.3	22.7	16.3	29.7	7.49	8.74	10.3	16.5	9.46	16.2	8.32	10.8
Period of Record	**Cycles 0-22**				**Cycles 0-65**							
3mass, mg kg^{-1}	3915	2074	4182	2296	4930	2177	6141	2628	5896	2620	5214	2349
3mass, mol kg^{-1}	0.0407	0.0647	0.0435	0.0716	0.0513	0.0679	0.0639	0.0820	0.0614	0.0817	0.0543	0.0733
mol S $kg^{-1}s^{-1}$ x 10^{10} (1)	30.6	48.6	32.7	53.8	13.0	17.3	16.3	20.9	15.6	20.8	13.8	18.6
mol O_2 $kg^{-1}s^{-1}$ x 10^{10} (2)	57.4	91.2	61.3	101	24.5	37.6	30.5	39.1	29.3	39.0	25.9	34.9

[1] Rate of sulfur release
[2] Rate of oxygen consumption
[3] Rate of oxygen consumption adjusted for target sulfur content of 0.85% in the TMA, relative to 0.63% in the tests.

Table I.B.3. Cumulative sulfur release and associated release rates accounting for change in solid-phase sulfate.

	ST1		ST2		IT1		IT2		LT1		LT2	
	SO_4	S(T)	SO_4	S(T)	SO_4	S(T)	SO_4	S(T)	SO_4	S(T)	SO_4	S(T)
Period of Record	**Cycles 0-22**				**Cycles 0-65**							
	Sulfur Mass Release to Drainage											
3mass, mg kg^{-1}	3915	2074	4182	2296	4930	2177	6141	2628	5896	2620	5214	2349
3mass, mol kg^{-1}	0.0407	0.0647	0.0435	0.0716	0.0513	0.0679	0.0639	0.0820	0.0614	0.0817	0.0543	0.0733
mol S $kg^{-1}s^{-1}$ x 10^{10} (1)	30.6	48.6	32.7	53.8	13.0	17.3	16.3	20.9	15.6	20.8	13.8	18.6
mol O_2 $kg^{-1}s^{-1}$ x 10^{10} (2)	57.4	91.2	61.3	101	24.5	37.6	30.5	39.1	29.3	39.0	25.9	34.9
85/63x previous value (3)	77.4	123	82.7	136	33.1	50.7	41.2	52.8	39.6	52.6	34.9	47.1
	Account for Change in Solid-Phase Sulfate Content											
♠solid phase SO_4, mol kg^{-1}(4)	-0.0221	-0.0221	-0.0221	-0.0221	NA	NA	NA	NA	NA	NA	NA	NA
net S release, mol kg^{-1}	0.0186	0.0426	0.0214	0.0495	NA	NA	NA	NA	NA	NA	NA	NA
net mol S, $kg^{-1}s^{-1}$ x 10^{10} (1)	14.0	32.0	16.1	37.2	NA	NA	NA	NA	NA	NA	NA	NA
net mol O_2, $kg^{-1}s^{-1}$ x 10^{10} (2)	26.2	60.0	30.1	69.8	NA	NA	NA	NA	NA	NA	NA	NA
85/63 x net mol O_2 (3)	35.3	81.0	40.6	94.2	NA	NA	NA	NA	NA	NA	NA	NA

[1]Rate of sulfur release = net S release in mol kg^{-1}/(22 cycles x 7 d/cycle x 24 hr/d x 3600 s/hr) = net S release/1.33 x 10^7

[2] Rate of oxygen consumption = 1.875 x rate of sulfur release.

[3] Rate of oxygen consumption (mol O_2 $kg^{-1}s^{-1}$ x 10^{10}) adjusted for difference between sulfide content in test (0.63%) and 0.85% target sulfide content.

[4] Difference between hydroxylamine hydrochloride extraction of solids leached in short term humidity cells and unleached solids.

Table I.B.4. Calculation summary for AP and NP depletion in short-term tests.

Method of Calculation	Depletion, kg $CaCO_3$ eq t^{-1}				Depletion, percent			
	AP		CO_3-NP		AP		NP	
	ST1	ST2	ST1	ST2	ST1	ST2	ST1	ST2
Change in solid phase during test[1]	3.9	-2.6	12	14	16	-11	14	16
Release of SO_4, Ca, Mg during test[2]	4.08	4.36	5.9	6.5	17	18	6.6	7.3
SO_4 release + leach extraction result[2]	7.2	9.3	NA	NA	29	38	NA	NA
SO_4 release + alkalinity release[2]	NA	NA	5.6	6.1	NA	NA	6.2	6.8

NA: Not applicable

[1] Table 3.4 of GWQPE Appendix A3 (EIR Appendix 4.2-16). Sobek NP depletion for ST1 and ST2 reported respectively as 17 kg $CaCO_3$ eq/t (23%) and 18 kg $CaCO_3$ eq/t (24%).

[2] Table 3.5 of GWQPE Appendix A3 (EIR Appendix 4.2-16).

Table I.B.5. Cumulative calcium and magnesium release and associated NP depletion for depyritized tailings.

Cycles	ST1		ST2		Cycles	IT1		IT2		LT1		LT2	
	mg kg^{-1}	$CaCO_3$ [1]	mg kg^{-1}	$CaCO_3$ [1]		mg kg^{-1}	$CaCO_3$ [1]	mg kg^{-1}	$CaCO_3$ [1]	mg kg^{-1}	$CaCO_3$ [1]	mg kg^{-1}	$CaCO_3$ [1]
	Calcium												
0-5	1053	2.63	1079	2.69	0-9	1038	2.59	1218	3.04	1174	2.93	1106	2.76
6-22	393	0.98	513	1.28	10-65	749	1.87	920	2.29	895	2.23	827	2.06
0-22	1446	3.61	1591	3.97	0-65	1787	4.46	2138	5.33	2069	5.16	1933	4.82
	Magnesium												
0-5	384	1.58	399	1.64	0-9	388	1.60	500	2.06	446	1.84	414	1.70
6-22	164	0.67	220	0.91	10-65	342	1.41	423	1.74	412	1.70	381	1.57
0-22	548	2.26	619	2.55	0-65	730	3.00	923	3.80	858	3.53	795	3.27
	Calcium + Magnesium												
0-5		4.21		4.33	0-9		4.19		5.10		4.77		4.46
6-22		1.65		2.19	10-65		3.28		4.03		3.93		3.63
0-22		5.87		6.52	0-65		7.46		9.13		8.69		8.09

[1] kg $CaCO_3$ eq/t

Note: Initial NP[$(Ca/Mg)CO_3$] = 0.834 x CO_3 NP = 0.834 x 89.6 = 74.7 kg $CaCO_3$ eq/t

Table I.B.6. NAG test summary. Summarized from Tables 2 and 3 of Attachment H of GWQPE Appendix A1 (EIR Appendix 4.2-15).

Sample ID	Initial Sample			Residue			Reacted		Percent Reacted			Leachate Analysis			
	Pct S_T	AP[1]	CO_3-NP[1]	Pct S_T	AP[1]	CO_3-NP[1]	AP[1]	CO_3-NP[1]	S_T	CO_3-NP[3]	CO_3-NP eq[2]	pH after H_2O_2 rxn	pH after heating	Acidity	Alkalinity
NAG-1A	0.85	27	151									4.2	5.3	285	30
NAG-1B				0.05	1.56	126	25	25	94	17	17	4.3	5.4	283	30
NAG-2A	0.76	24	124									4.7	6.0	344	55
NAG-2B				0.06	1.88	98	22	26	92	21	18	4.4	5.6	257	36
NAG-3A	0.71	22	87									4.8	6.2	297	58
NAG-3B				0.04	1.25	56	21	31	94	36	24	4.9	6.2	235	40
NAG-4A	1.12	35	86									5.1	6.3	176	34
NAG-4B				0.03	0.94	51	34	35	97	41	40	5.2	6.8	122	32
NAG-5A	1.66	52	84									5.8	7.0	22	10
NAG-5B				0.04	1.25	35	51	49	98	58	60	6.1	5.8	34	10
NAG-6A	2.00	68	82									6.0	4.8	80	8
NAG-6B	2.00	63	81	0.20	6.25	36	56	46	90	56	69	6.0	5.1	70	4
limestone												4.8	4.7	2142	101
H_2O_2 blank												1.5	1.6	7990	0

[1] AP based on S_T; AP and NP expressed as kg $CaCO_3$ eq t^{-1}

[2] Percent CO_3 eq reacted assumes NP depletion equal to AP depletion.

[3] Values in this column reported as 25.7, 25.1, 40.7, 44.6, 60.9, and 60.4 in Table 3 of Attachment H of GWQPE Appendix A1 (EIR Appendix 4.2-15).

Table I.C.1. Waste rock particle size distribution for large scale humidity cell tests. From EIR Section 3.5 and EIR Appendix 3.5-31 (Foth and Van Dyke, 1998e).

Sieve	Percent Finer Than							
	Master Composites				High Sulfur Composites			
	Skunk Lake	Rice Lake	U. Mole Lake	L. Mole Lake	Skunk Lake	Rice Lake	U. Mole Lake	L. Mole Lake
1.5 in.	100	100	100	100	100	100	100	100
1 in.	97.8	99.1	98.0	99.4	99.1	99.2	98.8	99.7
3/8 in.	43.6	35.5	41.1	44.2	36.8	42.1	39.3	45.0
#4	24.6	21.0	23.5	26.1	20.1	24.7	22.4	26.6
#10	13.5	12.0	13.1	14.7	10.5	13.8	12.2	15.9
#200	1.9	1.6	1.7	1.5	1.2	2.0	1.7	2.1

Table I.C.2. Bulk chemistry of master and high sulfur composites. From Tables 3.5-17 and 3.5-18 of EIR Section 3.5 (Foth and Van Dyke, 1998e). All values expressed in mg kg^{-1}.

	Master Composites				High Sulfur Composites			
Parameter	Skunk	Rice	U. Mole	L. Mole	Skunk	Rice	U. Mole	L. Mole
Al	63,600	68,000	71,000	68,300	64,300	65,600	66,800	63,500
Sb	20	20	30	30	20	20	20	60
As	61	<40	<40	61	61	61	46	190
Ba	390	340	360	290	230	270	330	260
Cd	5.0	7.0	6.0	8.0	9.0	7.0	7.0	16
Ca	1,100	7,700	13,400	9,900	3,800	1,700	3,600	6,600
C	800	3,300	5,300	4,400	2,400	500	1,600	3,800
Cr	7.0	11	12	9.0	9.0	10	9.0	9.0
Co	21	19	25	28	13	16	19	25
Cu	860	210	240	330	160	490	56	490
Ga	14	14	15	13	13	13	15	12
Fe	46,000	62,100	65,900	70,400	54,900	56,100	65,500	78,300
Pb	140	150	260	180	160	220	160	480
Mg	21,200	36,000	32,100	28,700	29,800	22,500	26,400	19,800
Mn	630	1,400	1,300	1,300	710	390	480	640
Hg	<0.3	<0.3	<0.3	<0.3	0.70	<0.3	0.70	2.3
Mo	<20	<20	<20	<20	<20	<20	<20	<20
Ni	6.0	15	10	10	<5	<5	18	8.0
K	17,900	12,400	11,400	11,900	18,000	16,300	18,400	21,200
Se	<3	<3	<3	<3	4.0	5.0	<3	<3
Si	311,000	285,000	285,000	273,000	303,000	313,000	286,000	280,000
Ag	<0.01	<0.01	<0.01	0.045	<0.01	<0.01	0.01	0.28
Na	1,100	5,100	6,900	7,300	1,200	2,800	3,000	3,500
S[1]	100?	<100?	400?	2,200?	39,300	33,300	44,400	44,400
Sn	<10	<10	60	<10	<10	20	<10	60
Ti	560	380	690	620	460	440	650	540
U	<10	<10	<10	<10	<10	<10	<10	<10
Zn	240	190	190	360	1,300	200	180	4,200

[1]S contents presented in EIR Appendix 3.5-34 are 0.14, 0.05, 0.10, 0.34, 3.95, 3.26, 4.49, and 4.15 percent, respectively.

Table I.C.3. Rates of sulfate release from waste rock master composites in large scale humidity cell tests. Cross-sectional area of cells was 0.164 m^2.

	Skunk Lake	Rice Lake	Upper Mole Lake	Lower Mole Lake
Percent S	0.14	0.05	0.10	0.34
Mass, kg	84.55	126.59	133.18	77.73
3 SO_4, mg/kg				
Cycle 9	26	9	12	31
Cycle 54	90	28	41	85
Final[1]	133	36	42	88
SO_4 release, mg/kg				
Cycle 9-54	64	19	29	54
Cycle 9-final[1]	107	27	30	57
SO_4 release rate, mol SO_4/kg rock/s[2]				
Cycle 9-54	$2.4x\ 10^{-11}$	7.3×10^{-12}	1.1×10^{-11}	2.1×10^{-11}
Cycle 9-final[1]	1.9×10^{-11}	4.9×10^{-12}	1.1×10^{-11}	2.0×10^{-11}
O_2 consumption rate, mol O_2/kg rock/s[2]				
Cycle 9-54	$4.5x\ 10^{-11}$	1.4×10^{-11}	2.1×10^{-11}	3.9×10^{-11}
Cycle 9-final[1]	3.6×10^{-11}	9.2×10^{-12}	2.1×10^{-11}	3.8×10^{-11}
O_2 consumption rate x 10, mol O_2/kg rock/s				
Cycle 9-54	$4.5x\ 10^{-10}$	1.4×10^{-10}	2.1×10^{-10}	3.9×10^{-10}
Cycle 9-final[1]	3.6×10^{-10}	9.2×10^{-11}	2.1×10^{-10}	3.8×10^{-10}

[1] 104 cycles for Skunk and Rice Lake, 58 cycles for Upper and Lower Mole Lake
[2] (SO_4 release)/[(cycles in period) x 7 x 24 x 3600 x 96.1 x 10^3]
[3] Sulfate release rate x 1.875

Table I.C.4. Rates of sulfate release from high sulfur composites in large scale humidity cell tests. Cross-sectional area of cells was 0.164 m^2.

	Skunk Lake	Rice Lake	Upper Mole Lake	Lower Mole Lake
Percent S	3.95	3.26	4.49	4.15
Mass, kg	73.64	81.14	78.18	74.32
3 SO_4, mg/kg				
Cycle 9	149	251	312	1058
Cycle 54	670	2055	1898	4267
Final[1]	1345	2228	2141	4574
SO_4 release, mg/kg				
Cycle 9-54	521	1804	1586	3209
Cycle 9-final[1]	1196	1977	1829	3516
Release Rate, mol SO_4/kg rock/s[2]				
Cycle 9-54	2.0×10^{-10}	6.9×10^{-10}	6.1×10^{-10}	1.2×10^{-9}
Cycle 9-final[1]	2.2×10^{-10}	6.9×10^{-10}	6.4×10^{-10}	1.2×10^{-9}
O_2 consumption rate, mol O_2/kg rock/s[3]				
Cycle 9-54	3.7×10^{-10}	1.3×10^{-9}	1.1×10^{-9}	2.3×10^{-9}
Cycle 9-final[1]	4.1×10^{-10}	1.3×10^{-9}	1.2×10^{-9}	2.3×10^{-9}
O_2 consumption rate x 10, mol O_2/kg rock/s				
Cycle 9-54	3.7×10^{-9}	1.3×10^{-8}	1.1×10^{-8}	2.3×10^{-8}
Cycle 9-final[1]	4.1×10^{-9}	1.3×10^{-8}	1.2×10^{-8}	2.3×10^{-8}

[1] 104 cycles for Skunk Lake, 58 cycles for Rice Lake, Upper and Lower Mole Lake
[2] (SO_4 release)/[(cycles in period) x 7 x 24 x 3600 x 96.1 x 10^3]
[3] Sulfate release rate x 1.875

Table I.C.5. Long-term mass release rates from waste rock master composites. Rates determined as average of cycles 17, 33 and 54; 5, 9 and 54 (Cd, Cr, Pb); or 5 and 9 (Sb, Be, Mo, Co, Hg, Ni, Ag). Rates calculated using detection limits for values reported below detection.

	Mass Release Rate, mg kg^{-1} wk^{-1}			
Parameter	Skunk Lake	Rice Lake	Upper Mole	Lower Mole
Al	4.60E-3	2.35E-2	3.51E-2	4.83E-2
Sb	2.60E-3	1.74E-3	1.52E-3	2.60E-3
As	6.63E-4	1.17E-3	6.62E-4	1.77E-3
Ba	3.40E-4	4.15E-4	5.28E-4	4.28E-4
Be	2.60E-4	1.74E-4	1.52E-4	2.60E-4
Cd	3.20E-4	2.37E-4	1.64E-4	3.56E-4
Ca	6.23E-1	8.05E-1	8.77E-1	1.36E0
Cr	2.67E-4[1]	1.98E-4	1.97E-4	2.65E-4[2]
Cu	5.07E-3	2.03E-3	1.45E-3	1.04E-3
Fe	7.88E-3	3.12E-2	5.45E-2	5.95E-2
Pb	1.44E-3	9.57E-4	8.48E-4	1.44E-3
Mg	3.55E-1	3.26E-1	4.25E-1	5.29E-1
Mn	9.01E-3	3.84E-3	4.68E-3	5.82E-3
Mo	1.14E-3	6.95E-4	1.22E-3	1.04E-3
Co	5.19E-4	4.43E-4	4.62E-4	7.90E-4
Hg	1.04E-5	6.95E-6	6.09E-6	1.58E-5
Ni	1.04E-3	6.95E-4	6.09E-4	1.58E-3
K	2.13E-1	1.77E-1	2.12E-1	2.46E-1
Se	5.87E-4	2.62E-4	3.34E-4	3.87E-4
Ag	2.60E-4	1.74E-4	1.52E-4	2.60E-4
Na	6.27E-2	1.02E-1	2.60E-1	1.36E-1
SO_4	1.88E0	4.84E-1	1.06E0	1.46E0
Zn	6.40E-3	1.52E-3	2.88E-2	4.46E-3

[1] Skunk Lake Cr rate reported as 2.41E-4 in NMC (2000a).
[2] Lower Mole Cr rate reported as 0.00E0 in NMC (2000a).

Table I.C.6. Long-term mass release rates from waste rock high sulfur composites. Rates determined as average of cycles 17, 33 and 54; 5, 9 and 54 (Cd, Cr, Co, Pb, Ni, Ag); or 5 and 9 (Sb, Be, Mo, Hg).

	Mass Release Rate, mg kg^{-1} wk^{-1}			
Parameter	Skunk Lake	Rice Lake	Upper Mole	Lower Mole
Al	2.19E-2	2.58E0	1.08E0	2.80E-1
Sb	2.86E-3	2.26E-3	2.74E-3	3.14E-3
As	3.95E-4	3.95E-4	3.48E-4	9.45E-4
Ba	5.34E-4	1.45E-3	1.42E-3	5.42E-4
Be	2.86E-4	3.98E-4	2.74E-4	2.83E-4
Cd	2.87E-4	6.68E-4	4.79E-4	8.25E-3
Ca	3.34E0	1.96E0	6.11E0	2.00E1
Cr	2.87E-4	5.04E-4	4.10E-4	2.98E-4
Cu	1.30E-3	6.76E-1	9.76E-2	1.06E0
Fe	2.12E-2	1.63E0	4.07E-1	3.80E-1
Pb	1.58E-3	1.36E-3	2.45E-3	2.48E-3
Mg	1.81E0	2.59E0	4.03E0	8.75E0
Mn	4.79E-2	1.13E-1	3.47E-1	1.06E0
Mo	1.14E-3	9.05E-4	1.48E-3	2.31E-3[1]
Co	6.13E-4	2.27E-2	1.08E-2	4.32E-2
Hg	1.14E-5	9.05E-6	1.10E-5	1.77E-5
Ni	1.15E-3	1.63E-3	1.09E-3	6.09E-3
K	1.77E-1	3.30E-1	2.92E-1	3.02E-1
Se	9.95E-4	1.35E-3	8.72E-4	1.29E-2
Ag	2.87E-4	2.42E-4	2.65E-4	2.98E-4
Na	5.15E-2	8.28E-2	6.85E-2	1.01E-1
SO_4	1.40E1	4.09E1	3.99E1	9.48E1
Zn	5.70E-2	4.82E-1	2.17E-1	4.08E0

[1] Rate from cycle 17 only.

Table I.C.7. Drainage volume (Table 1, EIR Appendix 3.5-34), concentrations (EIR Appendix 3.5-33), and long-term mass release rates from the 84.55 kg Skunk Lake Master Composite.

	Concentration, mg L^{-1} unless noted			Mass Release Rate, mg kg^{-1} wk^{-1}[1]		
Parameter	Cycle 17	Cycle 33	Cycle 54	Cycle 17	Cycle 33	Cycle 54
Volume, L	8.16	4.32	4.77	8.16	4.32	4.77
Al	0.068	0.092	0.045	0.00656	0.00470	0.00254
Sb[2]	<0.050[2]	<0.050[2]		<0.00264[2]	<0.00255[2]	
As	0.010	0.010	0.0091	0.000965	0.000511	0.000513
Ba	<0.005	<0.005	<0.005	<0.000483	<0.000255	<0.000282
Be[2]	<0.005[2]	<0.005[2]		<0.000264[2]	<0.000255[2]	
Cd[2]	0.008[2]	<0.005[2]	<0.005	0.000422[2]	<0.000255[2]	<0.000282
Ca	9.2	9.5	8.8	0.888	0.485	0.496
Cr[2]	<0.005[2]	0.005[2]	<0.005	<0.000264[2]	0.000255[2]	<0.000282
Cu	0.022	0.025	0.21	0.00212	0.00128	0.0118
Fe	0.097	0.23	0.044	0.00936	0.0118	0.00248
Pb[2]	<0.040[2]	<0.040[2]	<0.003	<0.00211[2]	<0.00204[2]	<0.000169
Mg	5.0	5.4	5.4	0.483	0.276	0.305
Mn	0.17	0.10	0.098	0.0164	0.00511	0.00553
Mo[2]	<0.020[2]	0.024[2]		<0.00105[2]	0.00123[2]	
Co[2]	<0.010[2]	<0.010[2]		<0.000527[2]	<0.000511[2]	
Hg, ug/L[2]	<0.2[2]	<0.2[2]		<0.0000105[2]	<0.0000102[2]	
Ni[2]	<0.020[2]	<0.020[2]		<0.00105[2]	<0.00102[2]	
K	4.7	2.6	0.93	0.454	0.133	0.0525
Se	0.006	0.011	0.011	0.000579	0.000562	0.000621
Ag[2]	<0.005[2]	<0.005[2]		<0.000264[2]	<0.000255[2]	
Na	1.1	0.90	0.64	0.106	0.0460	0.0361
SO_4	33	27	19	3.18	1.38	1.07
Zn	0.040	0.046	0.23	0.00386	0.00235	0.0130

[1] Mass release rate = V*c/84.55 where V = drainage volume, L; c = concentration, mg/L.
[2] Cycles 5 and 9 with respective volumes of 4.46 and 4.32 L.
Note increases in Cu and Zn concentrations at cycle 54.

Table I.C.8. Drainage volume (Table 1, EIR Appendix 3.5-34), concentrations (EIR Appendix 3.5-33), and long-term mass release rates from the 126.59 kg Rice Lake Master Composite.

	Concentration, mg L^{-1} unless noted			Mass Release Rate, mg kg^{-1} $wk^{-1(1)}$		
Parameter	Cycle 17	Cycle 33	Cycle 54	Cycle 17	Cycle 33	Cycle 54
Volume, L	7.48	3.72	3.84	7.48	3.72	3.84
Al	0.99	0.18	0.22	0.0585	0.00529	0.00667
Sb[2]	<0.050[2]	<0.050[2]		<0.00134[2]	<0.00213[2]	
As	0.026	0.035	0.031	0.00154	0.00103	0.000940
Ba	0.014	0.008	0.006	0.000827	0.000235	0.000182
Be[2]	<0.005[2]	<0.005[2]		<0.000134[2]	<0.000213[2]	
Cd	<0.005	0.009	<0.005	<0.000295	0.000264	<0.000152
Ca	16	18	31	0.945	0.529	0.940
Cr	<0.005	<0.005	<0.005	<0.000295	<0.000147	<0.000152
Cu	0.096	0.009	0.005	0.00567	0.000264	0.000152
Fe	1.4	0.13	0.23	0.0827	0.00382	0.00698
Pb[2]	<0.040[2]	<0.040[2]	<0.003	<0.00107[2]	<0.00171[2]	<0.0000910
Mg	9.5	8.0	6.0	0.561	0.235	0.182
Mn	0.11	0.048	0.020	0.00650	0.00141	0.000607
Mo[2]	<0.020[2]	<0.020[2]		<0.000537[2]	<0.000853[2]	
Co	<0.010	<0.010		<0.000591	<0.000294	
Hg, ug/L[2]	<0.2[2]	<0.2[2]		<0.00000537[2]	<0.00000853[2]	
Ni[2]	<0.020[2]	<0.020[2]		<0.000537[2]	<0.000853[2]	
K	6.4	3.2	1.9	0.378	0.0940	0.0576
Se	<0.005	0.008	0.0084	<0.000295	0.000235	0.000255
Ag[2]	<0.005[2]	<0.005[2]		<0.000134[2]	<0.000213[2]	
Na	3.6	2.0	1.1	0.213	0.0588	0.0334
SO_4	15	11	8	0.886	0.323	0.243
Zn	0.057	<0.020	<0.020	0.00337	<0.000588	<0.000607

[1] Mass release rate = V*c/126.59 where V = drainage volume, L; c = concentration, mg/L.
[2] Cycles 5 and 9 with respective volumes of 3.40 and 5.40 L.

Table I.C.9. Drainage volume (Table 1, EIR Appendix 3.5-34), concentrations (EIR Appendix 3.5-33), and long-term mass release rates from the 133.18 kg Upper Mole Lake Master Composite.

	Concentration, mg L^{-1} unless noted			Mass Release Rate, mg kg^{-1} $wk^{-1(1)}$		
Parameter	Cycle 17	Cycle 33	Cycle 54	Cycle 17	Cycle 33	Cycle 54
Volume, L	7.99	4.32	5.02	7.99	4.32	5.02
Al	1.6	0.14	0.13	0.0960	0.00454	0.00490
Sb[2]	<0.050[2]	<0.050[2]		<0.00141[2]	<0.00163[2]	
As	0.011	0.020	0.018	0.000660	0.000649	0.000678
Ba	0.020	0.006	<0.005	0.00120	0.000195	<0.000188
Be[2]	<0.005[2]	<0.005[2]		<0.000141[2]	<0.000163[2]	
Cd[2]	<0.005[2]	<0.005[2]	<0.005	<0.000141[2]	<0.000163[2]	<0.000188
Ca	21	19	20	1.26	0.616	0.754
Cr[2]	<0.005[2]	0.008[2]	<0.005	<0.000141[2]	0.000261[2]	<0.000188
Cu	0.066	0.006	<0.005	0.00396	0.000195	<0.000188
Fe	2.6	0.093	0.12	0.156	0.00302	0.00452
Pb[2]	<0.040[2]	<0.040[2]	<0.003	<0.00113[2]	<0.00130[2]	<0.000113
Mg	12	8.6	7.3	0.720	0.279	0.275
Mn	0.22	0.014	0.010	0.0132	0.000454	0.000377
Mo	0.030	<0.020		0.00180	<0.000649	
Co	<0.010	<0.010		<0.000600	<0.000324	
Hg, ug/L[2]	<0.2[2]	<0.2[2]		<0.00000565[2]	<0.00000652[2]	
Ni[2]	<0.020[2]	<0.020[2]		<0.000565[2]	<0.000652[2]	
K	6.9	4.3	2.2	0.414	0.139	0.0829
Se	<0.005	0.010	0.010	<0.000300	0.000324	0.000377
Ag[2]	<0.005[2]	<0.005[2]		<0.000141[2]	<0.000163[2]	
Na	4.3	2.2	1.2	0.258	0.0714	0.0452
SO_4	41	12	9	2.46	0.389	0.339
Zn	1.4	0.038	0.031	0.0840	0.00123	0.00117

[1] Mass release rate = V*c/133.18 where V = drainage volume, L; c = concentration, mg/L.
[2] Cycles 5 and 9 with respective volumes of 3.76 and 4.34 L.
NOTE: Cr reported as <0.005 on cycle 17, no Cr reported for cycle 33.

Table I.C.10. Drainage volume (Table 1EIR, Appendix 3.5-34), concentrations (EIR Appendix 3.5-33), and long-term mass release rates from the 77.73 kg Lower Mole Lake Master Composite.

	Concentration, mg L^{-1} unless noted			Mass Release Rate, mg kg^{-1} $wk^{-1(1)}$		
Parameter	Cycle 17	Cycle 33	Cycle 54	Cycle 17	Cycle 33	Cycle 54
Volume, L	8.50	3.79	4.28	8.50	3.79	4.28
Al	1.2	0.19	0.085	0.131	0.00926	0.00468
Sb[2]	<0.05[2]	<0.05[2]		<0.00280[2]	<0.00240[2]	
As	0.024	0.029	0.023	0.00262	0.00141	0.00127
Ba	0.007	<0.005	<0.005	0.000765	<0.000244	<0.000275
Be[2]	<0.005[2]	<0.005[2]		<0.000280[2]	<0.000240[2]	
Cd	0.005	<0.005	<0.005	0.000547	<0.000245	<0.000275
Ca	18	21	20	1.97	1.02	1.10
Cr[2]	<0.005[2]	<0.005[2]	<0.005	<0.000280[2]	<0.000240[2]	<0.000275
Cu	0.021	0.011	<0.005	0.00230	0.000536	<0.000275
Fe	1.5	0.19	0.096	0.164	0.00926	0.00529
Pb[2]	<0.040[2]	<0.040[2]	<0.003	<0.00224[2]	<0.00192[2]	<0.000165
Mg	8.6	6.6	5.9	0.940	0.322	0.325
Mn	0.14	0.031	0.012	0.0153	0.00151	0.000661
Mo[2]	<0.020[2]	<0.020[2]		<0.00112[2]	<0.000960[2]	
Co	<0.010	<0.010		<0.00109	<0.000489	
Hg, ug/L	<0.2	<0.2		<0.0000219	<0.00000979	
Ni	<0.020	<0.020		<0.00219	<0.000979	
K	5.0	2.2	1.5	0.547	0.107	0.0826
Se	0.005	<0.005	0.0067	0.000547	<0.000244	0.000369
Ag[2]	<0.005[2]	<0.005[2]		<0.000280[2]	<0.000240[2]	
Na	2.6	1.5	0.94	0.284	0.0731	0.0518
SO_4	25	18	14	2.73	0.878	0.771
Zn	0.063	<0.020	0.10	0.00689	<0.000975	0.00551

[1] Mass release rate = V*c/77.73 where V = drainage volume, L; c = concentration, mg/L.
[2] Cycles 5 and 9 with respective volumes of 4.36 and 3.73 L.
NOTE: Mo and Co were determined, no rates reported. Cr reported < 0.005 for cycle 33; not reported for cycle 17. Note increase in Zn at cycle 54.

Table I.C.11. Drainage volume (Table 1, EIR Appendix 3.5-34), concentrations (EIR Appendix 3.5-33), and long-term mass release rates from the 73.64 kg Skunk Lake High Sulfur Composite.

	Concentration, mg L^{-1} unless noted			Mass Release Rate, mg kg^{-1} $wk^{-1(1)}$		
Parameter	Cycle 17	Cycle 33	Cycle 54	Cycle 17	Cycle 33	Cycle 54
Volume, L	9.05	4.11	4.29	9.05	4.11	4.29
pH	7.85	6.55	7.02	7.85	6.55	7.02
Al	0.47	0.092	0.046	0.0578	0.00513	0.00268
Sb[2]	<0.050[2]	<0.050[2]		<0.00265[2]	<0.00306[2]	
As	<0.005	<0.005	<0.005	<0.000614	<0.000279	<0.000291
Ba	0.007	0.007	0.006	0.000860	0.000391	0.000350
Be[2]	<0.005[2]	<0.005[2]		<0.000265[2]	<0.000306[2]	
Cd[2]	<0.005[2]	<0.005[2]	<0.005	<0.000265[2]	<0.000306[2]	<0.000291
Ca	34	48	54	4.18	2.68	3.15
Cr[2]	<0.005[2]	<0.005[2]	<0.005	<0.000265[2]	<0.000306[2]	<0.000291
Cu	0.021	0.012	0.011	0.00258	0.000670	0.000641
Fe	0.46	0.077	0.050	0.0565	0.00430	0.00291
Pb[2]	<0.040[2]	<0.040[2]	<0.003	<0.00212[2]	<0.00244[2]	<0.000175
Mg	19	29	25	2.34	1.62	1.46
Mn	0.78	0.47	0.37	0.0959	0.0262	0.0216
Mo[2]	<0.020[2]	<0.020[2]		<0.00106[2]	<0.00122[2]	
Co[2]	<0.010[2]	<0.010[2]	0.012	<0.000530[2]	<0.000611[2]	0.000699
Hg, ug/L[2]	<0.2[2]	<0.2[2]		<0.0000106[2]	<0.0000122[2]	
Ni[2]	<0.020[2]	<0.020[2]	<0.020	<0.00106[2]	<0.00122[2]	<0.00117
K	3.1	1.8	0.87	0.381	0.100	0.0507
Se	0.013	0.015	0.0094	0.00160	0.000837	0.000548
Ag[2]	<0.005[2]	<0.005[2]	<0.005	<0.000265[2]	<0.000306[2]	<0.000291
Na	0.74	0.63	0.49	0.0909	0.0352	0.0285
SO_4	160	210	180	19.7	11.7	10.5
Zn	0.25	0.95	1.5	0.0307	0.0530	0.0874

[1] Mass release rate = V*c/73.64 where V = drainage volume, L; c = concentration, mg/L.
[2] Cycles 5 and 9 with respective volumes of 3.90 and 4.50 L and pH values of 6.09 and 7.37. No Cr cycles 17, 33.

Table I.C.12. Drainage volume (Table 1, EIR Appendix 3.5-34), concentrations (EIR Appendix 3.5-33) and long-term mass release rates from the 81.14 kg Rice Lake High Sulfur Composite.

	Concentration, mg L^{-1} unless noted			Mass Release Rate, mg kg^{-1} wk^{-1}[1]		
Parameter	Cycle 17	Cycle 33	Cycle 54	Cycle 17	Cycle 33	Cycle 54
Volume, L	7.80	4.35	4.46	7.80	4.35	4.46
pH	3.37	2.88	2.58	3.37	2.88	2.58
Al	18	60	51	1.73	3.22	2.80
Sb[2]	<0.050[2]	<0.050[2]		<0.00182[2]	<0.00270[2]	
As	<0.005	0.008	<0.005	<0.000481	0.000429	<0.000275
Ba	0.030	0.018	0.009	0.00288	0.000965	0.000495
Be[2]	0.007[2]	0.010[2]		0.000255[2]	0.000540[2]	
Cd[2]	0.007[2]	<0.005[2]	0.027	0.000255[2]	<0.000270[2]	0.00148
Ca	25	33	31	2.40	1.77	1.70
Cr	<0.005	0.010	0.009	<0.000481	0.000536	0.000495
Cu	10	8.6	11	0.961	0.461	0.605
Fe	9.4	20	53	0.904	1.07	2.91
Pb[2]	<0.040[2]	<0.040[2]	0.0082	<0.00146[2]	<0.00216[2]	0.000451
Mg	27	45	50	2.60	2.41	2.75
Mn	1.6	1.8	1.6	0.154	0.0965	0.0879
Mo[2]	<0.020[2]	<0.020[2]		<0.000730[2]	<0.00108[2]	
Co	0.37	0.36	0.24	0.0356	0.0193	0.0132
Hg, ug/L[2]	0.2[2]	<0.2[2]		0.00000730[2]	<0.0000108[2]	
Ni[2]	0.043[2]	0.039[2]	0.022	0.00157[2]	0.00211[2]	0.00121
K	5.8	1.9	<0.60	0.558	0.102	<0.0330
Se	0.024	0.020	0.012	0.00231	0.00107	0.000660
Ag[2]	<0.005[2]	<0.005[2]	<0.005	<0.000182[2]	<0.000270[2]	<0.000275
Na	1.5	1.2	0.73	0.144	0.0643	0.0401
SO_4	370	740	860	35.6	39.7	47.3
Zn	4.8	7.1	11	0.461	0.381	0.605

[1] Mass release rate = V*c/81.14 where V = drainage volume, L; c = concentration, mg/L.
[2] Cycles 5 and 9 with respective volumes of 2.96 and 4.38 L and pH values of 4.02 and 3.85.

Table I.C.13. Drainage volume (Table 1, EIR Appendix 3.5-34), concentrations (EIR Appendix 3.5-33), and long-term mass release rates from the 78.18 kg Upper Mole Lake High Sulfur Composite.

	Concentration, mg L^{-1} unless noted			Mass Release Rate, mg kg^{-1} wk^{-1}[1]		
Parameter	Cycle 17	Cycle 33	Cycle 54	Cycle 17	Cycle 33	Cycle 54
Volume, L	8.16	3.36	3.87	8.16	3.36	3.87
pH	4.14	3.81	2.74	4.14	3.81	2.74
Al	2.1	7.2	55	0.219	0.309	2.72
Sb[2]	<0.050[2]	<0.050[2]		<0.00195[2]	<0.00352[2]	
As	<0.005	<0.005	0.0062	<0.000522	<0.000215	0.000307
Ba	0.023	0.026	0.015	0.00240	0.00112	0.000743
Be[2]	<0.005[2]	<0.005[2]		<0.000195[2]	<0.000352[2]	
Cd[2]	<0.005[2]	<0.005[2]	0.018	<0.000195[2]	<0.000352[2]	0.000891
Ca	59	110	150	6.16	4.73	7.43
Cr	<0.005	NA	0.006	<0.000522	NA	0.000297
Cu	0.76	1.5	3.0	0.0793	0.0645	0.149
Fe	1.0	4.1	19	0.104	0.176	0.941
Pb[2]	<0.040[2]	<0.040[2]	0.060	<0.00156[2]	<0.00281[2]	0.00297
Mg	36	67	110	3.76	2.88	5.45
Mn	2.8	7.3	8.8	0.292	0.314	0.436
Mo	<0.020	<0.020		<0.00209	<0.000860	
Co	0.095	0.22	0.26	0.00992	0.00946	0.0129
Hg, ug/L[2]	<0.2[2]	<0.2[2]		<0.00000780[2]	<0.0000141[2]	
Ni[2]	<0.020[2]	<0.020[2]	0.022	<0.000780[2]	<0.00141[2]	0.00109
K	5.8	4.2	1.8	0.605	0.181	0.0891
Se	0.011	0.018	0.014	0.00115	0.000774	0.000693
Ag[2]	<0.005[2]	<0.005[2]	<0.005	<0.000195[2]	<0.000352[2]	<0.000248
Na	1.1	1.1	0.87	0.115	0.0473	0.0431
SO_4	340	580	1200	35.5	24.9	59.4
Zn	1.3	4.7	6.4	0.136	0.202	0.312

[1] Mass release rate = V*c/78.18 where V = drainage volume, L; c = concentration, mg/L.
[2] Cycles 5 and 9 with respective volumes of 3.05 and 5.50 L, and pH values of 5.31 and 4.67.

Table I.C.14. Drainage volume (Table 1, EIR Appendix 3.5-34) concentrations (EIR Appendix 3.5-33) and long-term mass release rates from the 74.32 Lower Mole Lake High Sulfur Composite.

	Concentration, mg L^{-1} unless noted			Mass Release Rate, mg kg^{-1} $wk^{-1(1)}$		
Parameter	Cycle 17	Cycle 33	Cycle 54	Cycle 17	Cycle 33	Cycle 54
Volume, L	8.59	4.53	4.88	8.59	4.53	4.88
pH	3.89	3.89	2.93	3.89	3.89	2.93
Al	1.6	1.8	8.3	0.185	0.110	0.545
Sb[2]	0.062[2]	<0.050[2]		0.00319[2]	<0.00309[2]	
As	0.007	0.016	0.016	0.000809	0.000975	0.00105
Ba	0.007	0.008	<0.005	0.000809	0.000488	<0.000328
Be[2]	<0.005[2]	<0.005[2]		<0.000257[2]	<0.000309[2]	
Cd	0.056	0.085	0.20	0.00647	0.00518	0.0131
Ca	290	210	210	33.5	12.8	13.8
Cr[2]	<0.005[2]	<0.005[2]	<0.005	<0.000257[2]	<0.000309[2]	<0.000328
Cu	11	11	19	1.27	0.670	1.25
Fe	2.8	5.4	7.4	0.324	0.329	0.486
Pb[2]	<0.040[2]	0.057[2]	0.029	<0.00206[2]	0.00347[2]	0.00190
Mg	120	84	110	13.9	5.12	7.22
Mn	15	11	12	1.73	0.670	0.788
Mo	<0.020			<0.00231		
Co	0.71	0.39	0.36	0.0821	0.0238	0.0236
Hg, ug/L	<0.2	<0.2		0.0000231	0.0000122	
Ni	0.097	0.050	0.061	0.0112	0.00305	0.00401
K	5.3	3.1	1.6	0.613	0.189	0.105
Se	0.22	0.13	0.082	0.0254	0.00792	0.00538
Ag[2]	<0.005[2]	<0.005[2]	<0.005	<0.000257[2]	<0.000309[2]	<0.000328
Na	1.7	0.84	0.83	0.196	0.0512	0.0545
SO_4	1300	910	1200	150	55.5	78.8
Zn	31	43	92	3.58	2.62	6.04

[1] Mass release rate = V*c/74.32 where V = drainage volume, L; c = concentration, mg/L.
[2] Cycles 5 and 9 with respective volumes of 3.82 and 4.60 L, and pH values of 3.92 and 4.24.

Table I.C.15. Mass release from waste rock humidity cells during cycles 0-9[1].

	Skunk Lake Master Composite	Rice Lake Master Composite	Upper Mole Lake Master Composite	Lower Mole Lake Master Composite	Skunk Lake High Sulfur Composite	Rice Lake High Sulfur Composite	Upper Mole Lake High Sulfur Composite	Lower Mole Lake High Sulfur Composite
	mg kg^{-1}	mg kg^{-1}	mg kg^{-1}	mg kg^{-1}	mg kg^{-1}	mg kg^{-1}	mg kg^{-1}	mg kg^{-1}
Al	2.06E+00	9.79E+00	3.33E+00	2.44E+00	1.45E+00	3.24E+00	1.35E+00	7.53E+00
Sb	2.55E-02	1.69E-02	1.61E-02	2.79E-02	3.00E-02	2.62E-02	2.61E-02	3.38E-02
As	7.24E-03	1.09E-02	1.26E-02	3.12E-02	4.13E-03	3.10E-03	3.46E-03	1.78E-02
Ba	8.19E-03	2.02E-02	8.60E-03	7.03E-03	7.36E-03	2.07E-02	1.69E-02	5.98E-03
Be	2.55E-03	1.69E-03	1.61E-03	2.79E-03	3.00E-03	3.66E-03	2.61E-03	4.10E-03
Cd	3.12E-03	1.78E-03	1.61E-03	2.79E-03	3.00E-03	2.65E-03	2.61E-03	2.32E-02
Ca	6.80E+00	5.50E+00	4.92E+00	1.04E+01	2.91E+01	2.76E+01	4.64E+01	1.62E+02
Cr	3.93E-03	7.62E-03	2.83E-03	2.79E-03	3.16E-03	2.62E-03	2.61E-03	3.05E-03
Cu	1.06E-01	1.51E-01	3.63E-02	4.64E-02	3.73E-02	2.46E+00	1.17E-01	4.14E+01
Fe	3.37E+00	1.43E+01	4.85E+00	4.10E+00	1.60E+00	1.94E+00	1.80E+00	4.14E+01
Pb	2.04E-02	1.63E-02	1.28E-02	2.23E-02	2.40E-02	3.24E-02	2.10E-02	2.74E-02
Mg	5.29E+00	1.05E+01	5.24E+00	8.07E+00	2.37E+01	3.22E+01	4.16E+01	1.48E+02
Mn	1.72E-01	3.20E-01	8.74E-02	1.13E-01	6.93E-01	1.47E+00	1.32E+00	1.59E+01
Mo	1.01E-02	1.17E-02	1.15E-02	1.27E-02	1.20E-02	1.05E-02	1.04E-02	1.22E-02
Co	5.04E-03	5.60E-03	3.31E-03	5.28E-03	9.23E-03	2.46E-01	4.75E-02	1.56E+00
Hg	1.02E-04	6.77E-05	6.42E-05	1.63E-04	1.32E-04	1.05E-04	1.04E-04	4.72E-04
Ni	1.02E-02	7.93E-03	6.42E-03	1.12E-02	1.20E-02	1.80E-02	1.04E-02	2.30E-01
K	4.90E+00	4.19E+00	3.91E+00	5.86E+00	6.92E+00	1.10E+01	9.17E+00	3.33E+00
Se	1.02E-02	1.87E-03	2.87E-03	3.93E-03	9.19E-03	1.46E-02	9.31E-03	1.45E-01
Ag	2.55E-03	1.69E-03	1.61E-03	2.79E-03	3.00E-03	2.62E-03	2.61E-03	4.54E-03
Na	2.47E+00	6.16E+00	7.52E+00	1.16E+01	2.44E+00	7.18E+00	9.58E+00	4.84E+00
Ti	2.55E-02	2.27E-02	1.79E-02	2.79E-02	3.00E-02	2.62E-02	2.61E-02	3.05E-02
SO_4	2.60E+01	9.02E+00	1.17E+01	3.18E+01	1.48E+02	2.52E+02	3.13E+02	1.06E+03
Zn	4.25E-02	9.58E-02	3.25E-02	5.37E-02	1.47E-01	2.04E+00	3.26E-01	2.43E+01

[1] The concentrations of solutes for which samples were not analyzed were calculated as the average of previous and subsequent reported values. For concentrations reported as below detection limits, detection limits were used.

Table II.A.1. Summary of leakage rates for the TMA and RP as reported by NMC*.

Facility	Condition	Leakage Rate (mm/yr)	
		K_{GCL}=6.9x10^{-11} m/s	K_{GCL}=8.8x10^{-8} m/s
RP	design	4.63x10^{-4}	-
TMA (operations - 10 year average)	base-lower stage	-	0.164
	base-upper stage		0.215
	lower ss-1st stage		0
	lower ss-2nd stage		0
	upper ss-2nd stage		0
TMA (post-closure: years after cover placement - base grades only)	1	-	0.985
	2		0.378
	3		0.0297
	4		0.0259
	5		0.0233
	6		0.0212
	7		0.0194
	8-15		0.0140
	16-25		7.82x10^{-3}
	26-35		4.95x10^{-3}
	36-40		3.84x10^{-3}
	41-50		3.12x10^{-3}
	51-60		2.46x10^{-3}
	61-70		2.06x10^{-3}
	71-80		1.75x10^{-3}
	81-90		1.50x10^{-3}
	91-115		1.02x10^{-4}
	116-140		1.02x10^{-4}
	141-240		0
	241+		5.08x10^{-4}

*from Table 8.3-5 of Addendum 5 to the Feasibility Report, Foth & Van Dyke (1998g).

Table II.A2. Peak daily leakage rates for the TMA operations period from HELP Model records.

Facility	Condition	Leakage Rate (mm/yr)	
		K_{GCL}=6.9x10^{-11} m/s	K_{GCL}=8.8x10^{-8} m/s
TMA (operations)	base-lower stage	-	1.06
	base-upper stage		1.01
	lower ss-1st stage		5.03x10^{-5}
	lower ss-2nd stage		5.75x10^{-5}
	upper ss-2nd stage		9.85x10^{-5}

Table II.D.1. Summary of Parameters for TMA Liner.

Parameter	Units	Value
Saturated Hydraulic Conductivity of GCL	m/s	6.9×10^{-11}
Saturated Hydraulic Conductivity of Leachate Collection Layer	m/s	0.003
Frequency of Defects[a]	ha^{-1}	2.5
Diameter of Holes in Geomembrane	mm	11
Diameter of Pinholes in Geomembrane	mm	1
Max. Length of Side Slope	m	78
Max. Length of Drainage Run on Base Slope	m	171
Angle of Side Slope	degrees	18.4
Angle of Base Slope	degrees	1.14

[a]Defect assumed to consist of one hole (11-mm diameter) and one pinhole (1-mm diameter)

Table II.D.2. Summary of Parameters for TMA Cover.

Parameter	Units	Value
Saturated Hydraulic Conductivity of GCL: Design[a]	m/s	2×10^{-11}
Diameter of Holes in Geomembrane	mm	11
Diameter of Pinholes in Geomembrane	mm	1
Frequency of Defects: Single Composite Barrier[b]	ha^{-1}	2.5
Frequency of Defects: Upper Composite Barrier in Double Barrier Cover	ha^{-1}	2.5
Frequency of Defects: Lower Composite Barrier in Double Barrier Cover	ha^{-1}	5.0
Length of Drainage Run	m	385
Slope of Drain: Design	%	2
Slope of Drain: Reduced Performance	%	1
Saturated Hydraulic Conductivity of Drain: Design	m/s	0.003
Saturated Hydraulic Conductivity of Drain: Reduced Performance	m/s	0.0003
Impingement Rate to Lower Drain for Double Barrier	mm/yr	1

[a]Typical hydraulic conductivity of GCLs to dilute waters at confining stress comparable to those anticipated in the final cover (Kraus et al., 1997, Petrov and Rowe, 1997, Vasko et al., 2001). [b]Defect assumed to consist of one hole (11-mm diameter) and one pinhole (1-mm diameter).

Table II.E.1. Summary of Parameters for RP Liner.

Parameter	Units	Value
Saturated Hydraulic Conductivity of GCL: Design	m/s	6.9×10^{-11}
Saturated Hydraulic Conductivity of GCL: Reduced Performance	m/s	6.9×10^{-10}
Diameter of Holes in Geomembrane	mm	11
Diameter of Pinholes in Geomembrane	mm	1
Frequency of Defects: Upper Composite Liner[a]	ha^{-1}	2.5
Frequency of Defects: Lower Composite Liner	ha^{-1}	5.0
Length of Drainage Run	m	244
Slope of Drain	%	0.833
Saturated Hydraulic Conductivity of Drain	m/s	0.001

[a]Defect assumed to consist of one hole (11-mm diameter) and one pinhole (1-mm diameter)

Table II.F.1. Summary of Leakage Rates for TMA and RP.

Facility	Period	Condition	Leakage Rate for Review (mm/yr)[a]	Leakage Rate Predicted by NMC with HELP (mm/yr)
TMA	Operation	Sideslope	5.5×10^{-6}	0
		Base	3.3×10^{-4}	0.16-0.25
	End of Drain Down	Sideslope	5.2×10^{-9}	-
		Base	1.3×10^{-7}	-
		Upper Bound	3.1	
	Steady State (base only)	Design Cover	0.0037	5×10^{-4}
		Double Composite Cover	0.00031	
RP	Operation of TMA	Design	3.9×10^{-4}	4.6×10^{-4}
		Reduced Performance	1.1×10^{-2}	
	Post-Closure of TMA	Design	1.2×10^{-4}	
		Reduced Performance	3.2×10^{-3}	

[a]Note: 1 in/yr = 25.4 mm/yr.

Table III.B.1. Estimates of oxygen flux into exposed tailings surface during drain down.

Time (yr)	Effective Diffusion Coefficient (m^2/s)	Reaction Rate = $2.2x10^{-7}$ 1/s		Reaction Rate = $1.6x10^{-6}$ 1/s	
		Flux (moles O^2/m^2-yr)	Penetration (m)	Flux (moles O^2/m^2-yr)	Penetration (m)
0	1.60E-08	16.6	0.27	44.6	0.10
1	2.96E-07	71.5	1.16	192.0	0.43
2	3.72E-07	80.1	1.30	215.1	0.48
3	4.22E-07	85.3	1.39	229.1	0.52
4	5.09E-07	93.7	1.52	251.7	0.57
5	6.14E-07	102.9	1.67	276.5	0.62
6	6.57E-07	106.4	1.73	285.9	0.64
7	6.75E-07	107.9	1.76	289.9	0.65
8	7.04E-07	110.2	1.79	296.1	0.67
9	7.74E-07	115.6	1.88	310.4	0.70
10	7.89E-07	116.7	1.90	313.4	0.71

Table IV.B.1. Summary of process streams discharging to the TMA (Table 1 of GWQPE Appendix B).

Stream	Stream ID	Flow	Flow
		gpm	(%)
Zinc Tails Thickner Overflow	ZTTO	1328	56.1
Depyritized Tailings Process Water	DTPW	475	20.1
Pyrite Backfill PPSM Overflow	PBPO	197	8.3
Zinc Concentrate Thickner Overflow	ZCTO	240	10.1
Lead Hydroseparator Overflow	LHSO	55	2.3
Lead Concentrate Thickner Overflow	LCTO	30	1.3
Copper Concentrate Thickner Overflow	CCTO	42	1.8
Total		2367	100.0

Table IV.B.2. NMC summary of solute concentration estimates and calculated discharges to the TMA (GWQPE Appendix B).

Parameter	Units	STREAM ID (See Table IV.B.1 for Description)							Process Water Discharge to TMA
		ZTTO	DTPW	PBPO	ZCTO	LHSO	LCTO	CCTO	
Operating flow Operating pH	gpm s.u.	1328 11.2	475 6	197 6	240 11.8	55 8.5	30 8.5	42 7.2	2367 11.1
Acidity as $CaCO_3$	eq.		34	60		<0.0002			12
Aluminum	mg/L	1.4	<0.018	0.043	1.4	<0.022			0.94
Antimony	mg/L	0.1	0.017	0.014	0.1	0.0061			0.071
Arsenic	mg/L	0.1	0.0048	0.022	0.1	0.0025			0.069
Barium	mg/L	0.0196	0.063	0.091	0.0196	0.029			0.035
Beryllium	mg/L	0.0006	<0.00012	<0.00012	0.0006	<0.00033			0.0004
Boron	mg/L		0.021	0.021		0.022			0.021
Cadmium	mg/L	0.0002	0.018	0.027	0.0002	0.0018			0.0061
Calcium	mg/L	299	210	270	299	300			279(624)**
Chloride	mg/L		36	36		33			36
Chromium	mg/L	0.056	0.0022	0.0042	0.056	<0.00053			0.038
Cobalt	mg/L	0.041	0.037	0.038	0.041	0.030			0.039
Copper	mg/L	0.063	0.0081	0.039	0.063	0.0017			0.047
Cyanide, total	mg/L		<0.0034	<0.0034		<0.0034			<0.0034
Cyanide, WAD	mg/L		<0.0029	<0.0029		<0.0029			<0.0029
Flouride	mg/L		0.28	0.22		1			0.38
Iron	mg/L	0.41	0.049	0.6	0.41	<0.0023			0.33
Lead	mg/L	0.27	0.017	0.091	0.27	0.0044			0.019
Magnesium	mg/L	0.15	12	14	0.15	27			5.1
Manganese	mg/L	0.0046	2	2.5	0.0046	1.2			0.068
Mercury	mg/L	0.0002	0.00018	<0.00008	0.0002	<0.00008			0.0002
Nickel	mg/L	0.006	0.12	0.2	0.006	0.016			0.045
Potassium	mg/L	10.3	24	21	10.3	27			14.8
Selenium	mg/L	0.29	0.032	0.041	0.29	0.024			0.20
Silver	mg/L	0.1	<0.0003	0.00067	0.1	0.00028			0.066
Sodium	mg/L	30	2020	20	30	26			27
Sulfate	mg/L	868*	490	620	868*	901			773(1599)**
Zinc	mg/L	0.455	19	33	0.455	1.3			6.9

Note: eq = mg $CaCO_3$ eq/L

* Sulfate data was not available for this test, and was therefore calculated based on the ion balance

** Numbers in brackets are from the MINTEQA2 run TMA_PWS.out

Table IV.B.3. NMC sensitivity analyses of process water makeup (Table 2.1, Steffen, Robertson and Kirsten, 2000b).

Parameter	Units	STREAM ID[1]							Process Water Discharge to TMA		
		ZTTO	DTPW	PBPO	ZCTO	LHSO	LCTO	CCTO	GWQPE[2]	High DTPW Case	Low DTPW Case
Operating flow	**gpm**	1328	475	197	240	55	30	42	2367	2367	2367
Aluminum	mg/L	1.4	<0.018	0.043	1.4	<0.022			0.94	0.66	1.1
Antimony	mg/L	0.1	0.017	0.014	0.1	0.0061			0.071	0.054	0.079
Arsenic	mg/L	0.1	0.0048	0.022	0.1	0.0025			0.069	0.050	0.079
Barium	mg/L	0.0196	0.063	0.091	0.0196	0.029			0.035	0.043	0.030
Beryllium	mg/L	0.0006	<0.00012	<0.00012	0.0006	<0.00033			0.00045	0.00035	0.00050
Boron	mg/L		0.021	0.021		0.022			0.021	0.021	0.021
Cadmium	mg/L	0.0002	0.018	0.027	0.0002	0.0018			0.0061	0.0097	0.0043
Calcium	mg/L	299	210	270	299	300			279	261	288
Chloride	mg/L		36	36		33			36	36	35
Chromium	mg/L	0.056	0.0022	0.0042	0.056	<0.00053			0.038	0.027	0.043
Cobalt	mg/L	0.041	0.037	0.038	0.041	0.030			0.039	0.039	0.040
Copper	mg/L	0.063	0.0081	0.039	0.063	0.0017			0.047	0.036	0.052
Cyanide, total	mg/L		<0.0034	<0.0034		<0.0034			<0.0034	0.0034	0.0034
Cyanide, WAD	mg/L		<0.0029	<0.0029		<0.0029			<0.0029	0.0029	0.0029
Flouride	mg/L		0.28	0.22		1			0.38	0.34	0.42
Iron	mg/L	0.41	0.049	0.6	0.41	<0.0023			0.33	0.26	0.37
Lead	mg/L	0.27	0.017	0.091	0.27	0.0044			0.19	0.14	0.22
Magnesium	mg/L	0.15	12	14	0.15	27			5.1	7.5	3.9
Manganese	mg/L	0.0046	2	2.5	0.0046	1.2			0.68	1.08	0.48
Mercury	mg/L	0.0002	0.00018	<0.00008	0.0002	<0.00008			0.00018	0.00018	0.00018
Nickel	mg/L	0.006	0.12	0.2	0.006	0.016			0.045	0.068	0.034
Potassium	mg/L	10.3	24	21	10.3	27			15	18	13
Selenium	mg/L	0.29	0.032	0.041	0.29	0.024			0.20	0.15	0.23
Silver	mg/L	0.1	<0.0003	0.00067	0.1	0.00028			0.066	0.046	0.076
Sodium	mg/L	30	2020	20	30	26			27	25	28
Sulfate	mg/L	868*	490490	620	868*	901			773	697	811
Zinc	mg/L	0.455	19	33	0.455	1.3			6.9	11	5.1

Notes: * Sulfate data was not available for this test, and was therefore calculated based on the ion balance.
[1] See Table IV.B.1 for Stream IDs.
[2] GWQPE estimates shown for comparison only (see Table IV.B.2 for source).

Table IV.B.4. Sensitivity to composition of water chemistry for small volume streams. Case 1 assumes that the small volume streams LHSO, LCTO and CCTO are equivalent to the ZTTO water; Case 2 assumes concentrations equivalent to the PBPO stream; and Case 3 assumes concentrations equivalent to the DTPW stream. The "SRK Case" is the GWQPE estimate (see Table IV.B.2 for the source).

Parameter	Units	SRK Case Conc.		CASE 1 Conc.	Percent Change		CASE 2 Conc.	Percent Change		CASE 3 Conc.	Percent Change
Flow	gpm	2367		2367			2367			2367	
Al	mg/l	0.94		1.0	-7.6		0.94	-0.1		0.94	0.0
Sb	mg/l	0.071		0.076	-6.8		0.072	-0.6		0.07	-0.8
As	mg/l	0.069		0.074	-7.3		0.07	-1.5		0.07	-0.2
Ba	mg/l	0.035		0.034	1.3		0.038	-9.3		0.04	-5.3
Be	mg/l	0.0004		0.0005	-3.2		0.0004	2.5		0.0004	2.5
B	mg/l	0.0071		0.006	18.0		0.007	0.8		0.007	0.8
Cd	mg/l	0.0061		0.006	1.4		0.0074	-20.0		0.007	-13.3
Ca	mg/l	279		279	0.0		277	0.6		274	1.7
Cl	mg/l	12.0		10.2	15.9		12.2	-1.3		12.2	-1.3
Cr	mg/l	0.038		0.041	-7.6		0.038	-0.5		0.038	-0.2
Co	mg/l	0.039		0.040	-1.5		0.040	-1.1		0.040	-0.9
Cu	mg/l	0.047		0.050	-6.8		0.049	-4.2		0.047	-0.7
CN	mg/l	0.0034		0.003	0.0		0.0034	0.0		0.0011	99.1
CN(WAD)	mg/l	0.0029		0.003	0.0		0.0029	0.0		0.0010	99.1
F	mg/l	0.38		0.38	0.0		0.38	0.0		0.090	123.7
Fe	mg/l	0.33		0.35	-6.4		0.36	-9.2		0.33	-0.8
Pb	mg/l	0.19		0.20	-7.2		0.19	-2.4		0.19	-0.4
Mg	mg/l	5.12		3.7	32.7		4.4	14.6		4.3	17.1
Mn	mg/l	0.68		0.61	9.9		0.75	-9.8		0.72	-6.1
Hg	mg/l	0.0002		0.0002	-3.5		0.00018	0.0		0.0002	-2.9
Ni	mg/l	0.046		0.045	1.2		0.055	-19.6		0.051	-11.5
K	mg/l	14.8		14	6.2		14.5	2.2		14.7	1.1
Se	mg/l	0.20		0.22	-6.8		0.20	-0.4		0.20	-0.2
Ag	mg/l	0.066		0.072	-7.7		0.07	0.0		0.066	0.0
Na	mg/l	27		27	-0.8		27	1.2		27	1.2
SO4	mg/l	773		772	0.2		758	2.0		751	2.9
Zn	mg/l	6.9		6.9	0.7		8.6	-21.9		7.9	-12.8

Table IV.B.5. NMC estimates of solute concentrations with mine water substitution (modified from Table 2.6 of Steffen, Robertson and Kirsten, 2000b).

Parameter	Mine Water Substitution	
	Input (mg/l)	Equilibrated (mg/l)
Aluminum	2.4	0.0022
Antimony	0.068	0.012
Arsenic	0.072	
Barium	0.027	0.0033
Beryllium	0.00043	
Cadmium	0.083	
Calcium	245	549
Chromium	0.040	
Copper	1.5	
Flouride	0.40	
Iron	3.1	6.0
Lead	0.21	
Magnesium	8.2	325
Manganese	0.4	
Mercury	0.00020	
Nickel	0.031	
Potassium	12	
Selenium	0.20	
Silver	0.069	
Sodium	25	
Sulfate	750	2713
Zinc	19	38

Table IV.B.6. Sensitivity analysis for replacement of mill process water with mine water for tailings transport using GWQPE estimates of mine water quality (see Table IV.B.2 for GWQPE estimate and Steffen, Robertson and Kirsten, 2000b, for "SRK Case 2").

Parameter	GWQPE	SRK Case 2 475 gpm	Alternate 1 SRK Case 2 475 gpm	Alternate 2 SRK Case 2 300 gpm	Alternate 3 SRK Case 2 300 gpm	Alternate 4 SRK Case 2 600 gpm	Alternate 5 SRK Case 2 600 gpm
		With Mine Water					
Acidity							
Al	0.94	2.36	2.08	1.83	1.66	2.73	2.38
Sb	0.071	0.068	0.052	0.069	0.059	0.068	0.047
As	0.069	0.072	0.053	0.071	0.059	0.073	0.049
Ba	0.035	0.027	0.035	0.030	0.035	0.025	0.036
Be	0.00045	0.00043	0.00033	0.00044	0.00037	0.00042	0.00030
B	0.021	0.009	0.021	0.013	0.021	0.005	0.021
Cd	0.006	0.083	0.086	0.055	0.057	0.103	0.107
Ca	278.8	245.1	227.2	257.5	246.2	236.2	213.6
Cl	35.5	41.5	62.9	39.3	52.8	43.0	70.1
Cr	0.038	0.040	0.029	0.039	0.032	0.040	0.027
Co	0.039	0.040	0.039	0.040	0.039	0.040	0.039
Cu	0.047	1.510	1.499	0.971	0.964	1.895	1.881
CN	0.0034	0.0014	0.0034	0.0021	0.0034	0.0009	0.0034
CN(WAD)	0.0029	0.0029	0.0072	0.0029	0.0046	0.0029	0.0116
F	0.38	0.40	0.56	0.39	0.50	0.40	0.61
Fe	0.33	3.13	3.06	2.10	2.05	3.87	3.78
Pb	0.19	0.21	0.16	0.20	0.17	0.21	0.15
Mg	5.1213	8.1315	10.5095	7.0225	8.5244	8.9236	11.9274
Mn	0.68	0.42	0.82	0.51	0.77	0.35	0.86
Hg	0.00018	0.00020	0.00020	0.00019	0.00019	0.00021	0.00020
Ni	0.046	0.031	0.054	0.036	0.051	0.027	0.056
NO_3+NO_2-N							
NH_3-N							
K	14.8	11.8	14.5	12.9	14.6	11.0	14.4
Se	0.20	0.20	0.15	0.20	0.17	0.20	0.14
Ag	0.066	0.069	0.049	0.068	0.056	0.070	0.045
Na	26.9	25.3	23.3	25.9	24.7	24.9	22.4
SO_4	773.3	750.6	674.7	759.0	711.0	744.6	648.8
Tl							
Zn	6.9	19.0	22.7	14.5	16.9	22.1	26.8

Table IV.B.7. Sensitivity analysis for replacement of mill process water with wine water for tailings transport using estimates of mine water quality from the Preliminary Engineering Report (PER) for Wastewater Treatment Facilities (Foth and Van Dyke, 1998c; see Table IV.B.2 for GWQPE estimate).

Parameter	GWQPE	Alternate 1 PER Case 2 475 gpm	Alternate 2 PER Case 2 475 gpm	Alternate 3 PER Case 2 300 gpm	Alternate 4 PER Case 2 300 gpm	Alternate 5 PER Case 2 600 gpm	Alternate 6 PER Case 2 600 gpm
		With Mine Water					
Acidity							
Al	0.94	1.17	0.82	1.07	0.87	1.25	0.78
Sb	0.071	0.068	0.052	0.069	0.059	0.068	0.047
As	0.069	0.077	0.058	0.074	0.062	0.079	0.055
Ba	0.035	0.030	0.039	0.032	0.038	0.029	0.040
Be	0.00045	0.00044	0.00034	0.00044	0.00038	0.00043	0.00031
B	0.021	0.021	0.052	0.021	0.034	0.022	0.085
Cd	0.006	0.564	0.568	0.359	0.361	0.711	0.716
Ca	278.8	248.3	230.4	259.5	248.2	240.3	217.7
Cl	35.5	40.9	62.3	38.9	52.4	42.3	69.3
Cr	0.038	0.040	0.029	0.039	0.032	0.040	0.027
Co	0.039	0.040	0.039	0.040	0.039	0.040	0.039
Cu	0.047	12.888	12.877	8.157	8.150	16.268	16.254
CN	0.0034	0.0034	0.0054	0.0034	0.0047	0.0034	0.0060
CN(WAD)	0.0029	0.0029	0.0072	0.0029	0.0046	0.0029	0.0116
F	0.38	0.40	0.56	0.39	0.49	0.40	0.60
Fe	0.33	11.16	11.09	7.17	7.12	14.01	13.92
Pb	0.19	0.29	0.24	0.25	0.22	0.31	0.25
Mg	5.1213	12.9477	15.3257	10.0643	11.5662	15.0073	18.0111
Mn	0.68	0.64	1.04	0.65	0.90	0.63	1.13
Hg	0.00018	0.00020	0.00020	0.00019	0.00019	0.00021	0.00020
Ni	0.046	0.060	0.082	0.054	0.069	0.063	0.092
NO_3+NO_2-N							
NH_3-N							
K	14.8	11.8	14.6	12.9	14.7	11.0	14.5
Se	0.20	0.21	0.16	0.21	0.18	0.22	0.15
Ag	0.066	0.068	0.048	0.067	0.055	0.069	0.043
Na	26.9	27.3	25.3	27.2	25.9	27.5	24.9
SO_4	773.3	929.8	853.9	872.1	824.2	971.1	875.2
Tl							
Zn	6.9	103.9	107.6	68.1	70.5	129.4	134.1

Table IV.B.8. Concentration estimates in process water if 375 gpm of the DTPW stream or the ZTTO stream is replaced by treated effluent from the WWTP using treated water quality estimates from the Preliminary Engineering Report (PER) for Wastewater Treatment Facilities (Foth and Van Dyke, 1998c; see Table IV.B.2 for GWQPE estimate and Steffen, Robertson and Kirsten, 2000b, for "SRK Case 2").

Parameter	GWQPE	WWTP Effluent SRK Case 2 375 gpm DTPW	WWTP Effluent SRK Case 2 375 gpm ZTTO
Acidity			
Al	0.94	1.11	0.85
Sb	0.071	0.069	0.056
As	0.069	0.069	0.054
Ba	0.035	0.027	0.034
Be	0.00045	0.00046	0.00038
B	0.021	0.016	0.026
Cd	0.006	0.003	0.006
Ca	278.8	293.0	278.9
Cl	35.5	26.4	48.3
Cr	0.038	0.038	0.029
Co	0.039	0.040	0.039
Cu	0.047	0.046	0.037
CN	0.0034	0.0026	0.0042
CN(WAD)	0.0029	0.0029	0.0055
F	0.38	0.48	0.61
Fe	0.33	0.32	0.27
Pb	0.19	0.19	0.15
Mg	5.1213	7.5	9.4
Mn	0.68	0.46	0.77
Hg	0.00018	0.00016	0.00015
Ni	0.046	0.029	0.047
NO_3+NO_2-N			
NH_3-N			
K	14.8	15.3	17.5
Se	0.20	0.20	0.16
Ag	0.066	0.066	0.051
Na	26.9	27.9	26.3
SO_4	773.3	838.4	778.5
Tl			
Zn	6.9	4.0	7.0

Table IV.B.9. Concentrations in process water for solutes recycled from the Reclaim Pond to the mill. These calculations account for replacement of the mill water every 2.15 cycles. See Table IV.B.1 for description of Stream IDs.

Parameter	Units	Stream ID							Processwater discharge to TMA		Process water with TMA Recycle
		ZTTO	DTPW	PBPO	ZCTO	LHSO	LCTO	CCTO			
Flow (gpm)	gpm	1328	475	197	240	55	30	42	2367		2367
pH (SU)	SU	11.2	6	6	11.8	8.5	8.5	7.2			
Acidity											
Al	mg/L	1.4	0.018	0.043	1.4	0.022	0.022	0.022	0.94		2.0
Sb	mg/L	0.1	0.017	0.014	0.1	0.0061	0.0061	0.0061	0.07		0.153
As	mg/L	0.1	0.0048	0.022	0.1	0.0025	0.0025	0.0025	0.069		0.149
Ba	mg/L	0.0196	0.063	0.091	0.0196	0.028	0.028	0.028	0.035		0.075
Be	mg/L	0.0006	0.00012	0.00012	0.0006	0.00033	0.00033	0.00033	0.0004		0.001
B	mg/L	0	0.021	0.021		0.022	0.022	0.022	0.007		0.015
Cd	mg/L	0.0002	0.018	0.027	0.0002	0.0018	0.0018	0.0018	0.006		0.013
Ca	mg/L	299	210	270	299	300	300	300	279		599
Cl	mg/L	0	36	36		33	33	33	12.0		26
Cr	mg/L	0.056	0.0022	0.0042	0.056	0.00053	0.00053	0.00053	0.038		0.082
Co	mg/L	0.041	0.037	0.038	0.041	0.03	0.03	0.03	0.039		0.085
Cu	mg/L	0.063	0.0081	0.039	0.063	0.0017	0.0017	0.0017	0.047		0.100
CN	mg/L		0.0034	0.0034		0.0034	0.0034	0.0034	0.0034		0.007
CN(WAD)	mg/L		0.0029	0.0029		0.0029	0.0029	0.0029	0.0029		0.006
F	mg/L		0.28	0.22		1	1	1	0.380		0.817
Fe	mg/L	0.41	0.049	0.6	0.41	0.0023	0.0023	0.0023	0.33		0.713
Pb	mg/L	0.27	0.017	0.091	0.27	0.0044	0.0044	0.0044	0.190		0.409
Mg	mg/L	0.15	12	14	0.15	27	27	27	5.1		11
Mn	mg/L	0.0046	2	2.5	0.0046	1.2	1.2	1.2	0.68		1.5
Hg	mg/L	0.0002	0.00018	0.00008	0.0002	0.00008	0.00008	0.00008	0.0002		0.0004
Ni	mg/L	0.006	0.12	0.2	0.006	0.016	0.016	0.016	0.046		0.098
K	mg/L	10.3	24	21	10.3	27	27	27	15		32
Se	mg/L	0.29	0.032	0.041	0.29	0.024	0.024	0.024	0.20		0.44
Ag	mg/L	0.1	0.0003	0.00067	0.1	0.00028	0.00028	0.00028	0.066		0.14
Na	mg/L	30	20	20	30	26	26	26	27		58
SO4	mg/L	868	490	620	868	901	901	901	773		1663
Zn	mg/L	0.455	19	33	0.455	1.3	1.3	1.3	6.9		14.9

Table IV.B.10. Summary of NMC's estimates of incremental solute contribution of waste rock. From Table 2.4 of GWQPE Addendum 1 (Foth and Van Dyke, 2001a).

Parameter	Annual Solute Release (mg/yr)		Incremental Pond concentrations (mg/L)	
	BEJ	UB	BEJ	UB
Al	1.48E+09	2.04E+09	0.31	0.42
Sb	5.87E+07	8.10E+07	0.012	0.017
As	4.35E+07	6.00E+07	0.0090	0.0124
Ba	1.12E+07	1.54E+07	0.0023	0.0032
Be	5.87E+06	8.10E+06	0.0012	0.0017
Cd	6.00E+06	8.28E+06	0.0012	0.0017
Ca	3.25E+10	4.48E+10	6.69	9.23
Cr	3.89E+05	5.36E+05	0.0001	0.00011
Cu	3.24E+07	4.47E+07	0.0067	0.0092
Fe	1.83E+09	2.53E+09	0.38	0.52
Pb	4.70E+07	6.48E+07	0.0097	0.0134
Mg	1.38E+10	1.91E+10	2.85	3.94
Mn	1.94E+08	2.67E+08	0.040	0.055
Hg	3.48E+05	4.80E+05	0.00007	0.00010
Ni	3.48E+07	4.80E+07	0.0072	0.0099
K	7.32E+09	1.01E+10	1.51	2.08
Se	9.20E+06	1.27E+07	0.0019	0.0026
Ag	5.87E+06	8.10E+06	0.0012	0.0017
Na	3.87E+09	5.34E+09	0.80	1.10
Sulphate	4.15E+10	5.73E+10	8.6	12
Zn	8.74E+07	1.21E+08	0.018	0.025

Table IV.B.11. Summary of incremental solute contributions of waste rock to the TMA pond water using increased oxidation rates. See description in Section IV.B.3.2.

Parameter	Annual Solute Release (mg/yr)		Incremental Pond concentrations (mg/L)	
	Lower Range	Upper Range	Lower Range	Upper Range
Al	1.48E+10	2.04E+10	3.05E+00	4.21E+00
Sb	5.87E+08	8.10E+08	1.21E-01	1.67E-01
As	4.35E+08	6.00E+08	8.97E-02	1.24E-01
Ba	1.12E+08	1.54E+08	2.30E-02	3.18E-02
Be	5.87E+07	8.10E+07	1.21E-02	1.67E-02
Cd	6.00E+07	8.28E+07	1.24E-02	1.71E-02
Ca	3.25E+11	4.48E+11	6.69E+01	9.23E+01
Cr	3.89E+06	5.36E+06	8.02E-04	1.11E-03
Cu	3.24E+08	4.47E+08	6.68E-02	9.22E-02
Fe	1.83E+10	2.53E+10	3.78E+00	5.21E+00
Pb	4.70E+08	6.48E+08	9.68E-02	1.34E-01
Mg	1.38E+11	1.91E+11	2.85E+01	3.94E+01
Mn	1.94E+09	2.67E+09	3.99E-01	5.51E-01
Hg	3.48E+06	4.80E+06	7.18E-04	9.90E-04
Ni	3.48E+08	4.80E+08	7.18E-02	9.90E-02
K	7.32E+10	1.01E+11	1.51E+01	2.08E+01
Se	9.20E+07	1.27E+08	1.90E-02	2.62E-02
Ag	5.87E+07	8.10E+07	1.21E-02	1.67E-02
Na	3.87E+10	5.34E+10	7.98E+00	1.10E+01
Sulphate	4.15E+11	5.73E+11	8.56E+01	1.18E+02
Zn	8.74E+08	1.21E+09	1.80E-01	2.49E-01

Table IV.B.12. Estimates of NMC Best Engineering Judgement (BEJ) TMA pond water quality. From Table 2.10 of Steffen, Robertson and Kirsten (2001).

Parameter	Acidic Pond mg/L	Neutral Condition Initial mg/L	MINTEQA2 Equilibrated mg/L	Neutral Pond mg/L
Al	1.24	1.2	0.0063	0.0063
Sb	0.083	0.083	0.012	0.012
As	0.078	0.078		0.078
Ba	0.0370	0.037	0.0034	0.0034
Be	0.0017	0.0017		0.0017
Bi				
B	0.021	0.021		0.0212
Cd	0.0073	0.0073		0.0073
Ca	739	631	553	553
Cl	36	36		36
Cr	0.038	0.038		0.038
Co	0.039	0.039		0.039
Cu	0.053	0.053		0.053
F	0.38	0.38		0.38
Fe	0.71	0.71	0.67	0.67
Pb	0.20	0.20		0.20
Mg	439	8.0	328	328
Mn	0.72	0.72		0.72
Hg	0.00025	0.00025		0.00025
Ni	0.053	0.053		0.053
K	16	16		16
Se	0.21	0.21		0.21
Ag	0.068	0.068		0.068
Na	28	28		28
Sulphate	3534	1608	2669	2669
Zn	6.9	6.9		6.9

Table IV.B.13. Estimates of NMC Upper Bound (UB) TMA pond water quality. From Table 2.12 of Steffen, Robertson and Kirsten (2001).

Parameter	Acidic Pond	Neutral Condition Initial	MINTEQA2 Equilibrated	Neutral Pond
	mg/L	mg/L	mg/L	mg/L
Al	1.36	1.4	0.0057	0.0057
Sb	0.088	0.088	0.012	0.012
As	0.082	0.082		0.082
Ba	0.0379	0.038	0.0034	0.0034
Be	0.0021	0.0021		0.0021
Bi				
B	0.021	0.021		0.0212
Cd	0.0078	0.0078		0.0078
Ca	921	633	554	554
Cl	36	36		36
Cr	0.038	0.038		0.038
Co	0.039	0.039		0.039
Cu	0.056	0.056		0.056
F	0.38	0.38		0.38
Fe	0.85	0.85	0.81	0.81
Pb	0.20	0.20		0.20
Mg	550	9.1	329	329
Mn	0.73	0.73		0.73
Hg	0.00028	0.00028		0.00028
Ni	0.055	0.055		0.055
K	17	17		17
Se	0.21	0.21		0.21
Ag	0.068	0.068		0.068
Na	28	28		28
Sulphate	4392	1611	2666	2666
Zn	6.9	6.9		6.9

Table IV.B.14. Estimates of NMC BEJ average TMA pond water quality. From Table 2.11 of Steffen, Robertson and Kirsten (2001).

Parameter	Time Averaged Pond Water Quality (mg/L)			BEJ Estimate
Events/year	1	2	3	
Al	0.021	0.035	0.050	0.021
Sb	0.013	0.014	0.015	0.013
As	0.078	0.078	0.078	0.078
Ba	0.0038	0.0042	0.0046	0.0038
Be (<1)	0.0017	0.0017	0.0017	0.0017
Bi				
B	0.021	0.021	0.021	0.021
Cd	0.0073	0.0073	0.0073	0.0073
Ca	555	557	560	555
Cl	36	36	36	36
Cr	0.038	0.038	0.038	0.038
Co	0.039	0.039	0.039	0.039
Cu	0.053	0.053	0.053	0.053
F	0.38	0.38	0.38	0.38
Fe	0.67	0.67	0.67	0.67
Pb	0.20	0.20	0.20	0.20
Mg	329	331	332	329
Mn	0.72	0.72	0.72	0.72
Hg	0.00025	0.00025	0.00025	0.00025
Ni	0.053	0.053	0.053	0.053
K	16	16	16	16
Se	0.21	0.21	0.21	0.21
Ag	0.068	0.068	0.068	0.068
Na	28	28	28	28
SO4	2679	2689	2699	2679
Zn	6.9	6.9	6.9	6.9

Table IV.B.15. Estimates of NMC UB average TMA pond water quality. From Table 2.13 of Steffen, Robertson and Kirsten (2001).

Parameter	Time Averaged Pond Water Quality (mg/L)			UB Estimate
Events/year	1	3	5	
Al	0.053	0.15	0.24	0.24
Sb	0.015	0.020	0.025	0.025
As	0.082	0.082	0.082	0.082
Ba	0.0046	0.0070	0.0094	0.0094
Be	0.0021	0.0021	0.0021	0.0021
Cd	0.0078	0.0078	0.0078	0.0078
Ca	567	593	618	618
Cl	36	36	36	36
Cr	0.038	0.038	0.038	0.038
Co	0.039	0.039	0.039	0.039
Cu	0.056	0.056	0.056	0.056
F	0.38	0.38	0.38	0.38
Fe	0.81	0.81	0.81	0.81
Pb	0.20	0.20	0.20	0.20
Mg	336	352	367	367
Mn	0.73	0.73	0.73	0.73
Hg	0.00028	0.00028	0.00028	0.00028
Ni	0.055	0.055	0.055	0.055
K	17	17	17	17
Se	0.21	0.21	0.21	0.21
Ag	0.068	0.068	0.068	0.068
Na	28	28	28	28
SO4	2726	2847	2968	2968
Zn	6.9	6.9	6.9	6.9

Table IV.B.16. Suggested Lower Range Estimate (LRE) concentrations of solutes in the TMA pond, representing time averaged concentrations including summer, winter and acidic conditions.

Parameter	Time Averaged Pond Water Quality mg/L			Lower Range Estimate
Events/Year	1	2	3	
Al	0.078	0.155	0.231	0.08
Sb	0.279	0.279	0.279	0.279
As	0.223	0.223	0.223	0.223
Ba	0.004	0.005	0.006	0.0043
Be	0.013	0.013	0.013	0.0134
B	0.005	0.006	0.006	0.015
Cd	0.096	0.096	0.096	0.096
Ca	538	543	549	538
Cl	12.2	12.3	12.5	25.8
Cr	0.085	0.085	0.085	0.085
Co	0.030	0.031	0.031	0.085
Cu	10.4	10.4	10.4	10.4
F	0.291	0.297	0.302	0.000
Fe	1.087	1.087	1.088	1.09
Pb	0.487	0.487	0.487	0.49
Mg	170	175	180	170
Mn	11	11	11	11
Hg	0.001	0.001	0.001	0.00113
Ni	0.214	0.214	0.214	0.214
K	44	44	44	44
Se	0.56	0.56	0.56	0.56
Ag	0.155	0.155	0.155	0.155
Na	65	65	65	65
SO4	2906	2924	2942	2906
Zn	50	50	50	50

Table IV.B.17. Suggested Upper Range Estimate (URE) concentrations of solutes in the TMA pond, representing time averaged concentrations including summer, winter and acidic conditions.

Parameter	Time Averaged Pond Water Quality mg/L			Lower Range Estimate
Events/Year	1	3	5	
Al	0.700	2.100	3.499	3.50
Sb	0.354	0.354	0.354	0.354
As	0.210	0.210	0.210	0.210
Ba	0.003	0.003	0.003	0.0026
Be	0.019	0.019	0.019	0.0195
B	0.006	0.006	0.007	0.015
Cd	0.495	0.496	0.496	0.496
Ca	525	652	778	778
Cl	12.5	13.4	14.4	25.8
Cr	0.101	0.101	0.101	0.101
Co	0.031	0.034	0.038	0.085
Cu	70.7	70.8	70.8	70.8
F	0.302	0.332	0.363	0.000
Fe	3.807	3.840	3.874	3.87
Pb	0.567	0.567	0.567	0.57
Mg	602	667	732	732
Mn	66	66	67	67
Hg	0.002	0.002	0.002	0.00156
Ni	0.507	0.508	0.508	0.508
K	51	51	51	51
Se	1.22	1.22	1.22	1.22
Ag	0.162	0.162	0.162	0.162
Na	65	65	65	65
SO4	5284	5788	6292	6292
Zn	256	256	256	256

Table IV.B.18. Estimates of NMC TMA "Pond Water Dominated Zone" solute concentrations. From Table 2.14 of Steffen, Robertson and Kirsten (2001).

Parameter	BEJ Case (mg/L)			UB Case (mg/L)		
	Average TMA Pond	MINTQA2 Equilibrated (TP_BEJ2)	Pond Water Dominated Zone	Average TMA Pond	MINTEQA2 Equilibrated (TP_UP2)	Pond Water Dominated Zone
Al	0.021	0.011	0.011	0.24	0.0058	0.0058
Sb	0.013	0.012	0.012	0.025	0.012	0.012
As	0.078		0.078	0.082		0.082
Ba	0.0038	0.0034	0.0034	0.0094		0.0094
Be	0.0017		0.0017	0.0021		0.0021
Cd	0.0073		0.0073	0.0078		0.0078
Ca	555	553	553	618	549	549
Cr	0.038		0.038	0.038		0.038
Cu	0.053		0.053	0.039		0.039
F	0.38		0.38	0.056		0.056
Fe	0.67	0.63	0.63	0.81	3.0	3.0
Pb	0.20		0.20	0.20		0.20
Mg	329	332	332	367	364	364
Mn	0.72		0.72	0.73	0.73	0.73
Hg	0.00025		0.00025	0.00028		0.00028
Ni	0.053		0.053	0.055	0.055	0.055
K	16		16	17		17
Se	0.21		0.21	0.21		0.21
Ag	0.068		0.068	0.068		0.068
Na	28		28	28		28
SO4	2679	2675	2675	2968	2827	2827
Zn	6.9		6.9	6.9	44	44

Table IV.B.19. Final estimates of dissolved constituent concentrations in the oxidized neutral portion of the TMA.

Neutral Oxidized Zone TMA Pore Water			
	Lower Range		Upper Range
	Estimate		Estimate
Element	mg/L		mg/L
Al	0.07		40.01
Sb	2.0		9.5
As	33		179
Ba	0.017		0.019
Be	0.854		4.297
Bi	0.000		0.000
B	0.011		0.008
Cd	0.340		1.251
Ca	521		2325
Cl	94		94
Cr	0.40		1.77
Co	1.6		7.9
Cu	8.5		41.1
F	34		175
Fe	18.6		115.1
Pb	8.0		12.4
Mg	1087		9795
Mn	16.5		102.2
Hg	0.082		0.414
Ni	1.2		5.7
P	0.00		0.00
K	137		552
Se	4.20		8.64
Ag	0.33		0.04
Na	138		488
SO_4	5228		3813
Zn	98		375

Table IV.C.1. Solubility controls assumed in MINTEQA2 for final estimates.

Lower Range Estimate Solubility Controls	**Upper Range Estimates Solubility Controls**
Barite	Barite
Cerrargyrite	Cerrargyrite
Gibbsite [c]	Gibbsite
Gypsum	Gypsum
Smithsonite	Ferrihydrite
Ferrihydrite	Rhodocrosite
Rhodocrosite	Anglesite
Anglesite	Dolomite
Dolomite	
Siderite [d]	

Table IV.C.2. Final estimates of dissolved constituent concentrations in TMA leachate.

TMA Leachate Composition				
	Operational Period	Closure Period	Operational Period	Closure Period
	Average Lower Range Estimate	Average Lower Range Estimate	Average Upper Range Estimate	Average Upper Range Estimate
Element	mg/L	mg/L	mg/L	mg/L
Al	0.061	0.062	3.499	7.696
Sb	0.274	0.477	0.354	1.401
As	0.239	4.047	0.210	20.763
Ba	0.004	0.006	0.003	0.005
Be	0.013	0.110	0.019	0.511
Bi	0.000	0.000	0.000	0.000
B	0.015	0.015	0.015	0.015
Cd	0.025	0.061	0.496	0.583
Ca	527	527	778	956
Cl	26	34	26	34
Cr	0.082	0.119	0.101	0.293
Co	0.085	0.260	0.085	0.984
Cu	0.17	1.13	70.8	67.4
F	0.82	4.7	0.0	20.1
Fe	4.4	6.0	3.9	16.7
Pb	0.51	1.37	0.57	1.93
Mg	118	230	732	1774
Mn	6.2	7.4	66.5	70.6
Hg	0.001	0.010	0.002	0.049
Ni	0.214	0.332	0.508	1.108
P	0.000	0.000	0.000	0.000
K	47	57	51	109
Se	0.565	0.982	1.216	2.070
Ag	0.155	0.174	0.162	0.148
Na	66	74	65	114
SO_4	2593	2896	6292	6007
Zn	28	36	256	270

Table IV.C.3. Final estimates of dissolved constituent concentrations in Reclaim Pond water.

	Reclaim Pond Water Composition			
	Lower Range Estimates		Upper Range Estimates	
	Operations	Consolidation/ Closure	Operations	Consolidation/ Closure
Element	mg/L	mg/L	mg/L	mg/L
Al	0.075	0.062	3.499	7.696
Sb	0.279	0.477	0.354	1.401
As	0.225	4.047	0.210	20.763
Ba	0.004	0.006	0.003	0.005
Be	0.013	0.110	0.019	0.511
Bi	0.00	0.00	0.00	0.00
B	0.015	0.015	0.015	0.015
Cd	0.0852	0.061	0.4961	0.583
Ca	537	527	778	956
Cl	26	34	26	34
Cr	0.084	0.119	0.101	0.293
Co	0.085	0.26	0.085	0.98
Cu	8.8	1.1	70.8	67.4
F	0.12	4.68	0.00	20.10
Fe	1.6	6.0	3.9	16.7
Pb	0.49	1.4	0.57	1.9
Mg	162	230	732	1774
Mn	10	7	67	71
Hg	0.001	0.010	0.002	0.049
Ni	0.214	0.33	0.508	1.11
P	0.00	0.00	0.00	0.00
K	45	57	51	109
Se	0.56	0.98	1.22	2.07
Ag	0.155	0.174	0.162	0.148
Na	65	74	65	114
SO_4	2859	2896	6292	6007
Zn	47	36	256	270